NASA CR- 160034

# ADVANCED VERY HIGH RESOLUTION

# RADIOMETER, MOD 2

# FINAL ENGINEERING REPORT

(NASA-CR-160034) ADVANCED VERY HIGH RESOLUTION RADIOMETER, MOD 2 ENGINEERING REPORT Final Report (ITT Aerospace/Optical Div.) 104 p HC A06/MF A01 CSCL 14B

N80-32701

Unclas
G3/35 34116

PREPARED BY

ITT AEROSPACE/OPTICAL DIVISION
FORT WAYNE, INDIANA
46803

CONTRACT # NAS 5-23400

PREPARED FOR

NATIONAL AERONAUTICS AND SPACE ADMINISTRATION
GODDARD SPACE FLIGHT CENTER
GREENBELT, MARYLAND
20771

TABLE OF CONTENTS

## 1.0 INTRODUCTION

The Advanced Very High Resolution Radiometer, Mod 2 (AVHRR/2) is a modification of the original AVHRR (AVHRR/1) to expand the number of channels from four to five and provide additional sensing in the infrared region. Figure 1-1 gives a comparison of the spectral regions employed in the two instruments. As seen in this table, three of the channels are the same on both instruments. The difference in instruments is in the long wave IR region where a single channel has been replaced by two channels.

The modification from AVHRR/1 to AVHRR/2 has been done with a minimum of changes. The areas of change are highlighted in Figure 1-2 and the modifications by module are summarized in Figure 1-3. It can be seen that the primary changes are in the relay optics and in the cooler.

In this development program only two models are involved. The first model, the Optical Test Model (OTM) was constructed and tested to prove the performance and structural integrity of the optical system and the modified cooler. The second model constructed is the Protoflight (PFM).

This document will deal only with the areas of the AVHRR/2 which have been modified from the AVHRR/1 design. These are discussed in the sections which follow.

AVHRR + ADDITIONAL THERMAL CHANNEL = AVHRR MOD. 2

| CHANNEL | AVHRR/1 | AVHRR/2 |
|---|---|---|
| 1 | .58 TO .68 | NO CHANGE |
| 2 | .725 TO ≈ 1.00 | NO CHANGE |
| 3 | 10.5 TO 11.5 | 10.3 TO 11.3 |
| 4 | 3.55 TO 3.93 | NO CHANGE |
| 5 | NONE | 11.5 TO 12.5 |

FIGURE 1-1

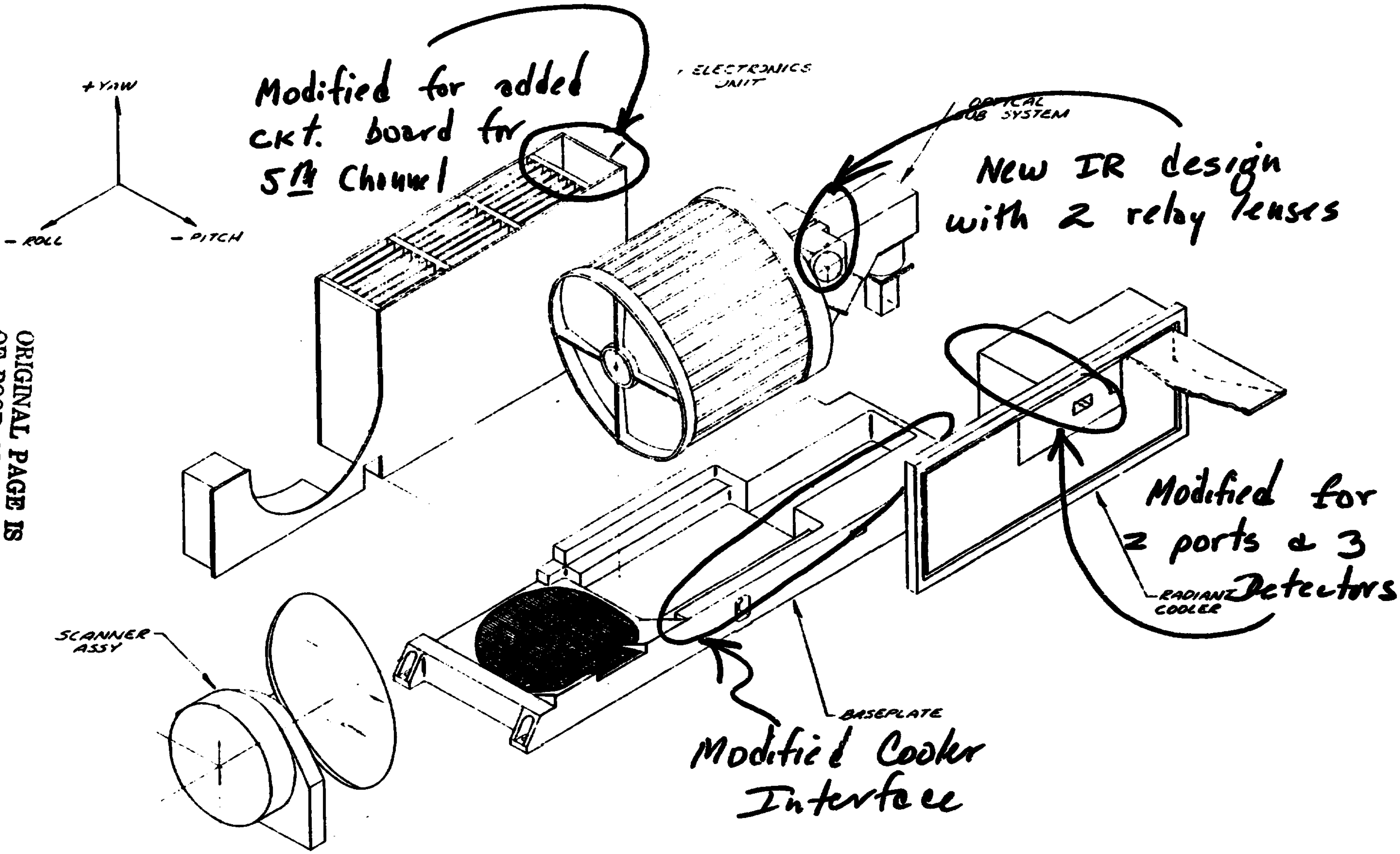


AVHRR/2 - MODIFIED AREAS

FIGURE 1-2

# AVHRR/2 MODULES

## SCANNER

SAME AS FOR AVHRR/1
BEING PROCURED AS COMMON PART ON AVHRR FLIGHT MODEL PROGRAM

## ELECTRONICS

PRESENT AVHRR/1 DESIGNED TO ACCOMMODATE 5 DATA CHANNELS
AVHRR/2 ADDS AMPLIFIERS, TM, AND COMMAND FOR 5TH CHANNEL
ADDED CIRCUITS ARE DUPLICATES OF EXISTING AVHRR/1 DESIGNS.

## OPTICS

TELESCOPE - SAME AS AVHRR/1
BEING PROCURED AS COMMON PART ON FM
PROGRAM FROM PERKIN-ELMER

RELAY OPTICS - CH. 1 AND CH. 2 SAME AS AVHRR/1
IR PORTION REDESIGNED TO PROVIDE FOR 3RD
THERMAL CHANNEL.
RELAY OPTICAL ELEMENTS ASSEMBLED BY ITT.

## COOLER

SIZE AND THERMAL CONSTRUCTION SAME AS AVHRR/1.
ADDED OPTICAL PORT INCORPORATED TO INTERFACE WITH
NEW IR RELAY OPTICS.

## BASEPLATE

ESSENTIALLY THE SAME AS AVHRR/1
MOUNTING INTERFACE WITH COOLER MODIFIED FOR
REVISED COOLER POSITION.

FIGURE 1-3

## 2.0 OPTICAL DESIGN

A comparison of the AVHRR/2 and AVHRR/1 optics is given in Figure 2-1. The scan mirror, telescope and Channel 1 and 2 relay optics are identical in both instruments. The transparent gold dichroic beamsplitter which reflects the infrared channels and transmits the Channels 1 and 2 is also retained both in function, size and location (just behind the telescope primary mirror). As indicated in Figure 2-2 one more dichroic beamsplitter is added to the five channel design which reflects the mid-IR band (Channel 4) and transmits the two far-IR bands (Channels 3 and 5). The aplanat lens designs used in AVHRR/1 have been retained in AVHRR/2 with the added Channel 5 aplanat lens being the same as Channel 4 except that the AR coating is modified for best transmission in the Channel 5 spectral region. The focus lenses are basically the same in function but radii of curvatures have been adjusted for the use of the Zn Se material in channels 3 and 5 and to reduce the thickness, and hence mass, of the Channel 4 lenses. Zinc selenide was selected for use in Channels 3 and 5 rather than germanium because it has negligible absorption and will provide more uniform spectral response.

Figure 2-3 illustrates the optical configuration of the AVHRR/2. After separation of the mid and far IR bands by dichroic D4, the far IR bands are re-directed by a flat folding mirror M3 in order to get the beam into the radiant cooler. Vacuum housing windows W1 and W3 are used to pressure seal the radiant cooler for bench testing. Windows W2 and W4 are used on the first stage radiator of the cooler for contamination protection of the cold patch and to reduce the radiant heat load on the patch. Channels 3 and 5 are arranged on the cold patch in AVHRR/2 in the same manner as Channels 3 and 4 in AVHRR/1.

Figure 2-4 and 2-5 give the detail design information for the reimaging optics for the infrared channels. In Figure 2-4 the germanium doublet lenses (surfaces 10, 11, 12 and 13) constitutes focus lens L6 in Figure 2-3, the two sapphire flat elements are cooler windows W3 and W4, the germanium flat element is filter F4 and the aplanatic lens (surfaces 20 and 21) is lens L7; the long wave channels have similar correspondence, the two zinc selenide lenses (surfaces 6, 7, 8 and 9) in Figure 2-5 being lens L1 in Figure 2-3, etc. The sensitive areas of the infrared detectors are located at the image plane identified for each channel and therefore serve as the field stops. The edge width of each of the three infrared detectors is 0.0068" $\pm$ 0.0003" which provides the IFOV (instantaneous field of view) of 1.31 milliradians.

The AVHRR/2 (as well as AVHRR/1) optical system is designed to cover a larger FOV than the required 1.31 m.r. by 1.31 m.r. This larger FOV is called the extended FOV and is illustrated in Figure 2-6. It is designed into the optical system so that the detectors can be displaced from their design nominal positions for purposes of registering the channels without serious optical performance

| ITEM | COMPARISON WITH MOD. 1 |
|---|---|
| SCAN MIRROR | SAME |
| TELESCOPE | SAME |
| CH. 1 & 2 RELAY OPTICS | SAME |
| BEAMSPLITTERS | ONE ADDED TO SEPARATE MID-IR BAND FROM TWO FAR-IR BANDS. |
| APLANAT LENSES | CH. 3 & 4 - SAME; CH. 5 - SAME DESIGN AS MOD 1, CH. 4 (AR COATING THICKNESS ADJUSTED). |
| FOCUS LENSES | CH. 3 & 5 USE ZN SE INSTEAD OF GE, RADIUS OF CURVES SLIGHTLY DIFFERENT; CH. 4 - SAME MTL (GE) BUT THICKNESS REDUCED TO REDUCE WEIGHT OF RELAY OPTICS. |

COMPARISON OF MOD. 1 & 2 OPTICS

FIGURE 2- 1

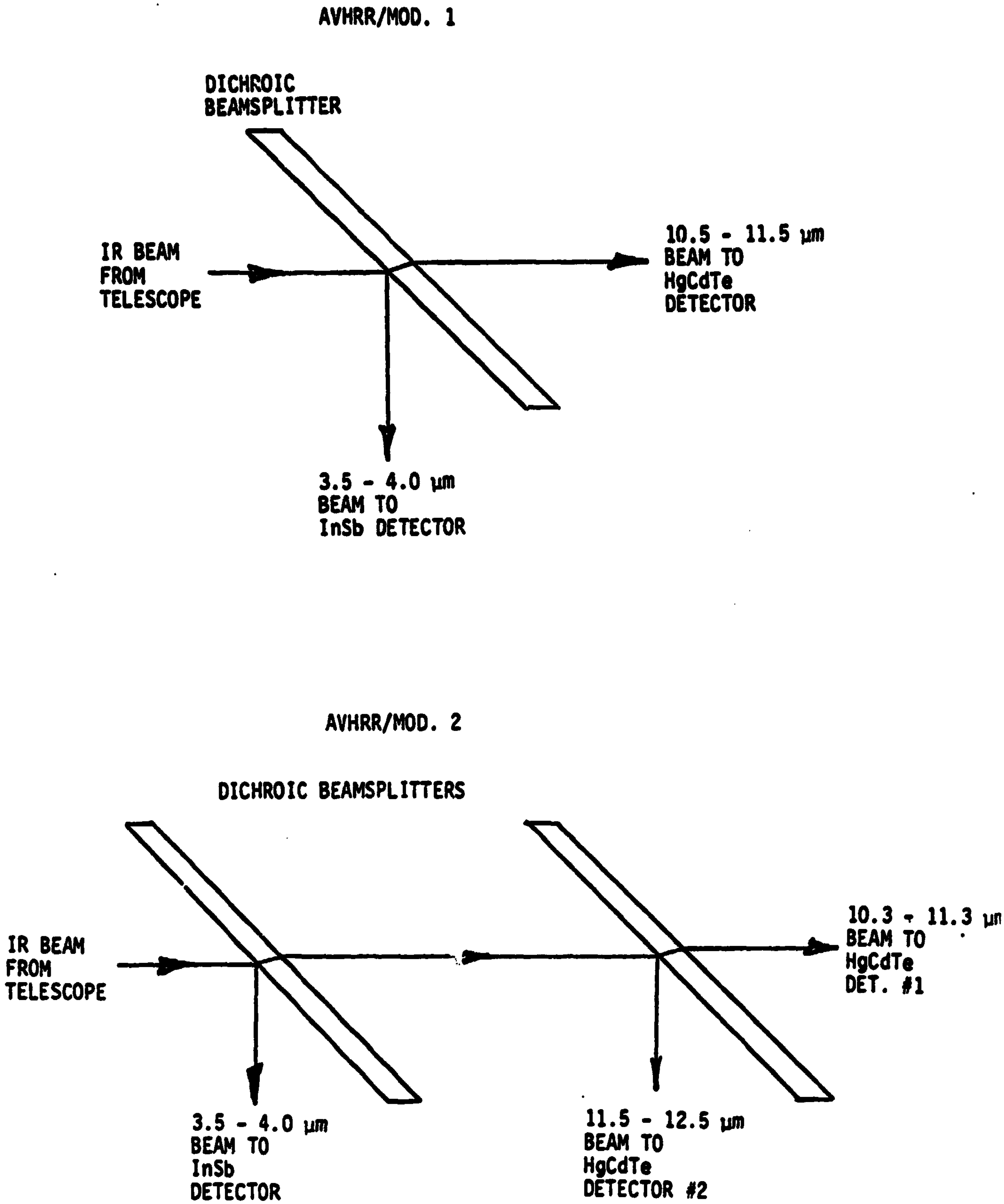


FIGURE 2-2 INFRARED DICHROIC BEAMSPLITTER ARRANGEMENT

M1 MIRROR,TELESCOPE PRIMARY
M2 MIRROR,TELESCOPE SECONDARY
D1 DICHROIC,THIN GOLD ON GLASS
M3,M4 FLAT FOLDING MIRRORS
L1 FAR-INFRARED FOCUS LENS
W1,W2 COOLER WINDOWS
D2/F3 INFRARED,DICHROIC & CHANNEL 3 FILTER
F1,F2,F4 BANDPASS FILTERS
L2,L3,L7 APLANAT LENSES
L4 FOCUS ACHROMAT LENS ASSY,CH.1
L5 FOCUS ACHROMAT LENS ASSY,CH.2
D3 BEAMSPLITTER,INCONEL
W3,W4 COOLER WINDOWS
D4 INFRARED DICHROIC
L6 FOCUS LENS,MID-INFRARED
F5 BANDPASS FILTER

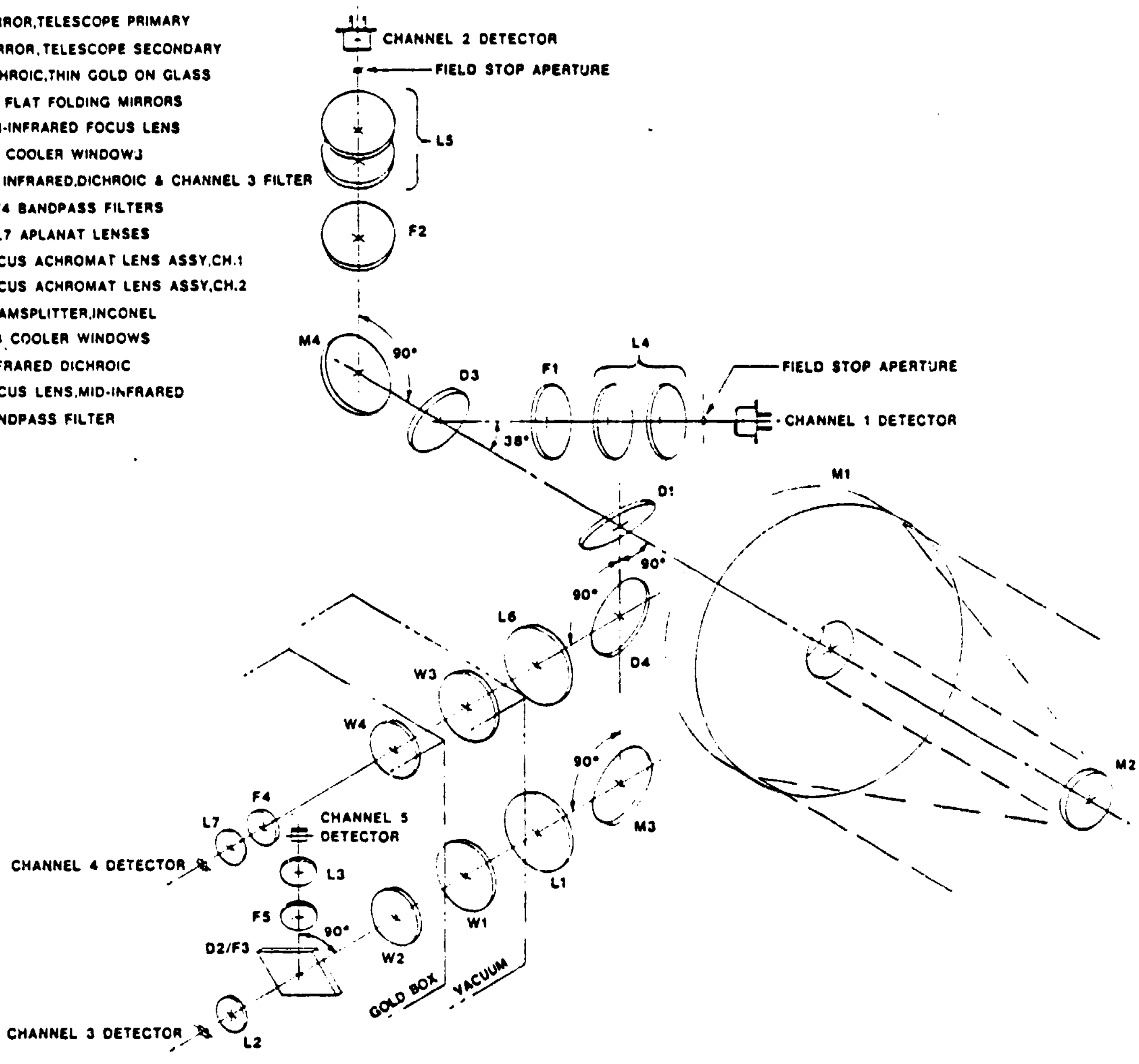


## AVHRR/2 OPTICAL CONFIGURATION

FIGURE 2-3

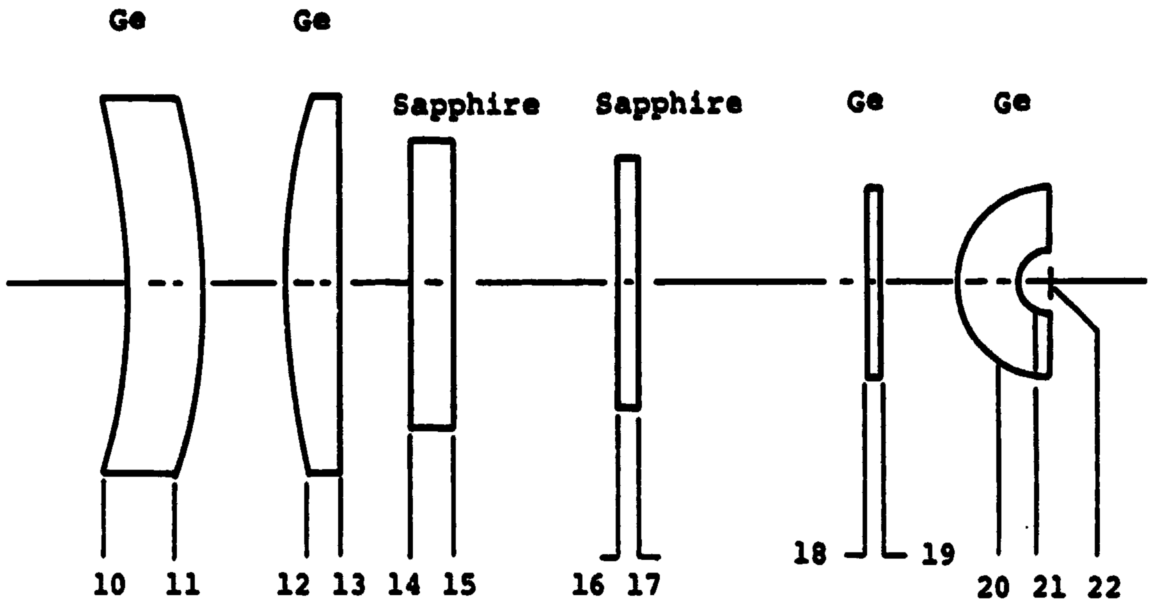


| SURFACE | RADIUS (m.m.) | AXIAL THICKNESS (m.m.) | HALF APERTURE (m.m.) |
|---|---|---|---|
| 10 | -101.905 | 6.364 | 19.716 |
| 11 | -91.542 | 17.283 | 20.619 |
| 12 | 135.471 | 6.353 | 18.832 |
| 13 | 255.382 | 23.898 | 18.113 |
| 14 | ∞ | 3.175 | 8.67 |
| 15 | ∞ | 11.681 | 8.22 |
| 16 | ∞ | 1.570 | 5.38 |
| 17 | ∞ | 2.990 | 5.16 |
| 18 | ∞ | 1.010 | 4.44 |
| 19 | ∞ | 1.143 | 4.38 |
| 20 | 3.900 | 2.997 | 3.55 |
| 21 | 1.930 | 1.570 | 1.53 |
| 22 | IMAGE PLANE, CHANNEL 4. | | |

* The two Ge lenses on the left are sized for the extended F.O.V., all others for Inst. F.O.V.

RELAY OPTICS FOR AVHRR/2, CHANNEL 4.

FIGURE 2 - 4

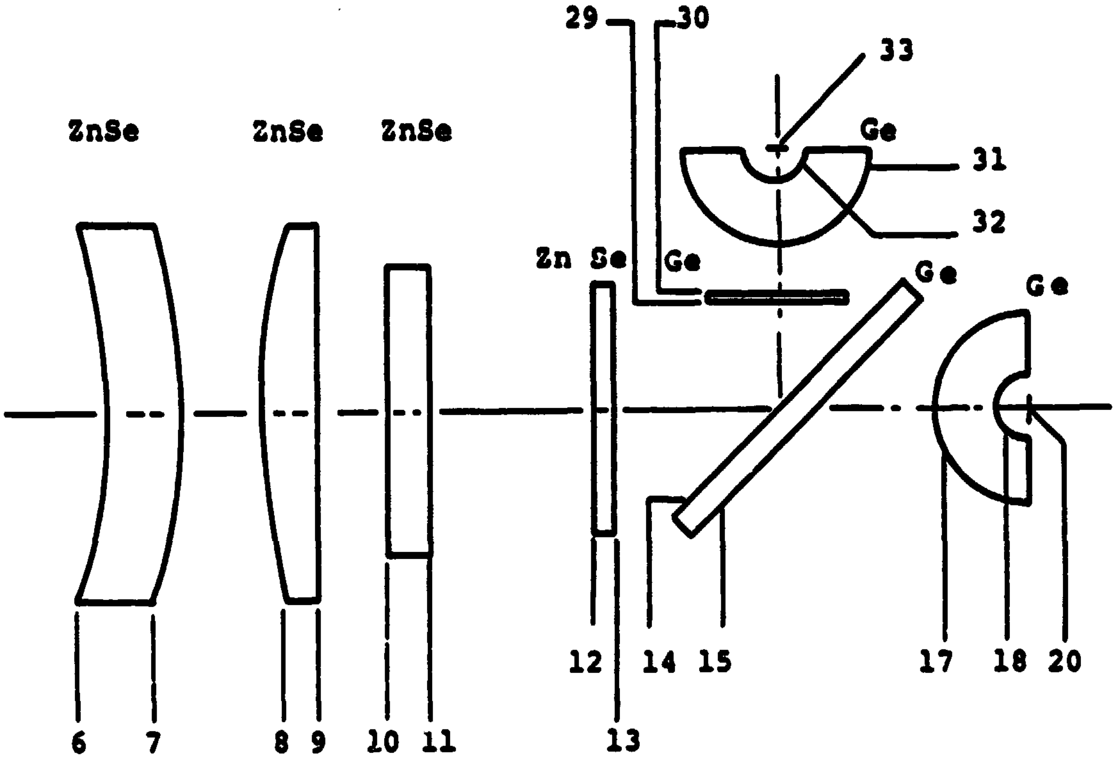


| SURFACE | RADIUS (m.m.) | AXIAL THICKNESS (m.m.) | HALF APERTURE (m.m.) |
|---|---|---|---|
| 6 | -57.92 | 7.00 | 20.64 |
| 7 | -65.481 | 15.00 | 22.20 |
| 8 | 108.189 | 7.00 | 23.17 |
| 9 | -597.276 | 4.363 | 22.73 |
| 10 | ∞ | 4.780 | 16.16 |
| 11 | ∞ | 17.404 | 15.67 |
| 12 | ∞ | 1.570 | 11.28 |
| 13 | ∞ | 15.255 | 11.12 |
| 14 | ∞ | 2.540 | ELLIP. |
| 15 | ∞ | 7.600 | ELLIP. |
| 17 | 4.580 | 2.997 | 4.47 |
| 18 | 2.800 | 2.480 | 2.49 |
| 20 | IMAGE PLANE, CHANNEL 3 | | |
| 14 | ∞ | 11.500 | ELLIP. |
| 29 | ∞ | 1.010 | 4.496 |
| 30 | ∞ | 0.254 | 4.434 |
| 31 | 3.900 | 2.997 | 3.685 |
| 32 | 1.928 | 1.653 | 1.621 |
| 33 | IMAGE PLANE, CHANNEL 5 | | |

* The two ZnSe lenses on the left are sized for the extended F.O.V., all others for Inst. F.O.V.

RELAY OPTICS FOR AVHRR/2 CHANNELS 3 & 5
FIGURE 2 - 5

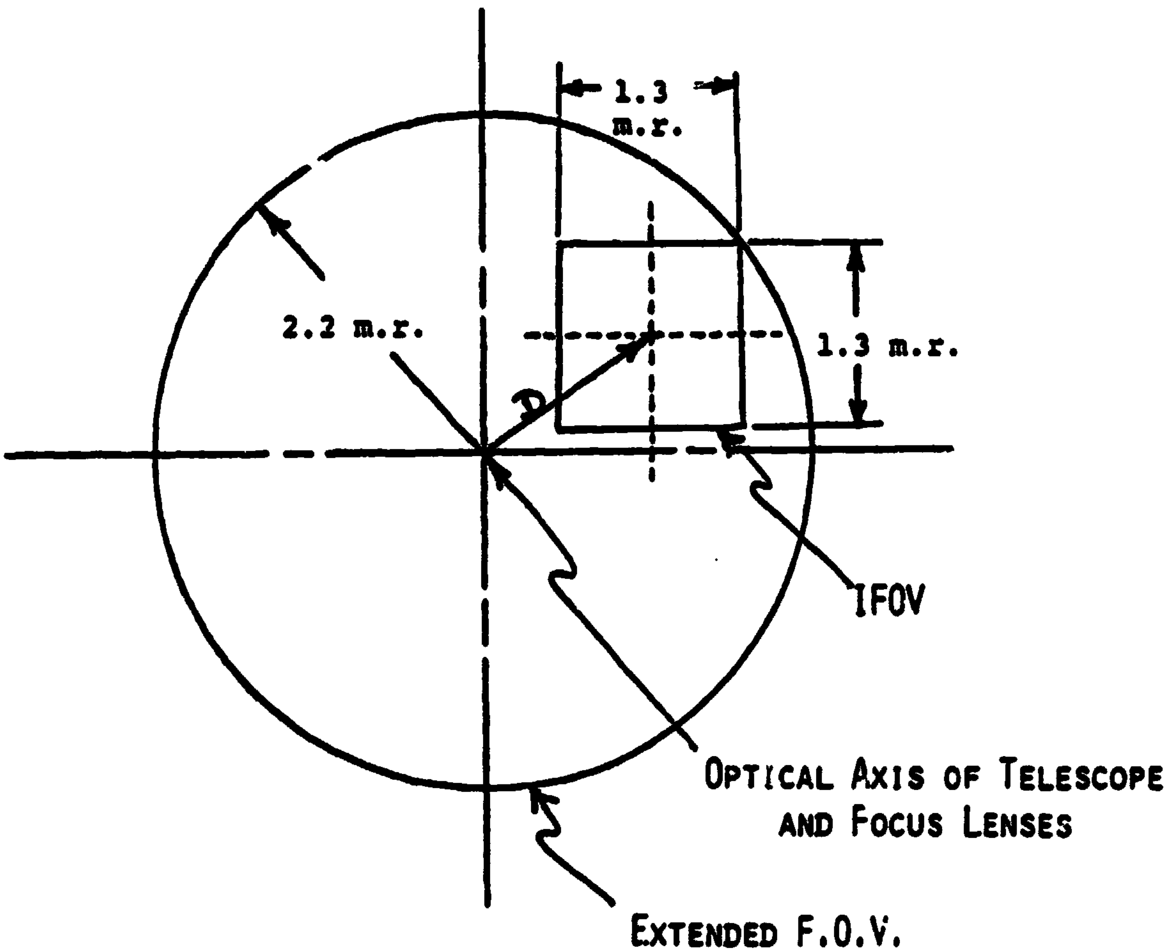


D = MAXIMUM APLANAT-DETECTOR OFFSET = 1.27 M.R.

D = 0.67 M.M. (=0.026")

ILLUSTRATION OF EXTENDED FOV FOR INFRARED
CHANNEL REGISTRATION (MAXIMUM OFFSET SHOWN)
FIGURE 2- 6

degradation. This relaxes the requirement for perfect optical and mechanical alignment. The maximum amount of infrared detector-aplanat assembly offset of each infrared channel without any vignetting occuring is 0.026"; the extended FOV for Channels 1 and 2 is the same as for AVHRR/1 and has proved to be adequate for registration.

The calculated optical performance for the infrared channels is given in Figure 2-7. The calculated performance of the AVHRR/2 infrared channels is generally as good or better than for AVHRR/1. The sine wave MTF for the three infared channels of AVHRR/2 is also given versus spatial frequency and target size in Figures 2-8, 2-9 and 2-10. The calculated performance is well above our internally specified minimum values in all cases. The measured optical performance of both the OTM and PFM met the internally specified limits.

## CHANNEL 3

| Spatial Frequency | On Axis Mod 1 | On Axis Mod 2 | IFOV Edge Mod 1 | IFOV Edge Mod 2 | EFOV Edge Mod 1 | EFOV Edge Mod 2 |
|---|---|---|---|---|---|---|
| 19 c/R | >99 | >99 | >99 | >99 | >99 | >99 |
| 256 c/R | 98 | 97.3 | 97 | 97.3 | 96 | 96.9 |
| 382 c/R | 97 | 95.5 | 95 | 95.8 | 94 | 94.6 |

## CHANNEL 4

| Spatial Frequency | On Axis Mod 1 | On Axis Mod 2 | IFOV Edge Mod 1 | IFOV Edge Mod 2 | EFOV Edge Mod 1 | EFOV Edge Mod 2 |
|---|---|---|---|---|---|---|
| 19 c/R | >99 | >99 | >99 | >99 | >99 | >99 |
| 256 c/R | 98.5 | 99.0 | 98 | 99.0 | 96 | 99.0 |
| 382 c/R | 97.7 | 98.2 | 97 | 98.2 | 94 | 98.2 |

## CHANNEL 5

| Spatial Frequency | On Axis Mod 1 | On Axis Mod 2 | IFOV Edge Mod 1 | IFOV Edge Mod 2 | EFOV Edge Mod 1 | EFOV Edge Mod 2 |
|---|---|---|---|---|---|---|
| 19 c/R | -- | >99 | -- | >99 | -- | >99 |
| 256 c/R | -- | 97.6 | -- | 97.6 | -- | 97.1 |
| 382 c/R | -- | 96.0 | -- | 96.0 | -- | 95.2 |

COMPARISON OF CALCULATED MTF FOR

AVHRR/1 & AVHRR/2

FIG. 2 - 7

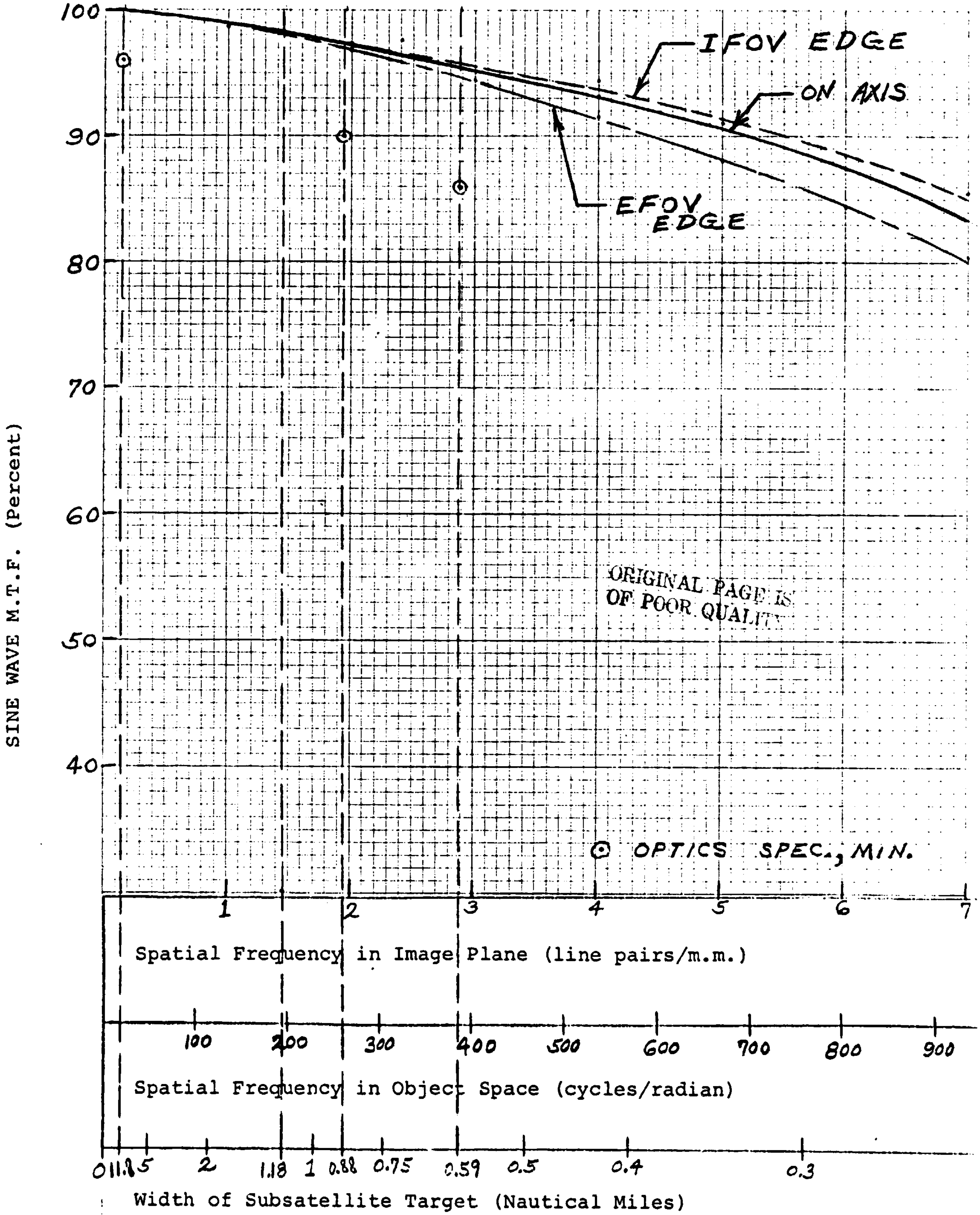


Channel 3 Optical M.T.F. vs. Spatial Freq. (or Tgt. Size)
FIGURE 2 - 8

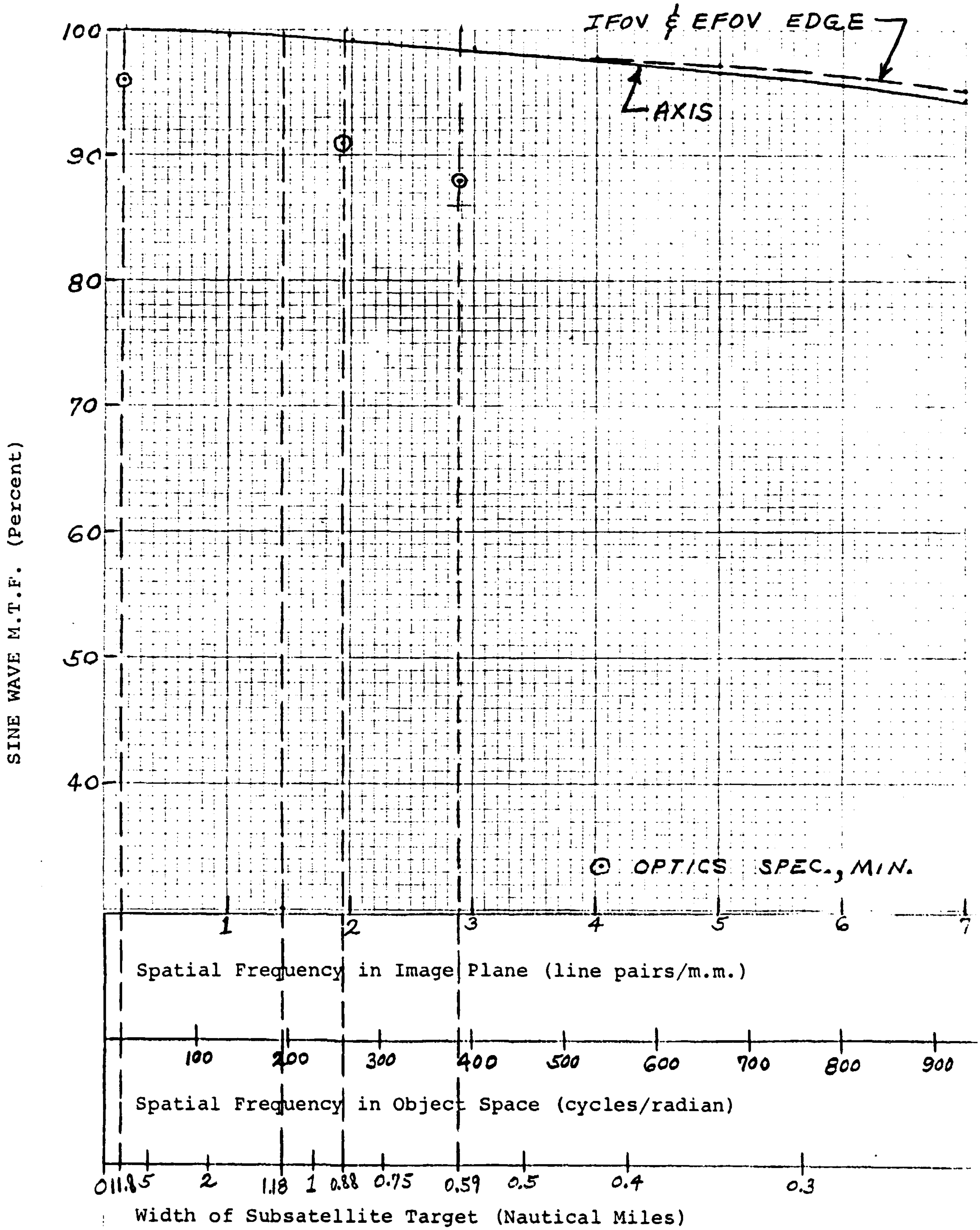


Channel 4 Optical M.T.F. vs. Spatial Freq. (or Tgt. Size)

FIG 2-9

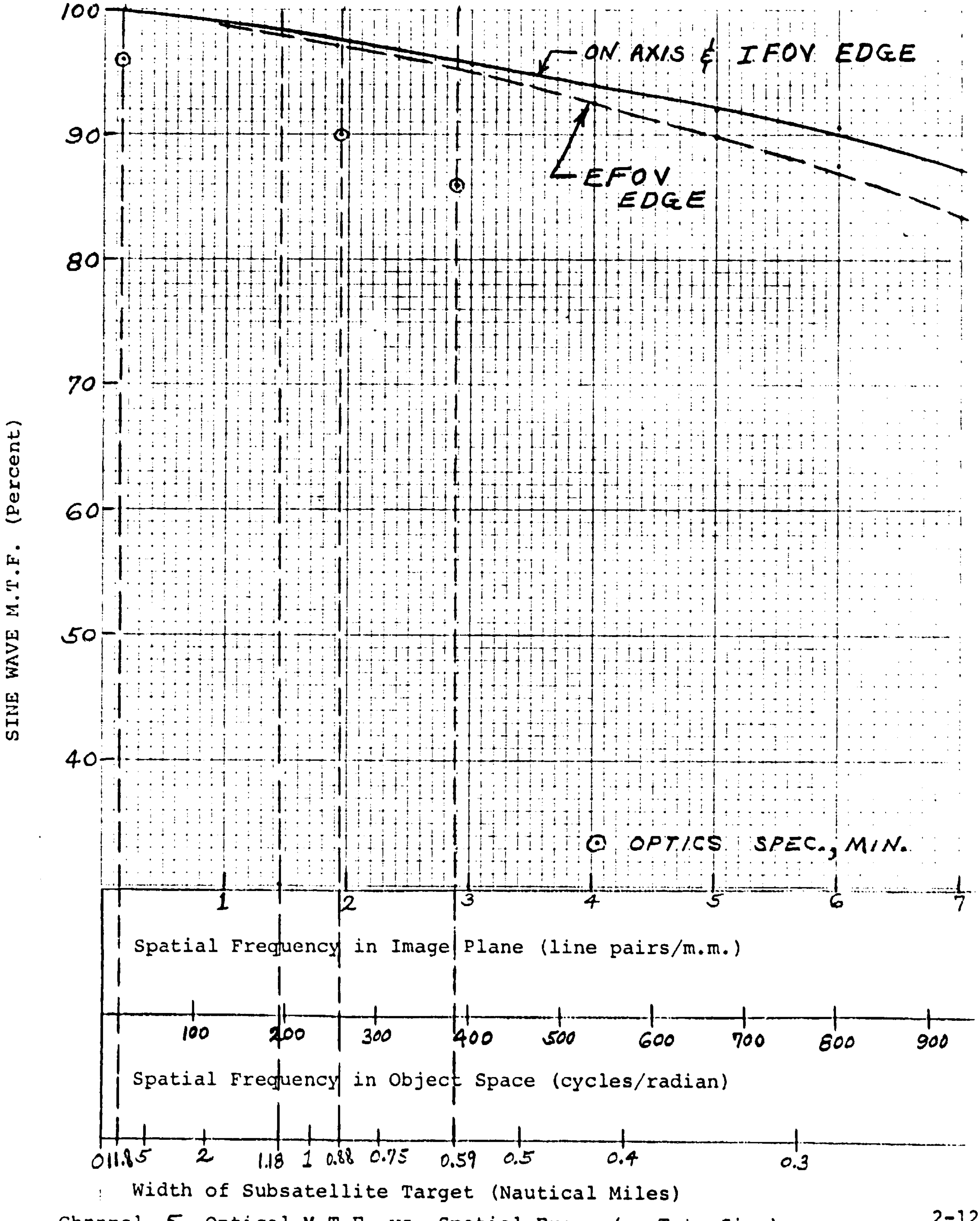


Channel 5 Optical M.T.F. vs. Spatial Freq. (or Tgt. Size)

FIG. 2 - 10

## 3.0 DETECTORS AND SENSITIVITY

In the infrared channels HgCdTe detectors are used in Channels 3 and 5 and an In Sb detector in Channel 4. These are purchased from outside manufacturers as indicated in Table 3-1 in accordance with detailed procurement specifications; some of the more pertinent performance requirements are also included in the table.

The sensitivity of the infrared channels can be expressed in terms of the NEΔT (noise equivalent temperature difference between two large targets scanned by the instrument which produces a change in output voltage equal to the r.m.s. noise output voltage. The equations used to calculate the NEΔTs from the AVHRR system parameters are found in Section 2.0 of the AVHRR/1 Technical Description document, Vol. 1 (Contract NAS5-21900). Using the detector detectivities and degradation factors listed in Table 3-2 for AVHRR/2, the NEΔT has been calculated for two values of optical system transmission for each infrared channel. The expected transmission ($\tau$) was obtained from typical measured data achieved on AVHRR/1 or, in the case of new components, values estimated to be realistic from past experience. The worst case transmission values listed in Table 3-2 is the product of the minimum specified transmission for each optical component given on the part procurement drawings. The expected and worst case NEΔT values given in Table 3-2 are the corresponding NEΔT values calculated from these two values of optical system transmission. The calculated worst case NEΔT values meet or exceed the specified instrument requirements for all three channels.

| Channel | 1 | 2 | 3 | 4 | 5 |
|---|---|---|---|---|---|
| Type | Silicon | Silicon | HgCdTe | InSb | HgCdTe |
| Manufacturer | IR Ind. | IR Ind. | Honeywell | Cincinnati Electronics | Honeywell |
| D* | -- | -- | $2.3 \times 10^{10}$ | -- | $2.3 \times 10^{10}$ |
| Responsivity | 0.37 A/W | 0.54 A/W | 5500 V/W | -- | 5500 V/W |
| Quantum Efficiency | -- | -- | -- | >0.75 | -- |
| Bias | -15 volts | -15 volts | 1.2 mwatt | ∿-15 mvolts | 1.2 mwatt |
| Size | 0.100 in | 0.100 in | 0.0068 in | 0.0068 in | 0.0068 in |

AVHRR/2 DETECTOR CHARACTERISTICS

TABLE 3-1

| PARAMETER | CH 3 | CH 4 | CH 5 | |
|---|---|---|---|---|
| DETECTOR D* | $2.3 \times 10^{10}$ | -- | $2.3 \times 10^{10}$ | $CMHZ^{\frac{1}{2}}W^{-1}$ |
| DEGRADATION FACTOR | 2.1* | 1.6 | 2.1* | |
| WORST CASE SYSTEM $\tau$ | .23 | .32 | .21 | |
| EXPECTED $\tau$ | .36 | .42 | .33 | |
| EXPECTED NE$\Delta$T | .08 | .05 | .09 | K @ 300K |
| WORST CASE NE$\Delta$T | .11 | .07 | .13 | K @ 300K |
| SPEC. NE$\Delta$T | $\leq$.12 | $\leq$.12 | $\leq$.13 | K @ 300K |

D* IS GUARANTEED MINIMUM AT 108K
CALCULATIONS ARE FOR NOMINAL SPECTRAL BANDPASS

*DEGRADATION FACTOR ACHIEVED IN CH 3 OF PFM WAS 1.6

AVHRR/2 THERMAL CHANNELS' SENSITIVITY PARAMETERS

TABLE 3-2 AVHRR/2 THERMAL CHANNELS' SENSITIVITY PARAMETERS

## 4.0 SPECTRAL RESPONSE

Channels 1, 2, and 4 of AVHRR/2 will be identical to the AVHRR/1 Flight Model responses. These are shown in Figure 4-1 thru Figure 4-3. The component changes in Channel 4 which could affect spectral response are the re-lacement of one mirror reflectance by a dichroic reflectance (which is flat between 3.5 and 4.0 microns) and the replacement of the Irtran 2 cooler windows by sapphire windows (having a more uniform spectral transmission).

The calculated spectral responses for Channels 3 and 5 O.T.M. instrument are given in Figure 4-4. It should be noted that an aplanat-detector incidence angle factor has not been incorporated into these calculated responses as was found necessary on the AVHRR/1 program to obtain agreement with measured data. The calculated responses indicate that no significant spectral overlap is anticipated; this occurs primarily because the bandpass filters manufactured by OCLI for Channel 3 were near the short wavelength limit of the allowable tolerance whereas Channel 5 filters are very near nominal values. The very steep cuton and cutoff slopes actually achieved on the manufactured filters also is responsible for the negligible spectral overlap.

Figure 4-5 shows the worse case spectral overlap between Channels 3 and 5 using idealized (trapezoidal) shaped response curves. The calculated worse case spectral overlap of 8.5% is not expected to cause any serious problem in data analysis even if it should get that large.

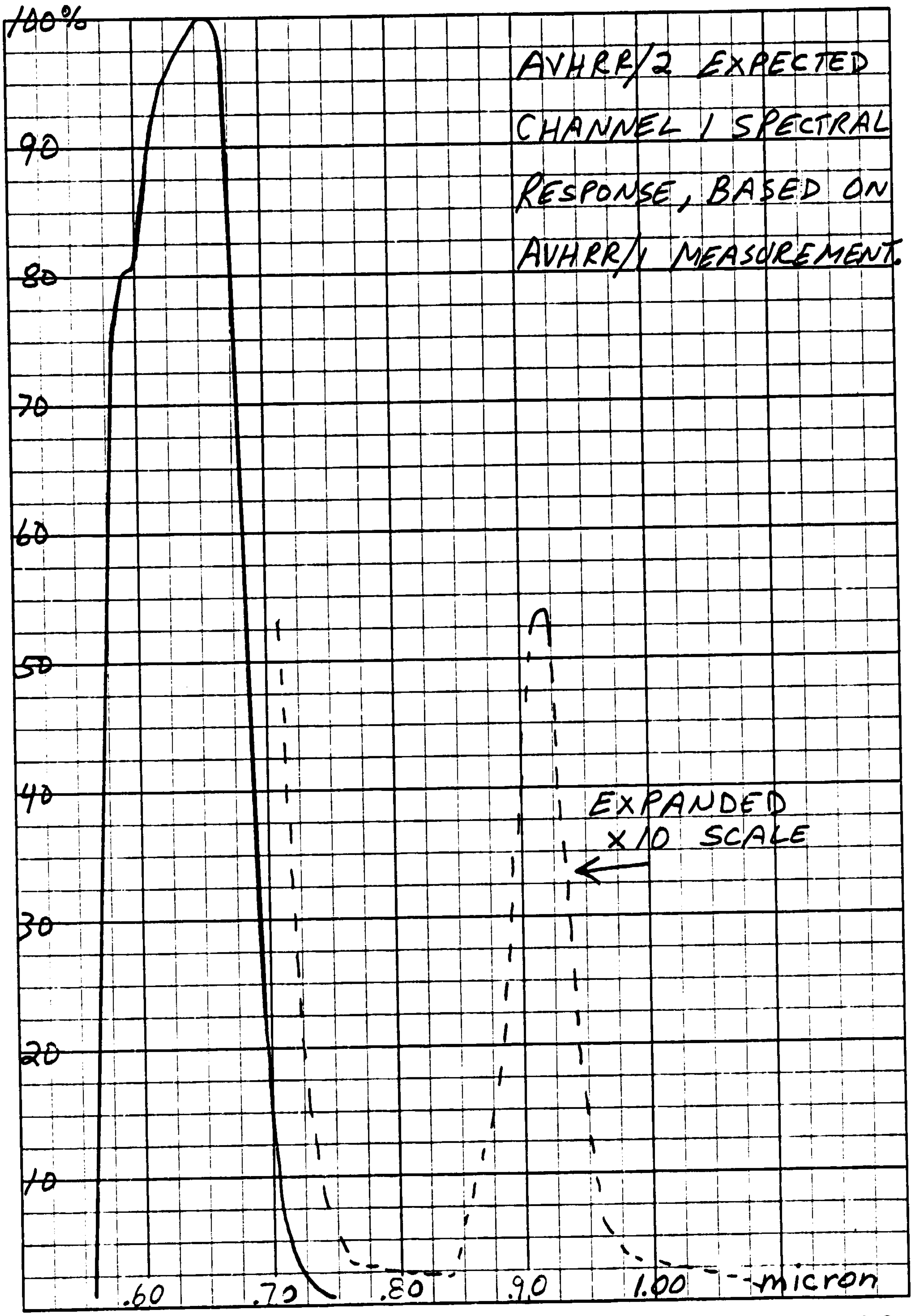
100%
90
80
70
60
50
40
30
20
10
AVHRR/2 EXPECTED
CHANNEL 1 SPECTRAL
RESPONSE, BASED ON
AVHRR/1 MEASUREMENT.
EXPANDED
X10 SCALE
.60
.70
.80
.90
1.00
micron

FIGURE 4 - 1

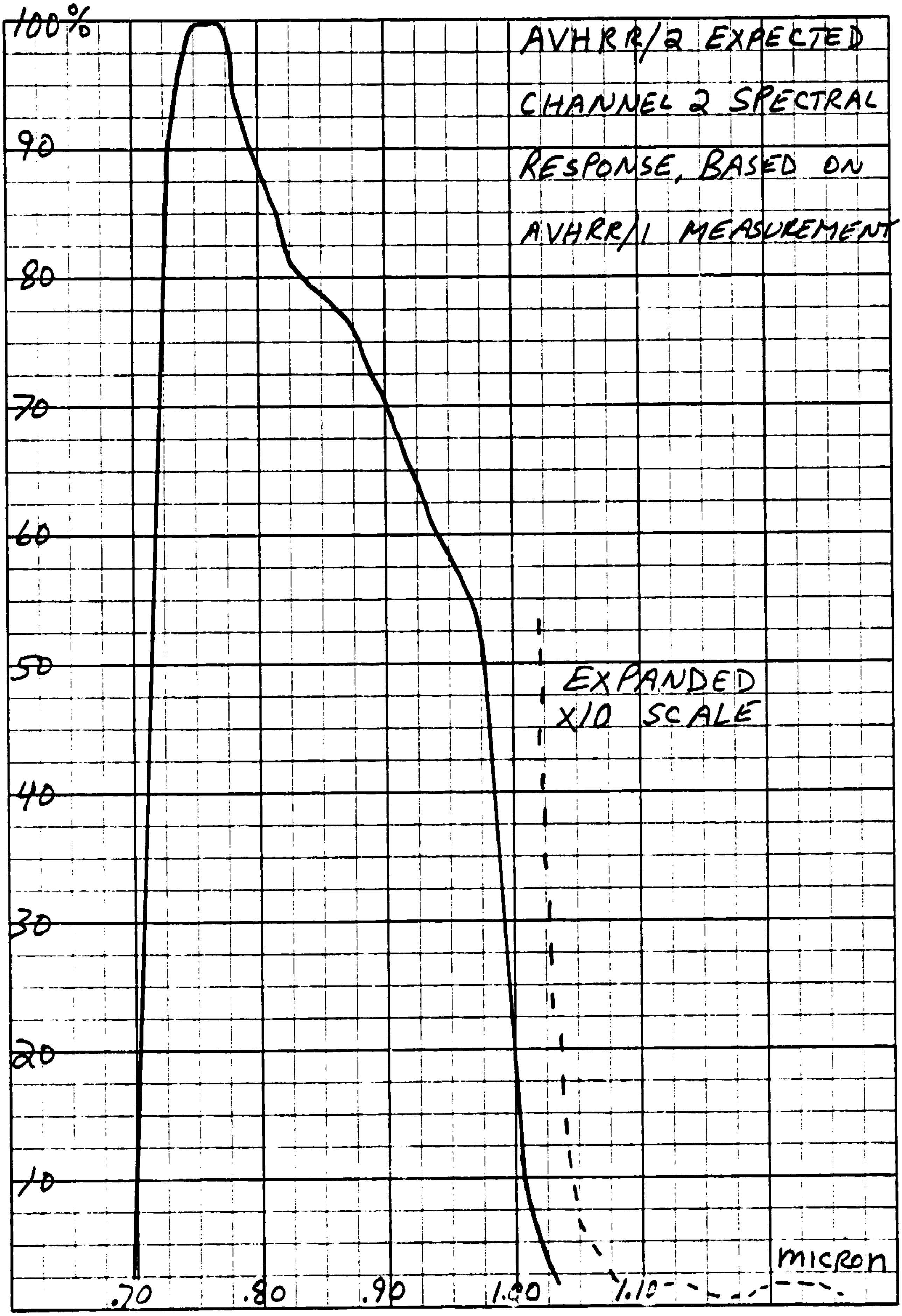
100%
90
80
70
60
50
40
30
20
10
.70
.80
.90
1.00
1.10
MICRON
AVHRR/2 EXPECTED CHANNEL 2 SPECTRAL RESPONSE, BASED ON AVHRR/1 MEASUREMENT
EXPANDED X10 SCALE

FIGURE 4 - 2

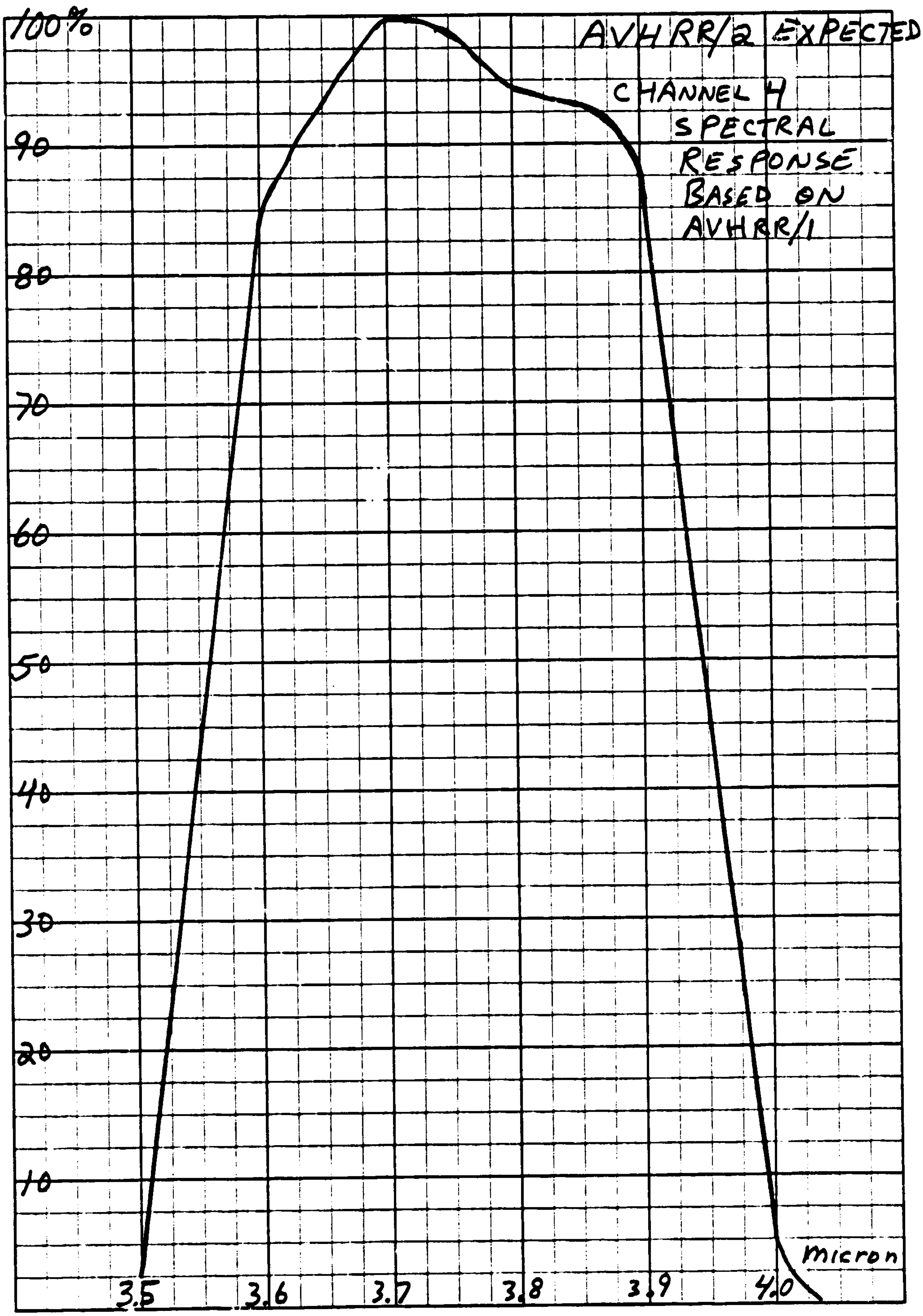
100%
90
80
70
60
50
40
30
20
10
3.5
3.6
3.7
3.8
3.9
4.0
micron
AVHRR/2 EXPECTED
CHANNEL 4
SPECTRAL
RESPONSE
BASED ON
AVHRR/1

FIGURE 4 - 3

AVHRR/2 O.T.M. CALCULATED SPECTRAL RESPONSE

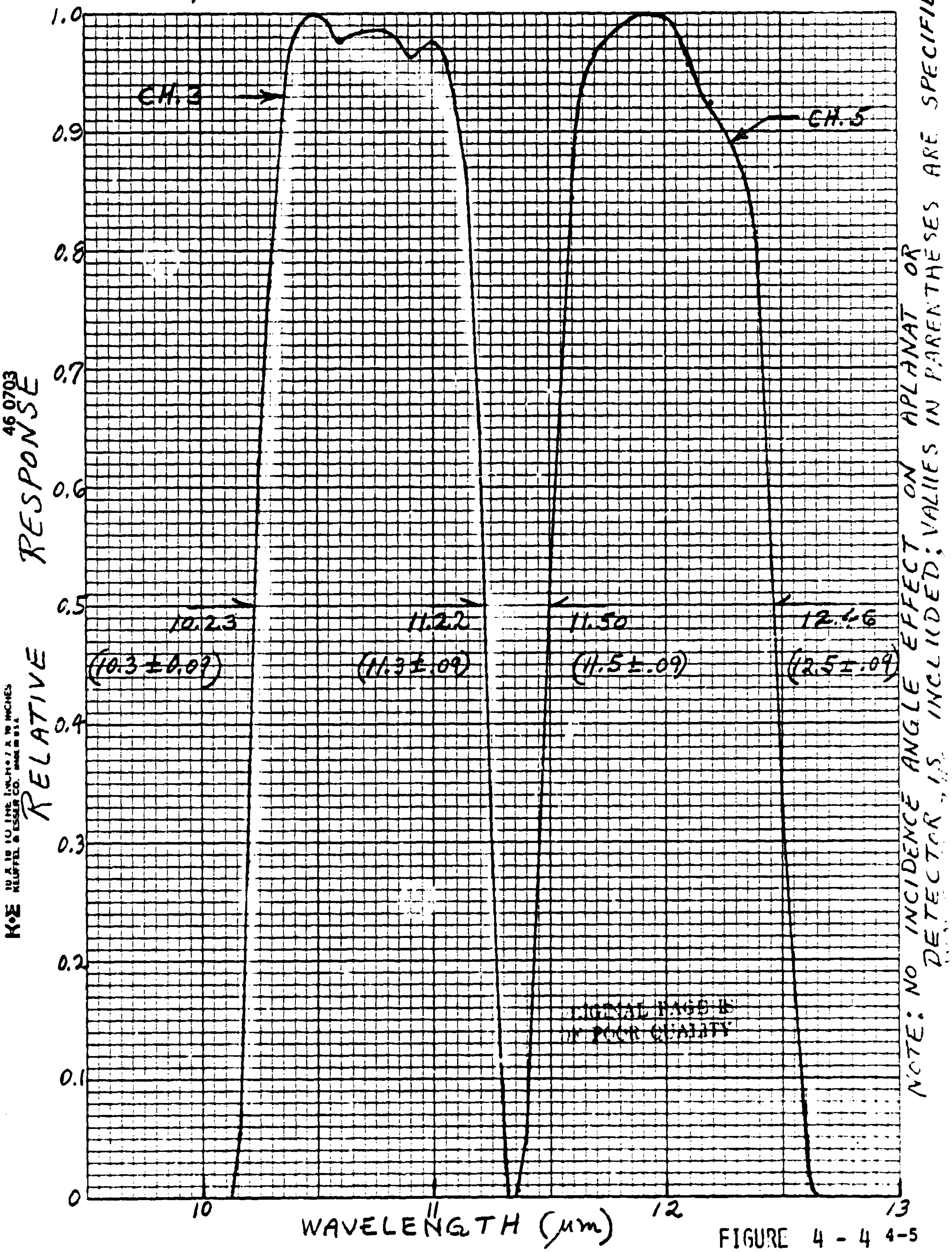


FIGURE 4 - 4

K•E 10 X 10 TO THE INCH • 7 X 10 INCHES KEUFFEL & ESSER CO. MADE IN U.S.A. 46 0703

Worse Case Spectral Overlap for 4% Slope & Idealized Response

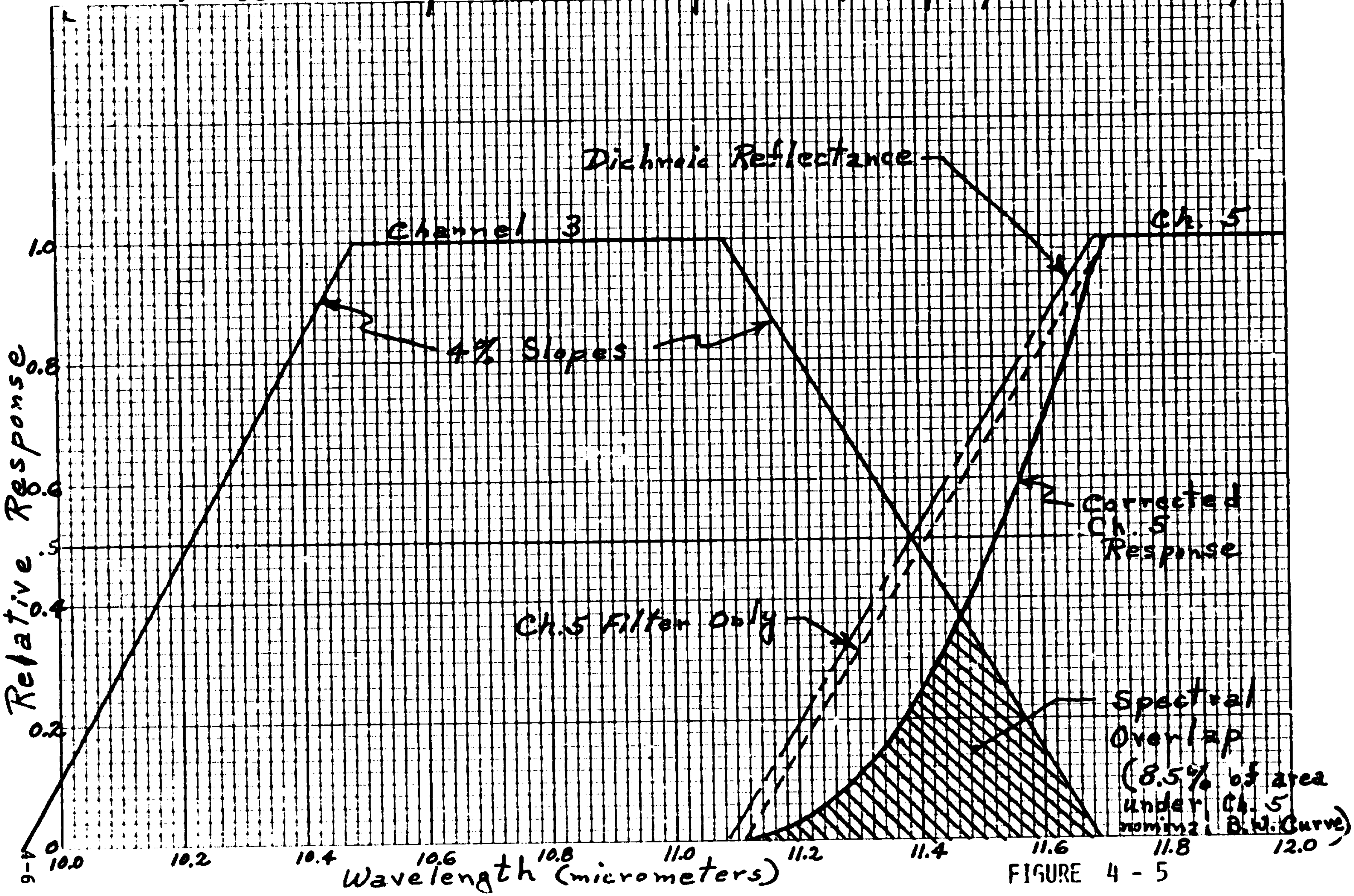


FIGURE 4 - 5

## 5.0 RADIANT COOLER

The basic design of the radiant cooler is unchanged from that used in Mod 1 (AVHRR Technical Description, Rev. B, Nov. 15, 1974, Section 6.0). In particular, we have preserved the design from AVHRR/1 to the maximum extent possible, consistent with the additional cool channel. As a result, the exterior of the cooler is unchanged from the Mod I design; this includes the earth shield, shield covers, and the radiating (black) areas for both stages. In addition, the rear surface of the radiator is insulated by means of a multilayer blanket, in the same manner as AVHRR/1. The common fronts on the coolers allow the use of a common bench cooler for both the four and five channel instruments.

The nominal characteristics of the radiant cooler for the AVHRR/2 are given in Tables 5.1 and 5.2. All the thermal predictions are based on the analytical model established on the Mod 1 program. The thermal influence of the third cooled channel shows up as changes in the optical port loadings from the second optical opening, as an increase in the insulated area on both stages that reflects the larger cooled optical assembly, and as an increase in the conductive input to the patch that reflects the large mass to be supported.

The thermal impact on the patch produced by the additional optical port is minimized by proper channel separation and spectral filtering. Thus Channels 3 and 5 (10.2 to 11.2μm and 11.9 to 12.9μm) share a common optical port to the cooler and are separated by a dichroic on the patch in the manner of Channels 3 and 4 in Mod 1. At the same time, the Zn Se radiator window is supplied with a band-pass filter (9.6μm — 13.2μm) that restricts the housing radiation that reaches the patch. The second optical port is used by Channel 4 (3.55 to 3.93μm). Here the use of a sapphire radiator window reduces the housing radiation that reaches the patch to a negligible value.

As a result of our experience on AVHRR/1, we have simplified the electrical wiring; all leads between the housing and radiator (first stage) are now copper and all leads between the radiator and patch (second stage) are nickel. The additional electrical leads (two to the third infrared sensor and two to the second heated radiator window) plus the change to all copper wires has increased the thermal conductance between the housing and the radiator from $1.905 \times 10^{-3}$ $Wk^{-1}$ to $2.237 \times 10^{-3}$ $WK^{-1}$.

The thermal analysis was carried out for an instrument base-plate regulated by the spacecraft louver system at a nominal 15°C. The corresponding cooler housing temperature is 17.5°C, while the infrared relay immediately in front of the cooler is at 20°C.

The result of the alterations in the optical chain is to actually reduce the optical port loading on the patch, from a nominal 25.3 mW in Mod 1 to 16.4mW in Mod 2. Part of this reduction is used to the added infrared detector bias (1.2 mW) and part for the additional conductive input (4.8 mW) from the additional mechanical support, additional electrical leads (2), and change to all nickel wires. The remainer ( 2.9 mW) partially offsets the increased insulation (rear) area on the patch and the increased radiator temperature (from its increased insulation area, thermal conductance, and optical port loading).

The in-orbit control power of 34.0 mW at the 105K control point corresponds to an uncontrolled temperature of 95.4K, so that the required thermal margin is achieved.

A detailed comparison of this prediction with the results of in-chamber tests on the Optical Test Model (OTM) of the radiant cooler is made in Section 5.5. When corrected to the nominal in-orbit conditions, the tests yielded a mean radiator temperature of 170.85K, a mean uncontrolled patch temperature of 97.0K, and a mean control power for operation at 105K of 29.05mW. The differences between the anlytical model and the test measurements are explored further in Section 5.5.

## 5.1 Cover Temperatures

Both the vertical and horizontal earth shields are insulated from external inputs by shield covers. The three optically polished shields are thermally and mechanically connected. However, the two vertical covers are not connected to the horizontal cover. The cover temperatures are determined by the thermal balance equation given in Figure 5.1 . The results are listed in Table 5.3 for the complete range of orbit normal to sun angles ($0^o$ to $68^o$) and for the nominal (833 km) and minimum (74 km) altitudes. The shading by the earth ends at a sun angle of $\beta_s = 90^o - \beta_e$, where $\beta_e$ is nadir to earth tangent line angle; the temperature of the horizontal cover is a maximum at this point. The nominal orbit (3:30 PM/8:30 AM) corresponds to a sun angle of $37.5^o$.

TABLE 5.3
Earth Shield Cover Temperatures

| | @ 833km ($\beta_e = 62.17^o$) | | | | @ 741km ($\beta_e = 63.61^o$) | | | |
|---|---|---|---|---|---|---|---|---|
| $\beta_s \rightarrow$ | $0^o$ | $27.83^o$ | $37.5^o$ | $68^o$ | $0^o$ | $26.39^o$ | $37.5^o$ | $68^o$ |
| Horizontal | 232.0 | 241.9 | 238.6 | 238.7 | 233.5 | 242.8 | 239.7 | 240.0 |
| Vertical | 167.8 | 187.4 | 190.1 | 195.7 | 170.2 | 188.4 | 191.5 | 197.0 |

All temperatures in kelvins.

TABLE 5.1
Nominal Characteristics of the Radiator (1st Stage)

| | | | |
|---|---|---|---|
| Temperature [a] | 168.8 | K | |
| Power radiated [a] | 1.590 | W | |
| Radiating area | | 55.2 $in^2$ | |
| Conductive input [a] | 0.272 | W | 17.1% |
| Insulation input [a] | 0.391 | W | 24.6 |
| Earth input | 0.198 | W | 12.5 |
| Covers input | 0.398 | W | 25.0 |
| Optical port input [a] | 0.331 | W | 20.8 |
| $dT/d\phi$ [b] | 2.14 | K/0.1W | |

(a) For housing 17.5°C, optics at 20°C.

(b) Rate of change of temperature with input power at temperature shown.

TABLE 5.2
Nominal Characteristics of the Patch (2nd Stage)

| | | |
|---|---|---|
| Temperature [a] | 105 K | |
| Power radiated | 96.6 mW | |
| Radiating area | 22.4 $in^2$ | |
| Conductive input [b] | 15.3 mW | 15.8 |
| Insulation input | 18.5 mW | 19.2 |
| Joule heat input | 3.5 mW | 3.6 |
| Optical port input | 16.4 mW | 17.0 |
| Shield input | 8.9 mW | 9.2 |
| Control power | 34.0 mW | 35.2 |
| $dT/d\phi$ | 0.32K $(mW)^{-1}$ @ 96K | |

(a) Nominal control point.

(b) Including effect of support shields.

Note: Values are for in-orbit operation.

Figure 5.1 Cooler Earth Shield Cover Thermal Balance Equation

$$\varepsilon_c \sigma T_c^4 = F_{ce} (\varepsilon_c W_e + \alpha_c W_r) + \alpha_c S_o < \sin i >,$$

where $\varepsilon_c$ = emissivity = 0.72 (silvered Teflon)

$\alpha_c$ = solar absorptivity = 0.08

$F_{ce}$ = view factor from cover to earth; $\sin^2 \beta_e$ for a horizontal cover and $\frac{1}{\pi} (\beta_e - \sin \beta_e \cos \beta_e)$ for a vertical cover, where $\beta_e$ is the mean angle from nadir to the earth-tangent line.

$<\sin i>$ = orbital average of the solar incidence angle, taken to be zero when the cover is shaded from direct sunlight; $\frac{1}{\pi} \sin \beta_s (1 - \sin \Delta u_e)$ for a horizontal surface and $\frac{1}{2\pi} \sin \beta_s (1 + \cos \Delta u_e)$ for a vertical surface.

$\Delta\mu_e$ = $\arccos (\cos \beta_e / \sin \beta_s)$; zero when $\sin \beta_s \leq \cos \beta_e$, i.e., when the spacecraft is in direct sunlight throughout its orbit.

$W_e$ = infrared exitance of earth = $2.1 \times 10^{-2}$ $Wcm^{-2}$

$W_r$ = reflected solar exitance of earth = $1.68 \times 10^{-2} \sin \beta_s$ $Wcm^{-2}$

$S_o$ = solar constant = 0.14 $Wcm^{-2}$

## 5.2 Radiator Thermal Analysis

The radiator and earth shield have a temperature, $T_r$, that is given in Figure 5.2. The thermal conductance, $K_r$, between the cooler housing and the first stage of cooling consists of $1.725 \times 10^{-3}$ $WK^{-1}$ from the synthane support tubes and $0.512 \times 10^{-3}$ $WK^{-1}$ from the copper electrical leads (2 leads of 0.0039 inch diameter and 18 leads of 0.0030 inch diameter, all with a free length of 3.15 inches).

The radiator temperature varies with sun angle and altitude as a result of changes in the direct load from the earth ($\phi_{er}$) and the indirect load from the shield covers ($\phi_{cr}$). The results are given in Table 5.4 for a nominal blanket insulation factor of 65; the nominal temperature (833 km, $\beta_s = 37.5^\circ$) is 168.8K.

TABLE 5.4

Radiator Temperatures

| $\beta_s \rightarrow$ | $0^\circ$ | $27.83^\circ/26.39^\circ$ | $37.5^\circ$ | $68^\circ$ |
|---|---|---|---|---|
| @ 833 km | 165.3 | 168.8 | 168.8 | 169.8 |
| @ 741 km | 166.2 | 169.5 | 169.7 | 170.7 |

Temperature in kelvins.

Nominal baseplate temperature ($15^\circ C$).

Nominal insulation blanket ($s_i = 65$).

To study the effect of the multilayer blanket on thermal performance, we varied its insulation factor to a minimum of 50 (experimental value on the AVHRR/1 breadboard model). The corresponding radiator temperatures are 171.2K in the nominal orbit and 173.2K in the worst case orbit.

Figure 5.2 Cooler First Stage Thermal Balance Equation

$$\varepsilon_r \sigma A_r T_r^4 = \phi_{er} + \phi_{cr} + \phi_i + \phi_k + \phi_o$$

where $\phi_{ab}$ = radiant power from a that is absored in b

$e$ = earth (infrared and reflected sunlight)

$r$ = black radiator, c = shield covers

$\phi_a$ = input from instrument through a

$i$ = multilayer insulation; k = supports and wires; o = optical port

$\phi_{er}$ = $F_{re}\ (\varepsilon_r W_e + \alpha_r W_r)\ A_r$

$\phi_{cr}$ = $\frac{\sigma A_c}{S_c}\ (T_c^4 - T_r^4) + K_c\ (T_c - T_r)$ for each cover

$F_{ab}$ = view factor from a to b; $A_a$ = area of a

$\varepsilon_a$ = emissivity of a; $\alpha_a$= solar absorptivity of a

$W_e$ = earth infrared exitance = $2.1 \times 10^{-2}$ $Wcm^{-2}$

$W_r$ = earth reflected sunlight exitance

= $1.68 \times 10^{-2} \sin \beta_s$ $Wcm^{-2}$; $\beta_s$ = orbit normal to sun angle

$A_c$ (horizontal) = 104 $in^2$; $A_c$ (2 vertical) = 7.5 $in^2$

$A_r$ = 55.2 $in^2$;

$F_{re}$ = 0.01837 (833 km), 0.02157 (741 km); computer calculations

$\varepsilon_r$ = $\alpha_r$ = 0.97(honeycomb cavity array covered with black paint)

$S_c$ = $\frac{2}{\varepsilon_c}$ -1; $\varepsilon_c$ = emissivity of gold plating on facing surfaces of shield and cover = 0.035.

$K_c$ = thermal conductance of supports between shield and cover

= $2.66 \times 10^{-3}$ $WK^{-1}$ (horizontal),

= $2.07 \times 10^{-3}$ $WK^{-1}$ (2 vertical)

$T_C$ = cover temperature

Figure 5.2 Cooler First Stage Thermal Balance Equation (Continued)

$$\Phi_i = \frac{\sigma A_i}{S_i} (T_h{}^4 - T_r{}^4); \; A_1 = 110 \text{ in}^2$$

$S_1$ = insulation factor of multilayer blanket between housing and radiator = 65 (nominal), 50 (minimum).

$T_h$ = housing temperature = 290.5K (17.5°C)

$\Phi_k$ = $K_r (T_h - T_r)$; $K_r$ = thermal conductance between h and r = $2.237 \times 10^{-3}$ $WK^{-1}$

$\Phi_o$ = 0.331 W (Section 5.4 )

## 5.3 Patch Thermal Analysis

The thermal balance equation for the patch is the solution to the equation described in Figure 5.3. The joule heat consists of 1.2 mW for each HgCdTe detector and 1.1 mW for the temperature sensor. The optical port loading is for a nominal baseplate temperature of 15°C and for an optics temperature of 20°C. The thermal conductance, $K_p$, between the radiator and patch consists of $1.414 \times 10^{-4}$ $WK^{-1}$ from the mechanical supports (3/16-inch OD x 5/32-inch ID and 2.00 inch free length) plus $0.630 \times 10^{-4}$ $WK^{-1}$ from the electrical leads (12,0.045-inch diameter nickel wires wound around the supports for 6.00 inches of free length).

The dual heat mode multiplier, M, was calculated by the technique described in the Technical Description of Mod 1 (Rev. B, Nov. 15, 1974, memorandum at the end of Section 6.0). A shield emissivity, $\varepsilon_s$, of 0.035 was used in the calculation and the analysis was carried out for the shield at the radiator temperature (i.e., the thermal gradient was evaluated at $x = \ell$).

The patch temperature varies with sun angle and altitude as a consequence of resultant variations in the radiator temperature. The results are given in Table . for a nominal radiator blanket insulation factor of 65; the nominal uncontrolled patch temperature is 95.4K, which corresponds to a control power of 34.0 mW at 105.0K.

TABLE 5.5
Patch Temperatures and Control Powers

| $\beta_s \rightarrow$ | 0° | 27.83°/26.39° | 37.5° | 68° |
|---|---|---|---|---|
| @ 833 km | 94.1(38.0)* | 95.4(34.0) | 95.4(34.0) | 95.8(32.9) |
| @ 741 km | 94.4(37.0) | 95.7(33.3) | 95.7(33.0) | 96.1(31.9) |

*Control power in milliwatts at 105.0K.

Temperature in kelvins; 15°C instrument baseplate; radiator insulation factor of 65.

For a minimum radiator insulation factor of 50, the nominal orbit uncontrolled patch temperature is increased from 95.4K to 96.3K (34.0 mW to 31.3 mW of control power) and the wrost case orbit uncontrolled patch is increased from 96.1K to 97.1K (31.9 mW to 28.9 mW). We will therefore have an in-orbit margin of greater than 10K with respect to the 108K control point under all conditions of spacecraft altitude, sun angle, and insulation factor.

The equation in Figure 5.3 does not include the input present during chamber testing as a result of reflection of the radiator power from the cold space target. Based on thermal tests and their analyses (Section 6.7 of the Mod 1 Technical Description) we estimate this input to be given by

$$7.5 \times 10^{-3} \left(\frac{T_r}{164}\right)^4 \text{ W}$$

for the 22.4 in² black radiating area. Under nominal conditions, this input is $8.42 \times 10^{-3}$W and increases the uncontrolled patch temperature to 98.0K, an increase of 2.6K.

$$\sigma\varepsilon_p A_p T_p^4 = \phi_s + \phi_k + \phi_i + \phi_j + \phi_o$$

where

| | | |
|---|---|---|
| $p$ | = | patch |
| $s$ | = | earth shield (upper side) |
| $k$ | = | thermal conductance including the influence of radiative inputs from the support shields |
| $i$ | = | gold-to-gold radiative insulation |
| $j$ | = | joule heat of detectors and temperature sensor |
| $o$ | = | optical port |
| $\phi_s$ | = | $\sigma\varepsilon_p\ \varepsilon_s A_p F_{ps} T_r^4$ |
| $\phi_k$ | = | $M\ K_p\ (T_r - T_p)$; $M$ = dual mode multiplier |
| $\phi_i$ | = | $\frac{\sigma A_i}{S_i}(T_r^4 - T_p^4)$; $S_i = \frac{2}{\varepsilon_i} - 1$ |
| $\phi_j$ | = | $3.5 \times 10^{-3}$ W |
| $\phi_o$ | = | $8.21 \times 10^{-3} + 8.214 \times 10^{-12}\ (T_r + 9K)^4$ W (Section 5.4 ) |
| $\varepsilon_p$ | = | 0.97 (black paint on honeycomb cavity array) |
| $\varepsilon_s$ | = | 0.035 (vacuum deposited aluminum) |
| $\varepsilon_i$ | = | 0.035 (gold plate) |
| $A_p$ | = | 22.4 $in^2$ ; $A_i$ = 41 $in^2$ |
| $F_{ps}$ | = | 0.3948 (computer calculation, including second reflections) |
| $K_p$ | = | $2.044 \times 10^{-4}\ WK^{-1}$; $M = 1.17$ |

Figure 5.3 Cooler Second Stage Thermal Balance Equation

## 5.4 Optical Port Loading

The optical port loading was calculated from an analytical model developed on the Mod 1 program (AVHRR Technical Description, Rev. B, Nov. 15, 1974, Section 6.8). This model is based on three separate thermal tests of the radiant cooler. The dimensions and opening materials for Mod 2 are shown in Figure , together with the resultant view factors. These data can be used to calculate the optical loading on the radiator and patch for each of the optical ports in Mod 2.

The optical loading on the radiator is given by

$$\Phi_{or} = \varepsilon_1 \sigma T_O^4 A_1 \left[ F_{12}'(1 - P_2) + (1 - F_{12}') \right]$$

where $A_1$ equals $\pi r_1^2$ and $p_2$ is the fraction of housing temperature radiation passed by the radiator window. The radiator window for Channels 3 and 5 is Zn Se coated with a bandpass filter that transmits from 9.6 to 13.2 μm. The radiator window for Channel 4 is sapphire. The corresponding values of $p_2$ are 0.23 and 0.03. The emissivity, $\varepsilon_1$, of the housing window is for greybody radiation emitted by the housing window or transmitted through the window from the optics. In Channels 3 and 5, the housing window is Zn Se and $\varepsilon_1$ is 0.9. In Channel 4, the housing window is sapphire and $\varepsilon_1$ is 0.6 (See Thermal Properties of Matter, Y.S. Touloukian and D. P. DeWitt, IFI/Plenum, 1972).

The emission temperature $T_O$ in Channels 3 and 5 is that of the relay optics or 293K(20°C); the emission temperature in Channel 4, however, is that of the housing window or 290.5K (17.5°C).

We then have

$$\Phi_{or} \text{ (Chs. 3 and 5)} = 0.277\text{W, and}$$

$$\Phi_{or} \text{ (Ch. 4)} = 0.054\text{W.}$$

The optical port loading on the patch consists of inputs from the ambient instrument optics and the radiator. We will restrict the radiator input to that from the inner window itself; radiation at the radiator temperature (i.e., the cold trap) is efficiently absorbed in the window. The input from the instrument to the patch is given by

$$\Phi_{13} = \varepsilon_1 \sigma T_O \; P_2 \tau_2 F_{31} \gamma_3 A_3$$

where $\tau_2$ is the transmittance of the inner window for greybody radiation at the temperature $T_O$ and where $\gamma_3$ is the effective absorptivity of the patch opening. For Channels 3 and 5, $\tau_2$ is 0.9 and $\gamma_3$ is 0.773 (experimental value from Mod 1). For Channel 4, $\tau_2$ is 0.95 and $\gamma_3$ is 0.9. For Channels 3 and 5, $p_2$ is again 0.23. In the case of Channel 4, $\tau_2$, $P_2$, and $\gamma_3$ are for the narrow spectral band (3.55 to 3.93μm) that is absorbed in the patch. (The patch opening is occupied by the spectral filter for Channel 4). As a result, the effective value of $p_2$ for the patch opening of Channel 4 is $9.12 \times 10^{-4}$ .

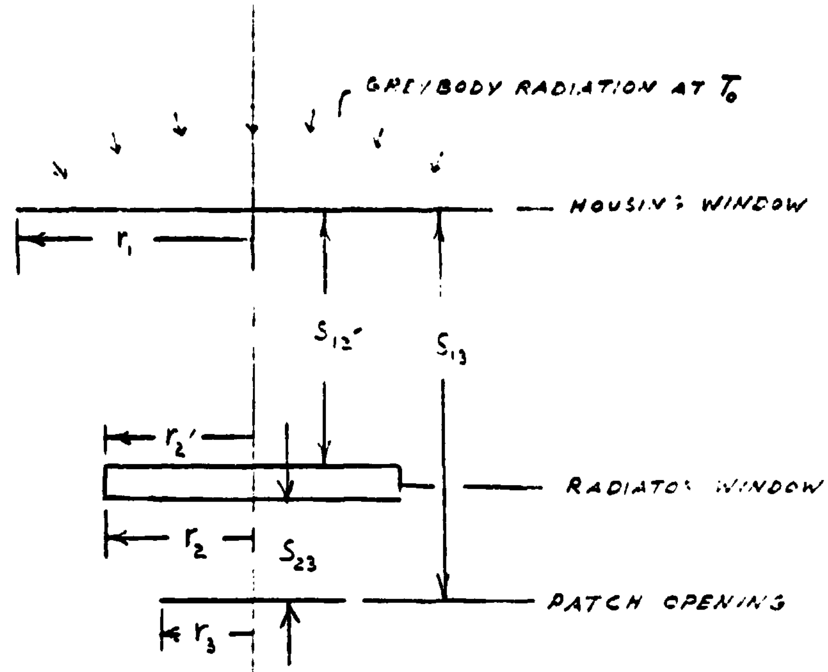


| | $r_1$ | $r_2$ | $r'_2$ | $r_3$ | $S_{13}$ | $S_{23}$ | $S_{12'}$ |
|---|---|---|---|---|---|---|---|
| Ch 3 & 5 | 15.77 | 11.37 | 11.77 | 10.96 | 19.05 | 1.27 | 15.35 |
| Ch 4 | 8.43 | 5.49 | 5.89 | 5.19 | 13.32 | 1.27 | 9.525 |

| | $F_{12'}$ | $F_{31}$ | $F_{32}$ | $F_{33'}$ |
|---|---|---|---|---|
| Ch 3 & 5 | 0.248 | 0.361 | 0.921 | 0.6675 |
| Ch 4 | 0.190 | 0.265 | 0.829 | 0.434 |

NOTE: $F_{1j}$ = view factor from area i to j

| | Housing Window | Radiator Window | Patch Opening |
|---|---|---|---|
| Ch 3 & 5 | Zn Se | Zn Se with bandpass | Optical elements and gold baffle |
| Ch 4 | Sapphire | Sapphire | Spectral filter |

(Dimensions in millimeters)

Figure 5.4 Dimensions and Opening Materials for Optical Port

Moreover, the input to Channel 4 as well as to Channels 3 and 5 is now from the relay at +20°C, so that we have

$$\Phi_{13} \text{ (Chs. 3 and 5)} = 8.21 \times 10^{-3}\text{W, and}$$

$$\Phi_{13} \text{ (Ch. 4)} = 6.9 \times 10^{-6} \text{ W.}$$

The input to the patch from the inner window attached to the raidator is given by

$$\Phi_{23} = \sigma T_w^4 \varepsilon_2 F_{32} \gamma_3 A_3$$

The window temperature, $T_w$, is a nominal 9K above the radiator. For an inner window of ZnSe and for greybody radiation at the window temperature, the window emissivity, $\varepsilon_2$, is approximately 0.45 (Y.S. Touloukian and D. P. DeWitt, op. cit.) and the effective patch absorptivity is still 0.773 (Channels 3 and 5). For an inner window of sapphire, $\varepsilon_2$, is about 0.5. The effective absorptivity, $\gamma_3$, of the patch opening in Channel 4 was calculated from

$$\gamma_3 = \frac{\alpha_3}{1 - \rho_2(1 - \alpha_3) F_{33'}}$$

where $\alpha_3$ is the actual absorptivity of the patch opening (spectral filter and $\rho_2$ is the (specular) reflectance of the inner window, both for the window radiation. For a sapphire radiator window and a germanium patch opening, we have $\alpha_2 = 0.63$ and $\rho_2 = 0.5$, so that $\gamma_3 = 0.685$. The thermal loads on the patch from the radiator windows are therefore

$$\Phi_{23} \text{ (Chs. 3 \& 5)} = 6.852 \times 10^{-12}(T_r + 9K)^4$$

$$\Phi_{23} \text{ (Ch. 4 )} = 1.362 \times 10^{-12}(T_r + 9K)^4$$

Thus, the total optical port loading on the radiator and patch are, respectively,

$$\Phi_{or} = 0.331 \text{ W, and}$$

$$\Phi_{or} = 8.21 \times 10^{-3} + 8.214 \times 10^{-12}(T_r + 9K)^4 \text{ W.}$$

## 5.5 OTM Cooler Thermal Tests

Chamber tests on the AVHRR/2 OTM radiant cooler were run in the period from February 28 to March 2, 1977. Two tests were run, one at a control point of 103.4K and a second at 108.3K. The results are listed in the first column of Table 5.6; the second column shows these measurements corrected to in-orbit operation under nominal conditions. The corrections are based on the analytical model of the radiant cooler (to be contained in the AVHRR/2 Technical Description), which predicted the temperatures listed in the third column.

We see that the cooler meets the specified requirement for a 10K margin at a 108K control point with about 1K to spare. To correct from chamber to nominal in-orbit conditions, we first used the measured temperatures to calculate an effective insulation factor for the multilayer blanket on the rear surface of the radiator. This was done by using the nominal thermal characteristics in the analytical model for everything but the blanket itself. The results are listed in the first column of Table 5.7; they show an average insulation factor of 51.5.

In retrospect, however, it is not fair to compare this value with that attained on the AVHRR/1. In particular, the insulation factor includes the net effect of heating the radiator windows, and in AVHRR/1 this effect is quite small. A nominal power of 0.050W is applied to each window; most of this is conducted into the radiator through the polyimide isolator. This input, however, is offset by radiant emission from the radiator optical port (chiefly from the cold trap back into the housing). We estimate the net input on the AVHRR/1 to amount to 0.020W. This corresponds to a radiator temperature change of 0.42K or an insulation factor change of about 2.3 or 4%. In the AVHRR/2, we have about the same input at the radiator optical port of Channels 3 and 5. However, the Channel 4 port is not an effective emitter and introduces a net load of approximately 0.044W into the first stage of cooling. If this is subtracted from the insulation input derived from the chamber tests, we find that the insulation factor increases to the values listed in the second column of Table 2 or to an average value of 58.0. This is less than the 65 achieved on recent models of the AVHRR/1, but it is nevertheless a very good value in view of the additional optical port and the resultant increase in the complexity of the multilayer blanket.

TABLE 5.6

AVHRR OTM Radiant Cooler THERMAL Performance

| | Chamber Test | | Analytical Model |
|---|---|---|---|
| | Measured | Corrected | Predicted |
| $T_h$ | 3.3°C | 17.5°C | 17.5°C |
| $T_o$ | 13°C | 20°C* | 20°C* |
| $T_r$ | 167.7K, 167.4K | 171.0K, 170.7K | 168.8K - 173.2K |
| Uncontrolled $T_p$ | -- -- | 96.9K, 97.1K | 95.4K - 97.1K |
| Controlled $T_p$ | 103.4K, 108.3K | 105K | 105K |
| Control Power | 22.04mW, 41.04mW | 29.4mW,28.7mW | 34.0mW - 28.7mW |
| Joule heat | 1.46mW | 3.5mW | 3.5mW |

T = temperature

h = cooler housing

o = optics

r = radiator

p = patch

* Except for Channel 4 input to radiator which is at 17.5°C.

TABLE 5.7

INSULATION FACTOR OF RADIATOR
(AVHRR/2 OTM)

| Test No. | Insulation Factor $S_i$ Uncorrected | Insulation Factor $S_i$ Corrected to -/1 Condition |
|---|---|---|
| 1 | 50.7 | 57.0 |
| 2 | 52.3 | 59.0 |

Returning now to our approach to the calculation of nominal in-orbit performance from the chamber test results, we next used the analytical model with the experimentally determined insulation factor to predict the radiator temperature under nominal orbital conditions. As shown in Table 5.6, the result is approximately 171K, which is in the middle of the predicted range of about 169K to 173K.

We then used the analytical model to predict all the in-chamber thermal loads on the patch. This prediction includes the measured control power and calculated radiant input from the first stage produced by reflection off the imperfect cold space target. It is also based on the measured radiator temperature and the nominal thermal properties used in the patch analytical model. The predicted chamber heat load was then compared with the calculated power emitted at the measured patch temperature. We found that the emitted power exceeded the predicted inputs by an amount we term the excess input ($\Phi_x$). The value of $\Phi_x$ varied from 2.07 mW at the 103.4K control point to 3.21 mW at the 108.3K point.

There are three potential sources of the excess heat load. The first is the inaccuracy contained in each measurement of temperature and power. The second is the inaccuracy in each term used in the analytical model; the prime suspect here is probably the optical port loading. And the third is the failure to attain a steady-state equilibrium in the cooler and its surroundings; in this case, the actual performance is better than that measured. In terms of temperature increments on the patch, the excess inputs correspond to 0.6K and 1.0K at 97K or 0.5K and 0.8K at 105K. Most of the increase (1.14 mW) in excess input between the two control points shows up in the control power. Thus the analytical model predicts that the control power should increase by 20.0 mW between 103.4K and 108.3K, whereas, the measured increase was 1.0 mW less (19.0 mW).

And finally, the calculated in-orbit radiator temperature was combined with the derived value of $\Phi_x$ to correct the measured patch temperature to orbital conditions. The corrected values were based on the predicted in-orbit optical temperature ($T_O$ in Table 5.6), the projected joule heat (3.5 mW; the 1.46 mW during the tests was dissipated in the temperature sensor), and the absence of a space target input.

## 6.0 MECHANICAL DESCRIPTION

The AVHRR/2 instrument, basically, is the same as the AVHRR/1 instrument with the exception of the 5th optical channel. The addition of the 5th optical channel required the following mechanical changes.

1. Redesign of relay optics to accommodate 5th channel.
2. Change patch to accommodate additional channel.
3. Slight change in radiator for the additional channel.
4. Addition of window and header in vacuum housing.
5. Baseplate modification to raise cooler.
6. Additional P.C. board and preamp module.
7. Slight size and weight increase.

The following paragraphs describe the changes required for the above seven items.

### 6.1 Relay Optics

The relay optics for the AVHRR/2 has been changed to add another I.R. channel, and, in addition, the folding optical assemblies are being retained in a more positive manner.

An additional I.R. focus lense was added directly above the existing I.R. focus lense which necessitated an increase in height of the relay optics housing of 1.94 inches (Figures 6-1 and 6-2).

The folding assemblies of the relay optics on the /1 design were retained in the optics housing by setscrews and the injection of RTV between the outer sleeve of the assembly and the relay optics housing. As a result of vibration testing, a clamp was added to the inside of the Channel 2 folding element to further restrain it during vibration (Figure 6-1). Structural adhesive was also applied around the periphery between the sleeve and the relay optics housing of Channel 2 folding mirror assembly and Channels 3 and 4 folding mirror assembly.

All of the above features were retained in the /2 design, and, in addition, a clamp, similar to the one used on Channel 2, has been added to Channel 3/5 lens assembly (Figure 6-2).

It was physically impossible to restrain the gold beam-splitter, neutral density and I.R. dichroic assemblies by the use of clamps, so two threaded holes have been added to the spacers of these assemblies and screws have been added to aid in alignment and retention of the assemblies (Figures 6-1 and 6-2.).

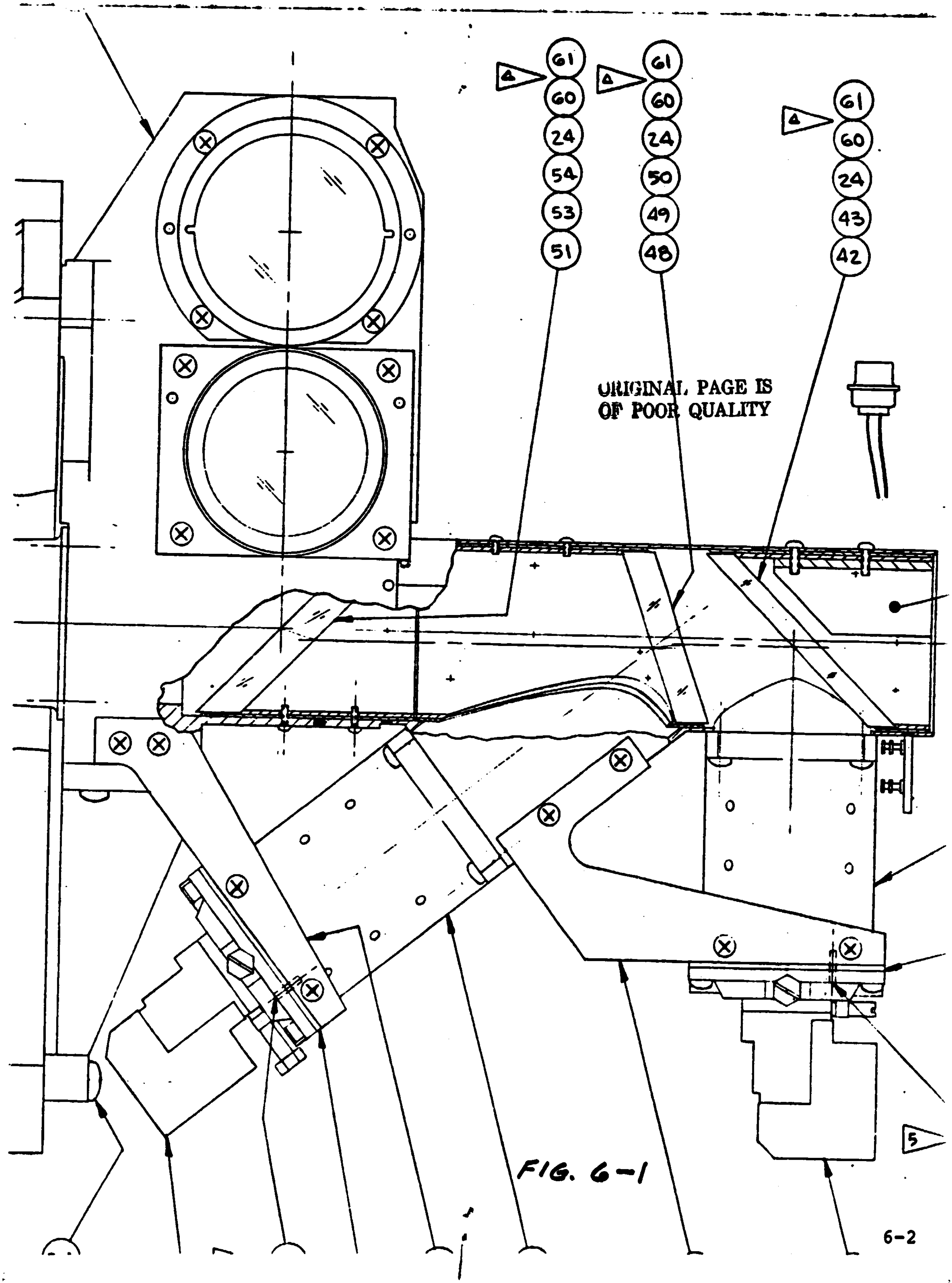


ORIGINAL PAGE IS
OF POOR QUALITY

FIG. 6-1

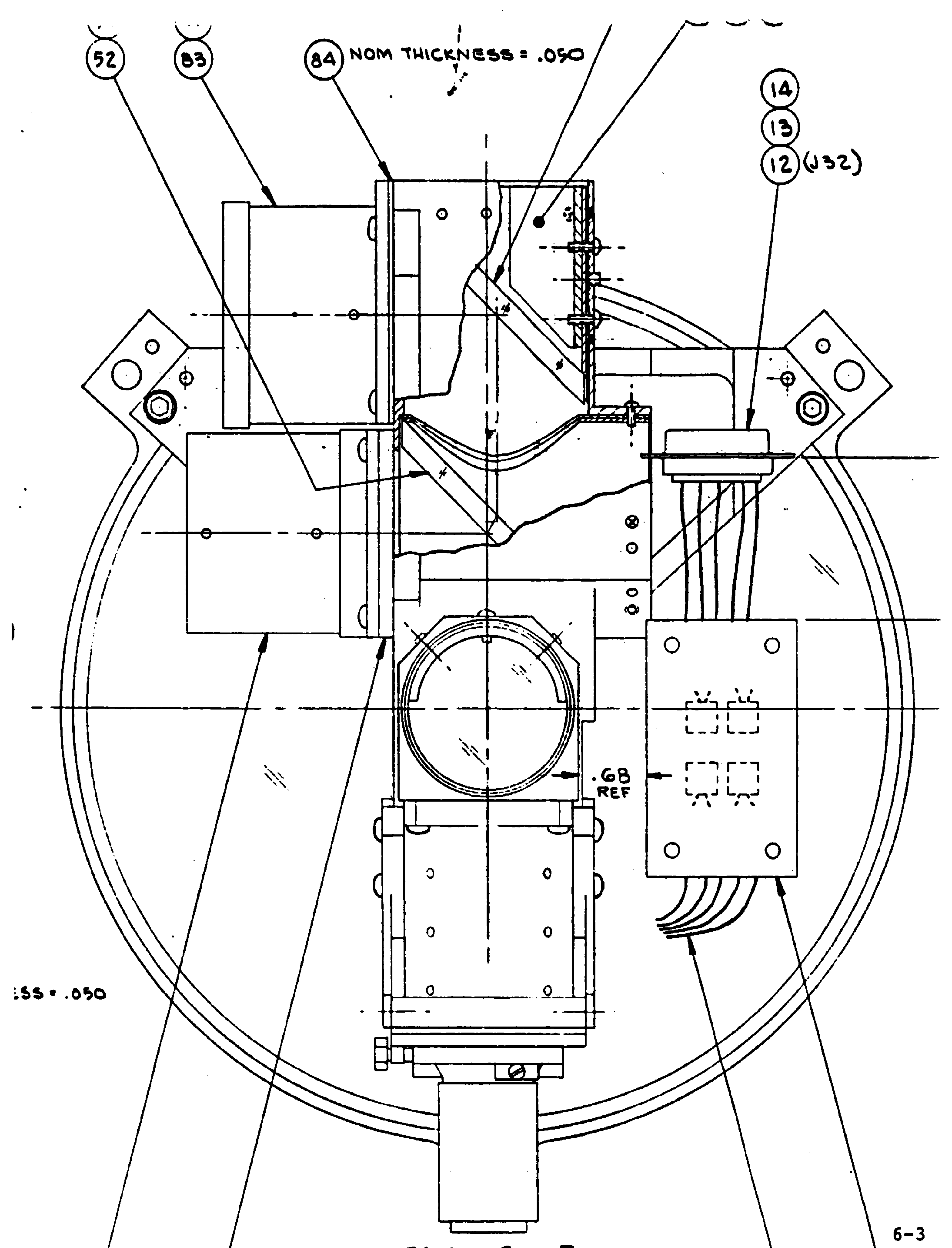


FIG. 6-2

## 6.2 Patch

The patch configurations has changed in several ways as can be seen in Figure 6-3. On the /1 design, the detectors and dichroic mounted on a frame that in turn mounted in an enclosure that mounted to the patch (Figure 6-4). The /2 design incorporates the detector frame and the enclosure into one piece. The detector mounting frame has also been rotated 90° and an additional detector for the added channel has been placed on the frame. With the new /2 configuration, Channels 3 and 5 share the same focus lens (new focus lense that was added) and Channel 4 utilizes the other focus lense. The patch support rods have been shortened .7 inch, and have been moved apart to compensate for the added mass during vibration.

Four small solid polurethane snubbers have been added to the patch to aid in reducing the tranmissibility to the patch during vibration. The snubbers are ¼ inch diameter and are located in the four corners of the patch. When the earth shield door is closed, the snubbers are designed to rest against the door, thereby limiting the patch excursion during vibration. The patch has seen the highest Q levels during the Y axis of vibration, however, the snubbers have proven to be very effective in reducing these levels.

## 6.3 Radiator

Minimal changes were made to the radiator. An additional window was added for the fifth optical channel and one radiator support rod was moved to allow room for the increased detector frame size.

## 6.4 Vacuum Housing

The vacuum housing for the /2 design has also changed very little. In addition to the added window for the fifth optical channel, a removable header plate was added to the back surface of the housing to make the assembly and trouble shooting easier. The flange size of the vacuum housing remains the same as /1 and will mount to /1 bench cooler.

## 6.5 Baseplate

The /2 baseplate is basically the same as /1 with the exception of a few minor changes. One change adds a mounting base between the baseplate and the cooler. This baseplate adapter, as it is called, accomplishes two objectives. One, it raises the cooler assembly the requited height for proper alignment with the added optical channel, and secondly, it provides for easier alignment of the cooler with the optical channels. Another minor change was made to the in-flight black body calibration target area of the baseplate. This change was made to simplify the machining and assembly of the baseplate target area.

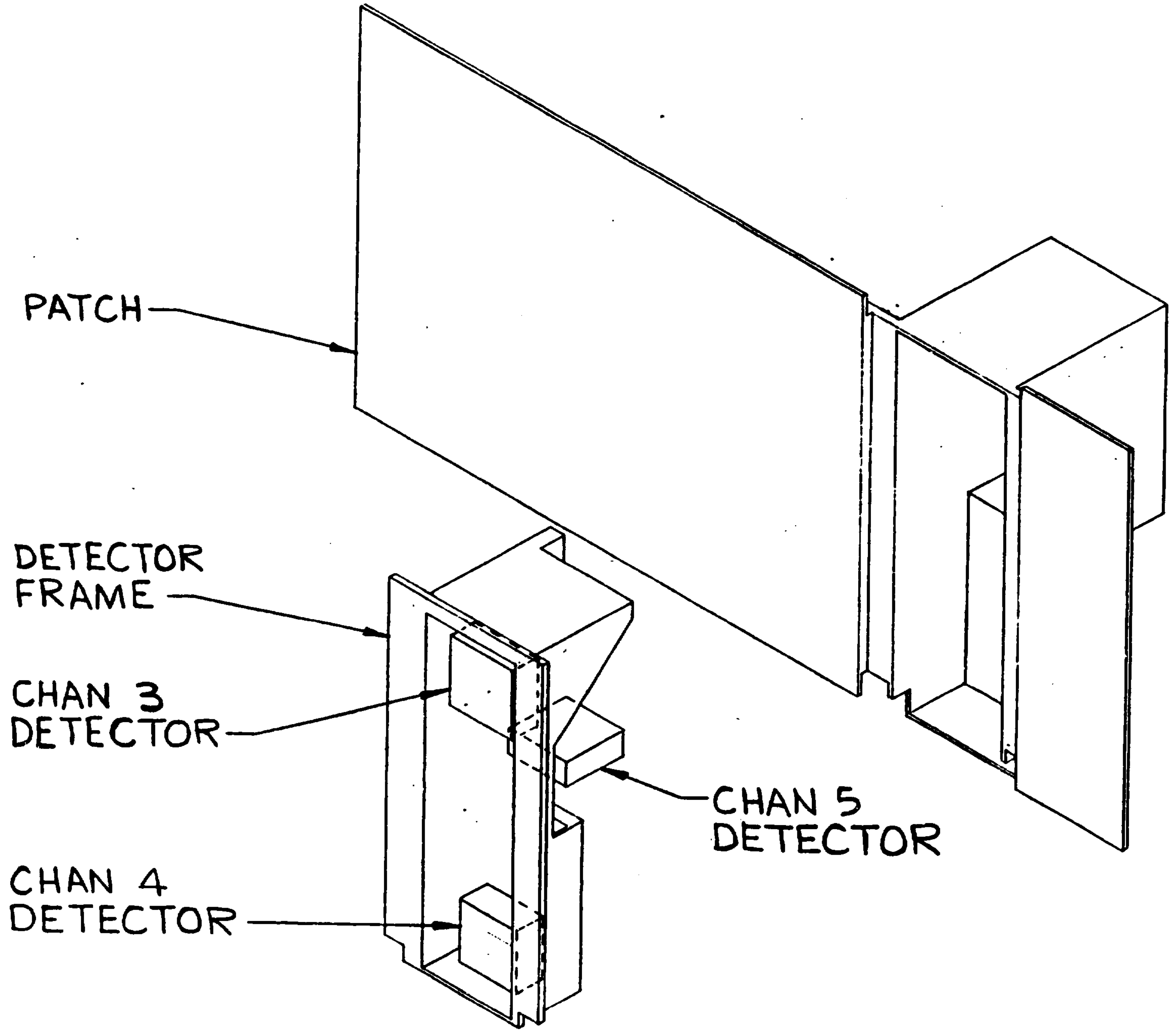
PATCH
DETECTOR FRAME
CHAN 3 DETECTOR
CHAN 4 DETECTOR
CHAN 5 DETECTOR

FIG. 6-3

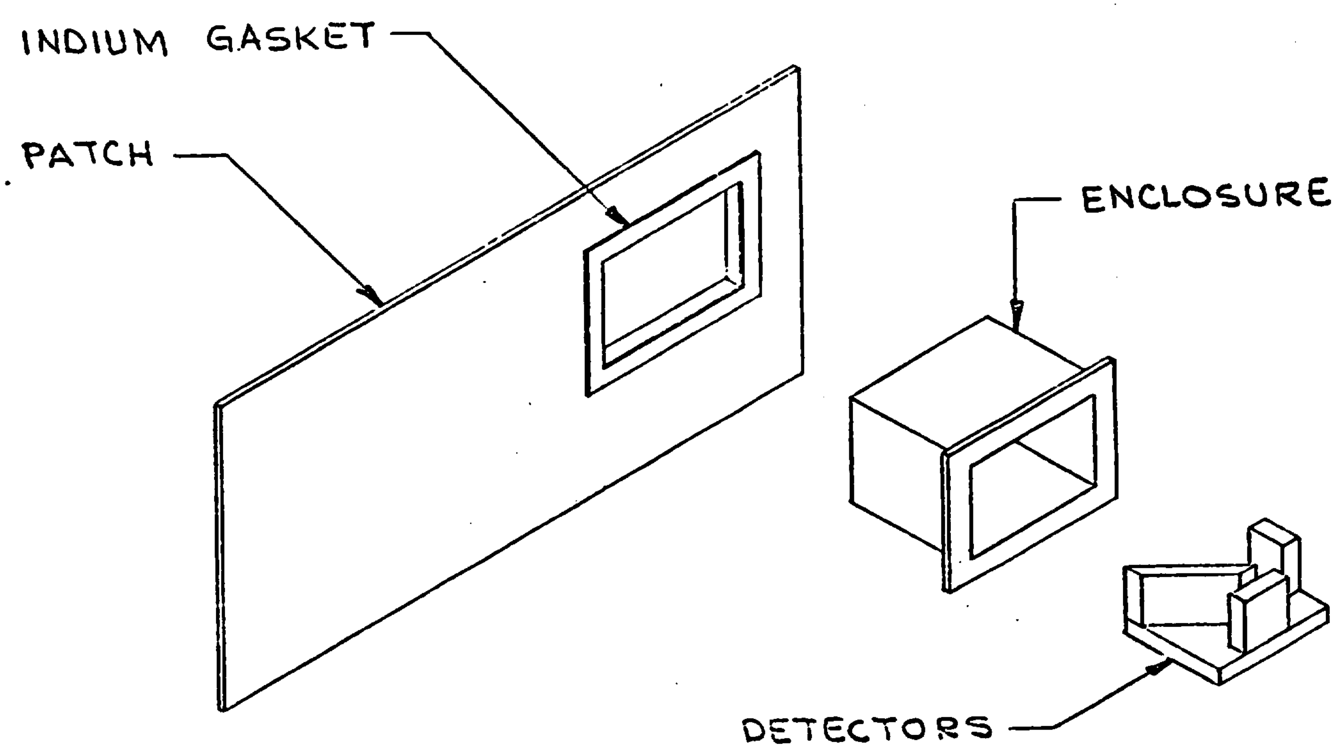


/1 PATCH DESIGN

FIG. 6-4

## 6.6 Electronics Module

The electronics module was extended approximately 1-3/8" in length to provide room for Channel 5 post amplifier p.c. board. Figure 6-5 shows the difference between the /1 and /2 designs. As can be seen in the figures, the A to D Converter was moved from the end wall of the electronics module to the side wall to make room for post amplifier board. Figure 6-5 also shows the location of the added Channel 5 pre-amplifier.

## 6.7 Size and Weight

The size of the AVHRR/2 is 30.25" x 11.19" x 14.31" without the Thermal blanket. The instrument weighs 63.31 lbs. with Thermal blanket installed.

The outline drawing of the instrument is shown in Figure 6-6.

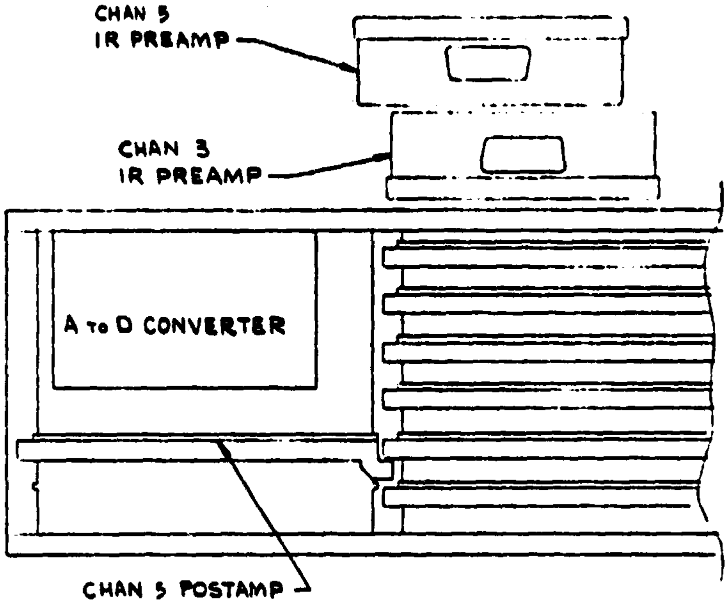


AVHRR / 2

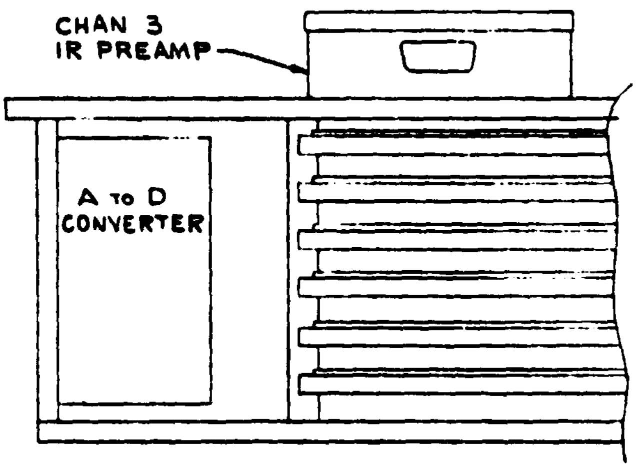


AVHRR / 1

FIG. 6-5

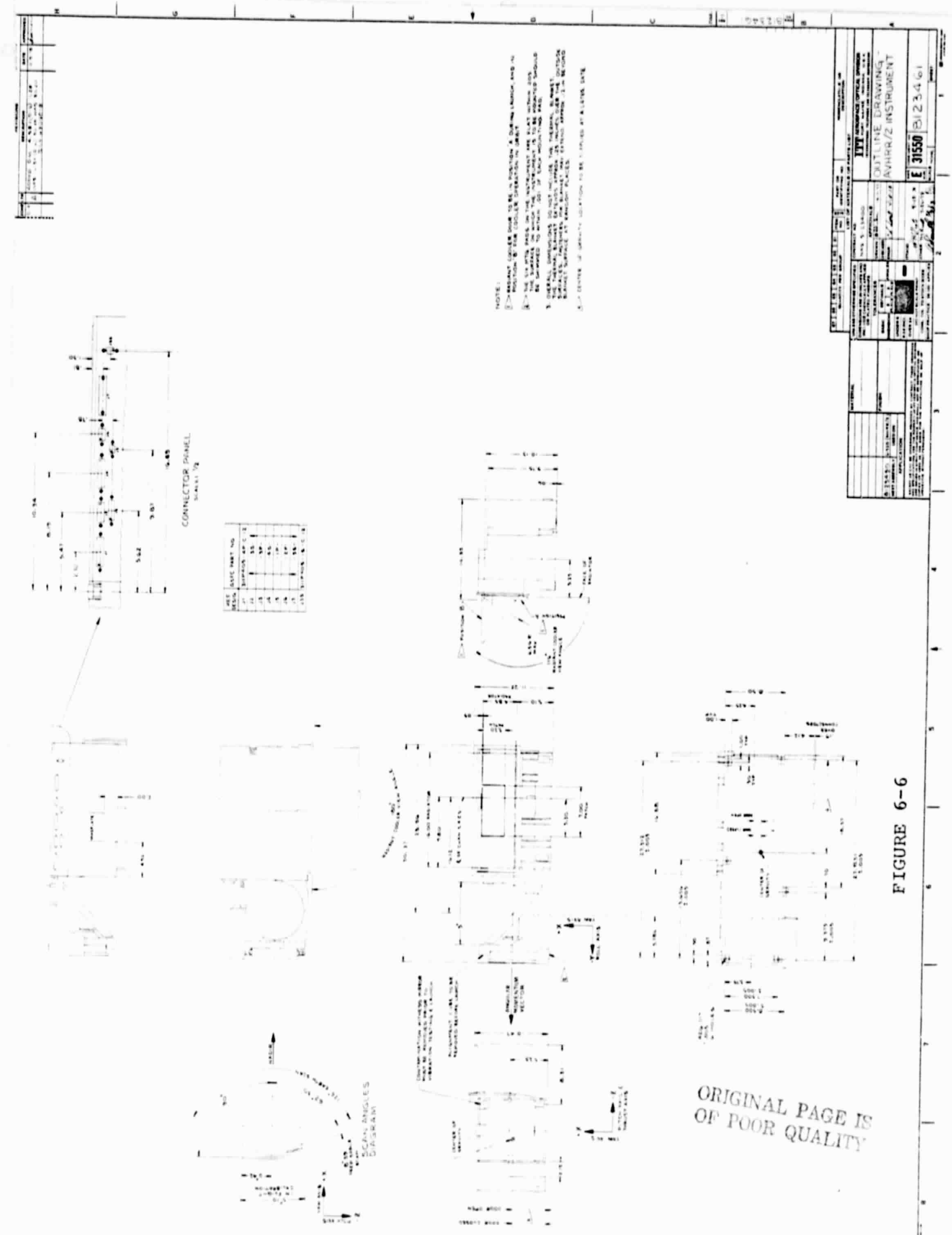
OUTLINE DRAWING
AVHRR/2 INSTRUMENT
31550
B1234G1
CONNECTOR PANEL
SCAN ANGLES DIAGRAM

FIGURE 6-6

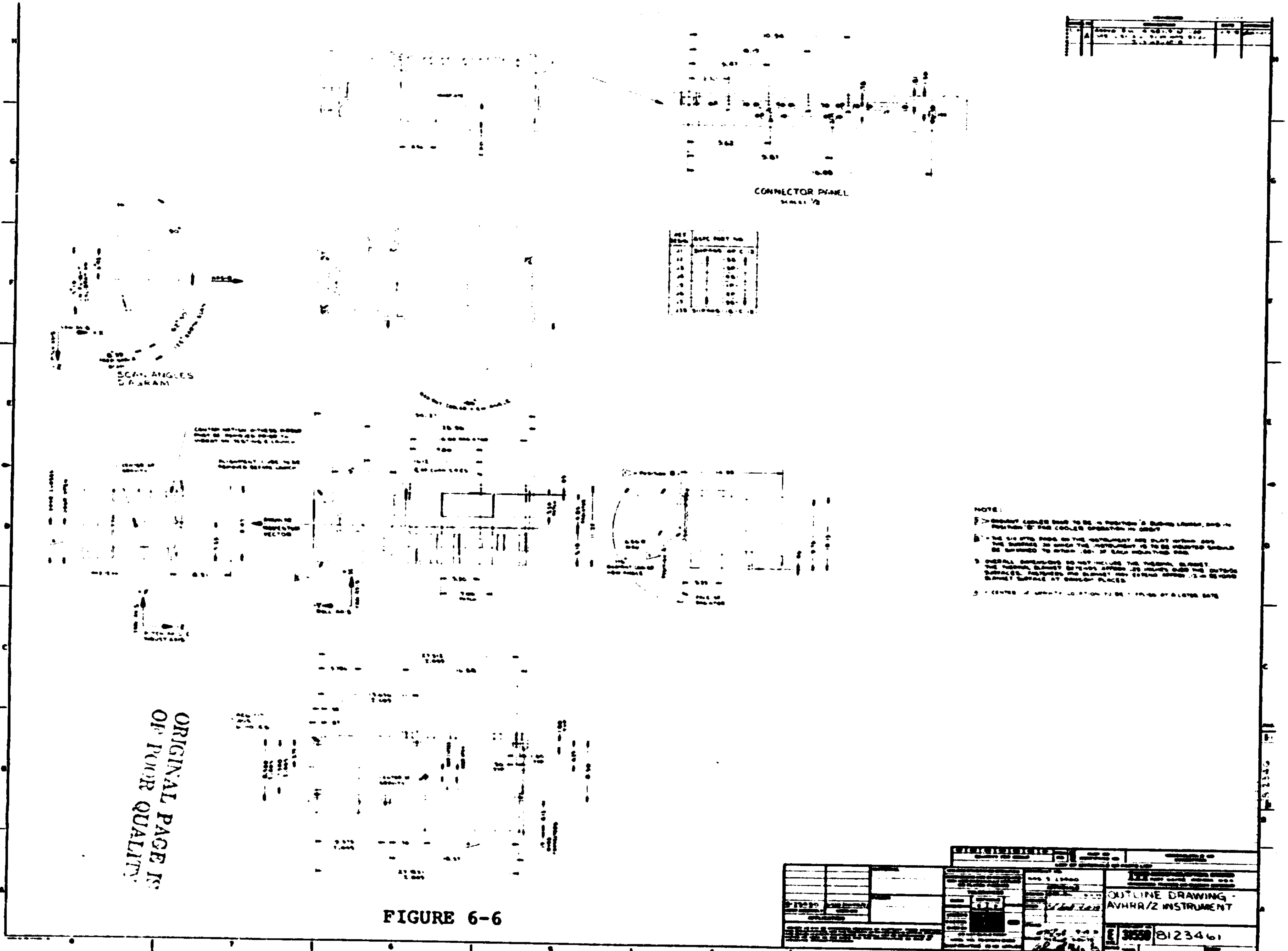
CONNECTOR PANEL
SCAN ANGLES DIAGRAM
NOTE:
OUTLINE DRAWING - AVHRR/2 INSTRUMENT
8123461
ORIGINAL PAGE IS OF POOR QUALITY

FIGURE 6-6

## 7.0 ELECTRONICS

The AVHRR/1 design anticipated the 5 channel design so that minimal electrical changes are required. The major change to the electrical system is the addition of the circuits for the fifth data channel. This requires the addition of a new p.c. assembly for the Channel 5 Post Amplifier and an additional pre-amplifier which is identical to the Channel 3 pre-amplifier.

### 7.1 Channel 5 Post Amplifier

The schematic for the Channel 5 Post Amplifier is shown in Figure 7-1. The amplifier section is identical to the Channel 3 Post Amplifier. This board contains all the linear regulators and enabling circuits for Channel 5. It also contains the sample and hold circuits for the Channel 5 BB Temperature IR TM.

### 7.2 Command Relay No. 4

An additional relay and command verification circuits have been added for enabling Channel 5. The remaining circuits are the same as the AVHRR/1 Command Relay No. 3.

### 7.3 Patch Temperature and Control TM

Component value changes have been made for the patch and cooler temperature TM circuits to accommodate the differences in connecting lead resistance and secondary control temperature. Values were selected to give the same telemetry equations as those for AVHRR/1.

### 7.4 Scan Count and Decode

Gating was added to the logic signal for the Ramp Calibration Signal. The additional gating is for disab ling Ramp Calibration from the test connector. This is done to remove the signal for such tests as registration and field of view instrument tests.

### 7.5 Worst Case and Stress Analysis

The following changes were made as a result of the worst case and stress analysis.

1) Multiplexer - Capacitor C11 was changed from 22 μf 15 volts to 6.8μf 35 volts. Voltage stress now 0.294, rated 0.6.

2) Logic Regulator - Resistor R22 changed from 510 ohm to 470 ohms. Base drive for transistor Q9 in the 5 volt regulator circuit now meets worst case conditions.

3) +15 volt Regulator - Resistor R23 changed from 8.2K ¼ watt to 6.8K ¼ watt. Base drive for transistor Q6 in the -15V Electronics enable circuit now meets worst case conditions. Power stress on R23 now 0.342, rated 0.5.

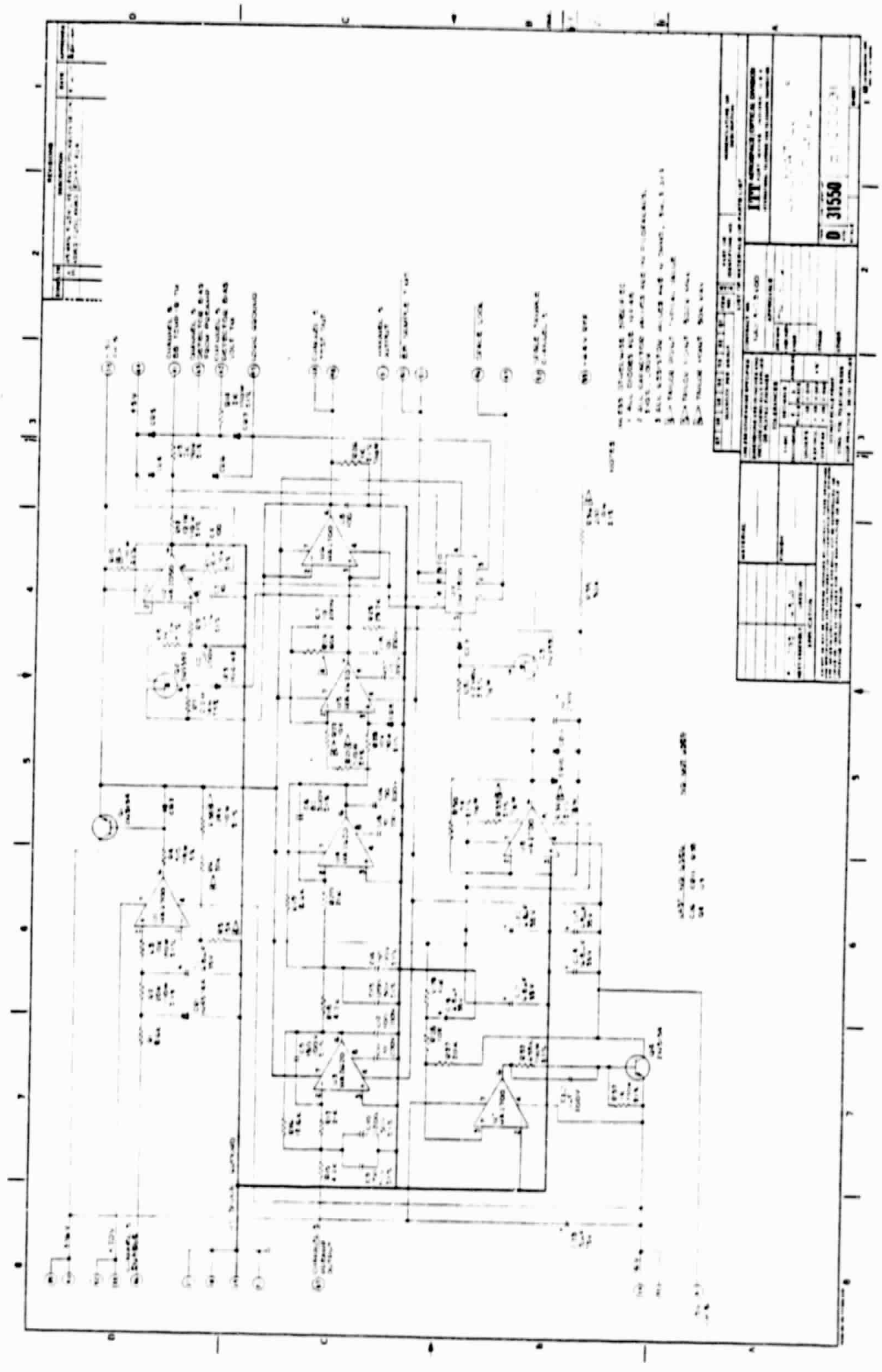

FIGURE 7-1

FIGURE 7-1

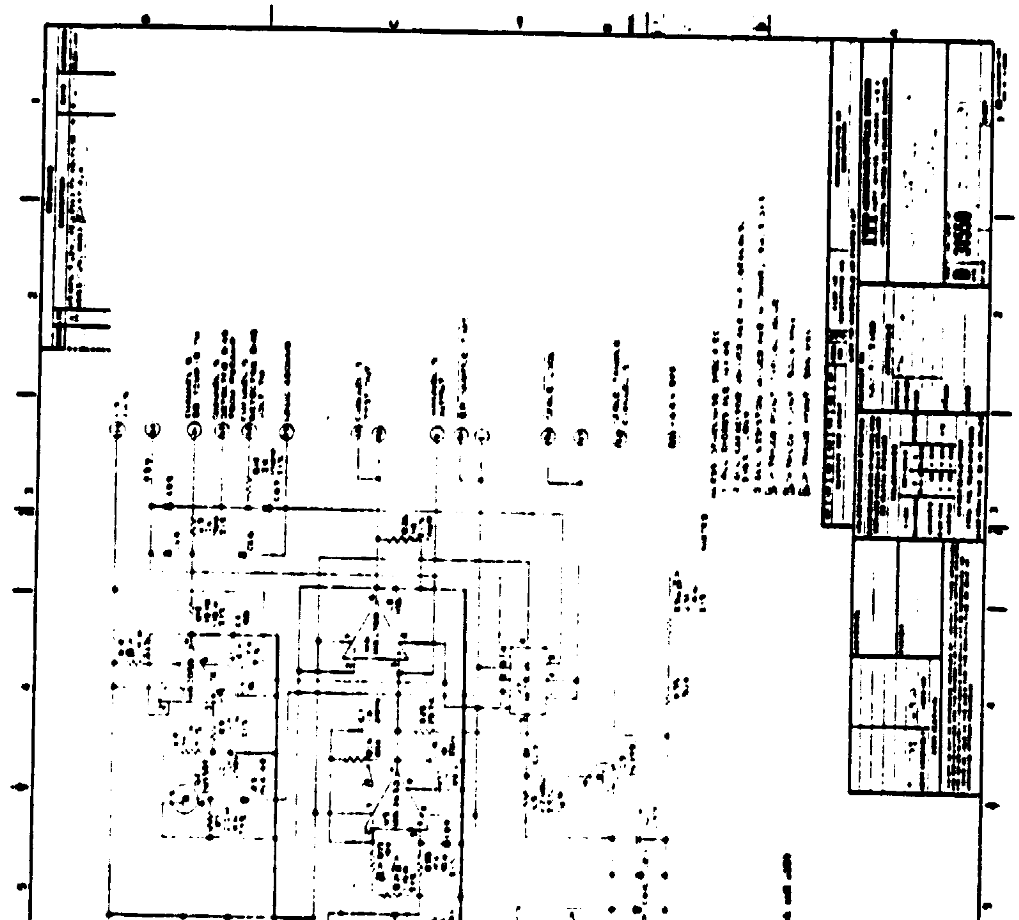

## 7.6 Interface Connections

The complete list for the AVHRR/2 interface connectors is given in Table 7-1.

## 7.7 Printed Circuit Board Drawings

A listing of all applicable drawings for each of the AVHRR/2 printed circuit boards is given in Table 7-2.

## 7.8 Power Profile

The Power Profile for the AVHRR/2 is shown in Table 7-3.

TABLE 7-1

J1 COMMAND

| PIN NO. | FUNCTION |
|---|---|
| 1 | Elec/Telemetry On |
| 2 | Elec/Telemetry Off |
| 3 | Motor/Telemetry On |
| 4 | Motor/Telemetry Off |
| 5 | Telemetry Not Locked On |
| 6 | Telemetry Locked On |
| 7 | Channel 1 Enable |
| 8 | Channel 1 Disable |
| 9 | Channel 2 Enable |
| 10 | Channel 2 Disable |
| 11 | Channel 3 Enable |
| 12 | Channel 3 Disable |
| 13 | Channel 4 Enable |
| 14 | Channel 4 Disable |
| 15 | Motor Low Power |
| 16 | Motor High Power |
| 17 | Patch Low |
| 18 | Patch High |
| 19 | |
| 20 | Patch Control Off |
| 21 | Patch Control On |
| 22 | Earth Shield Disable |
| 23 | Earth Shield Deploy |
| 24 | Cooler Heat Off |
| 25 | Cooler Heat On |
| 26 | Voltage Calibrate Off |
| 27 | Voltage Calibrate On |

J1 COMMAND (Continued)

| PIN NO. | FUNCTION |
|---|---|
| 28 | CHANNEL 5 ENABLE |
| 29 | CHANNEL 5 DISABLE |
| 37 | Chassis Ground |

J2 DIGITAL TM

| PIN NO. | FUNCTION |
|---|---|
| 1 | Earth Shield Status |
| 2 | Patch Control Status |
| 3 | Patch Mode Status |
| 4 | Motor Mode Status |
| 5 | Voltage Calibrate Status |
| 6 | Cooler Heat Status |
| 7 | Electronics/Telemetry Status |
| 8 | Motor/Telemetry Status |
| 9 | Telemetry Lock Status |
| 10 | Channel 1 Status |
| 11 | Channel 2 Status |
| 12 | Channel 3 Status |
| 13 | Channel 4 Status |
| 14 | CHANNEL 5 STATUS |
| 25 | Chassis Ground |

## J3 POWER

| PIN NO. | FUNCTION |
|---|---|
| 1 | +28V Buss |
| 2 | +28V Buss |
| 3 | +28V Buss (Motor) |
| 4 | +28V Buss (Motor) |
| 5 | Power Ground |
| 6 | Power Ground |
| 7 | AC 28V Return |
| 8 | AC 28V Return |
| 9 | +10V Buss |
| 10 | +10V Buss |
| 11 | +5V Buss |
| 12 | +5V Buss |
| 13 | Interface Power Ground |
| 14 | Interface Power Ground |
| 15 | Signal Ground |
| 16 | Signal Ground |
| 17 | Chassis Ground |
| 18 | Chassis Ground |

## J4 ANALOG TM

| PIN NO. | FUNCTION |
|---|---|
| 1 | Radiator Temp. TM |
| 2 | Patch Power TM |
| 3 | Patch Temp TM Low Range |
| 4 | Patch Temp TM Ext Range |
| 5 | Black Body #1 TM |
| 6 | Black Body #2 TM |
| 7 | Black Body #3 TM |
| 8 | Black Body #4 TM |
| 9 | Motor Current TM |
| 10 | Elect. Current TM |
| 11 | Earth Shield Position TM |
| 12 | Electronics Temp. TM |
| 13 | Base Plate Temp. TM |
| 14 | A/D Conv. Temp. TM |
| 15 | Motor Hsg. Temp TM |
| 16 | Cooler Hsg. Temp. TM |
| 17 | Detector Bias Volt Ch. 3 TM |
| 18 | DETECTOR BIAS VOLT CH 5 TM |
| 19 | BB Temp. IR Ch. 3 TM |
| 20 | BB Temp. IR Ch. 4 TM |
| 21 | Offset Voltage TM |
| 22 | BB TEMP IR CH 5 TM |
| 37 | Chassis Ground |

## J5 CLOCK

| PIN NO. | FUNCTION |
|---|---|
| 1 | Clock - Ref |
| 2 | Clock |
| 3 | Clock Shield |
| 4 | Chassis Ground |

## J6 DATA PROCESSOR

| PIN NO. | FUNCTION |
|---|---|
| 1 | $2^9$ MIRP Data |
| 2 | $2^8$ MIRP Data |
| 3 | $2^7$ MIRP Data |
| 4 | $2^6$ MIRP Data |
| 5 | $2^5$ MIRP Data |
| 6 | $2^4$ MIRP Data |
| 7 | $2^3$ MIRP Data |
| 8 | $2^2$ MIRP Data |
| 9 | $2^1$ MIRP Data |
| 10 | $2^0$ MIRP Data |
| 11 | Chassis Ground |
| 12 | Sample Pulse From MIRP |
| 13 | Chassis Ground |
| 14 | Sync Pulse |
| 15 | Chassis Ground |

## J7 TEST

| PIN NO. | FUNCTION |
|---|---|
| 1 | Test - Pick-up loss sim. |
| 2 | Ramp Cal. 3 level |
| 3 | Ch. 3 Test |
| 4 | Ch. 4 Test |
| 5 | Ch. 1 Test |
| 6 | Ch. 2 Test |
| 7 | REf. V Test Point |
| 8 | Pick-up #1 Test |
| 9 | Pick-up #2 Test |
| 10 | -15V Test |
| 11 | +15V Test |
| 12 | Clock Rcvr Test |
| 13 | Solenoid +28 |
| 14 | Solenoid +28 |
| 15 | +5V Test |
| 16 | SIGNAL GROUND |
| 17 | Sync Pulse |
| 18 | CHANNEL 5 TEST |
| 19 | RAMP CAL INHIBIT |
| 50 | Chassis Ground |

## J33 - PULSE LOAD HEATER

| PIN NO. | FUNCTION |
|---|---|
| 1 | Pulse Load Heater |
| 2 | Pulse Load Heater Ret. |
| 3 | Temp. Control Sensor |
| 4 | Temp. Control Sensor |
| 5 | |
| 6 | |
| 7 | Chassis Ground |
| 8 | |
| 9 | |

Table 7 -2 AVHRR/2 CIRCUIT BOARD DRAWING NUMBERS

| CIRCUIT NAME | SCHEMATIC | BOARD # | ASSEMBLY DRAWING | ASSEMBLY PROCEDURE | TEST PROCEDURE |
|---|---|---|---|---|---|
| POWER CONV. & SW. REG. | 8007970 | 8007971 | 8007972-G1 | 8008230 | 8008279 |
| LOGICS REGULATORS | 8123373 | 8007976 | 8007977-G2 | 8123378 | 8123372 |
| ±15V REGULATORS | 8123374 | 8123375 | 8007982-G2 | 8123376 | 8123377 |
| MOTOR SW. REG. | 8007944 | 8007945 | 8007946-G1 | 8008233 | 8008297 |
| COMMAND RELAY #1 | 8008800 | 8008801 | 8008802-G1 | 8008234 | 8008280 |
| COMMAND RELAY #2 | 8008794 | 8008795 | 8008796-G1 | 8008235 | 8008281 |
| COMMAND RELAY #4 | 8122573 | 8008795 | 8008796-G3 | 8122574 | 8122575 |
| PATCH TEMP CONT. & T/M | 8122569 | 8008121 | 8008122-G2 | 8122570 | 8122571 |
| T/M BOARD #2 | 8008127 | 8008128 | 8008129-G1 | 8008237 | 8008291 |
| MOTOR LOGICS | 8008045 | 8008046 | 8008047-G1 | 8008238 | 8008283 |
| SCAN COUNT & DEC. | 8123386 | 8123387 | 8008051-G2 | 8123388 | 8123309 |
| INTERFACE LOGICS #1 | 8009206 | 8009207 | 8009208-G1 | 8008240 | 8008293 |
| INTERFACE LOGICS #2 | 8009209 | 8009210 | 8009211-G1 | 8009225 | 8009228 |
| RAMP CAL. GEN. | 8007963 | 8007964 | 8007965-G1 | 8008241 | 8008285 |
| AUX SCAN LOGICS | 8008052 | 8008053 | 8008054-G1 | 8008242 | 8008286 |
| CH. 3 PREAMP | 8008101 | 8008102 | 8008103-G1 | 8008243 | 8008294 |
| CH. 4 PREAMP | 8009217 | 8009218 | 8009219-G1 | 8009226 | 8009229 |
| IR POST AMP | 8008078 | 8008079 | 8008080-G1 | 8008244 | 8008288 |
| DAYLIGHT PREAMP | 8008130 | 8008131 | 8008132-G1 | 8008245 | 8008295 |
| DAYLIGHT POST AMP | 8008096 | 8008097 | 8008098-G1 | 8008246 | 8008289 |
| MULTIPLEXER | 8123379 | 8008134 | 8008135-G2 | 8123380 | 8123381 |
| MOTOR POWER SUPPLY | 8007941 | 8007942 | 8007943-G1 | 8008248 | 8008296 |
| BLACK BODY MUX | 8008250 | 8008251 | 8008252-G1 | 8008249 | 8008287 |
| CHANNEL 5 POST AMP | 8122091 | 8122092 | 8122093-G1 | 8123416 | 8123417 |

POWER PROFILE

| FUNCTION | POWER | NORMAL OPERATION | TELEMETRY ONLY | MOTOR ON | COOLER HEATER | INSTRUMENT OFF |
|---|---|---|---|---|---|---|
| ANALOG TELEMETRY & MOTOR LOGICS | 3.22W | X | X | X | X | |
| A-D & ELECTRONICS ** | 12.94W | X | | | | |
| SCAN MOTOR HIGH | 4.84W | X | | X | | |
| SCAN MOTOR LOW | 3.98W | | | X | | |
| CHANNEL 1 | .67W | X | | | | |
| CHANNEL 2 | .89W | X | | | | |
| CHANNEL 3 | 1.4W | X | | | | |
| CHANNEL 4 | .95W | X | | | | |
| CHANNEL 5 | 1.8W | X | | | | |
| COOLER HEATER | 21.2W | | | | X | |
| COOLER COVER DEPLOY | 56.9W* | | | | | |
| STANDBY HEATER | 22.8W** | | | | | X |
| | | 26.71W | 3.22W | 7.20 or 8.06 | 24.75W | 22.8W** |

* Required only once for a period of approximately 1 sec.

** Supplied from TCE - not from +28V buss.

TABLE 7 - 3

## 8.0 THERMAL MODEL

The in-orbit nodal temperatures of the AVHRR/2 are given in Tables 8-1 thru 8-4 which follow.

The Thermal Interface Drawing for AVHRR/2 is given in Figure 8-5.

AVHRR/2 NODAL TEMPERATURES ($^{o}C$)
NOMINAL CASE

| NODE | DESCRIPTION | ORBIT 28° | 68° | 0° |
|---|---|---|---|---|
| 1 | PWR CONV | 33.97 | 33.83 | 33.76 |
| 2 | VOLT REG | 41.16 | 41.04 | 40.98 |
| 3 | RELAY123 | 28.19 | 28.03 | 27.96 |
| 4 | PATCH TM | 26.55 | 26.41 | 26.44 |
| 5 | TM # 2 | 27.92 | 27.87 | 27.92 |
| 6 | AUX SCAN | 30.24 | 30.23 | 30.28 |
| 7 | SCAN CTR | 29.14 | 29.14 | 29.20 |
| 8 | MTR LOGI | 30.41 | 30.40 | 30.47 |
| 9 | BLK BODY | 26.45 | 26.41 | 26.48 |
| 10 | AMPCH3&4 | 35.68 | 35.55 | 35.58 |
| 11 | POSTA1&2 | 37.54 | 37.49 | 37.53 |
| 12 | RAMP CAL | 34.03 | 34.01 | 34.06 |
| 13 | LOGIC #1 | 30.70 | 30.69 | 30.75 |
| 14 | LOGIC #2 | 31.11 | 31.09 | 31.16 |
| 15 | MULTPLX | 32.95 | 32.91 | 32.98 |
| 16 | POSTACH5 | 26.96 | 26.57 | 26.52 |
| 17 | P AMP3&5 | 28.06 | 27.48 | 27.33 |
| 18 | A/D CONV | 25.65 | 24.86 | 24.69 |
| 19 | CH 1 DET | 27.43 | 22.85 | 17.00 |
| 20 | CH 2 DET | 27.44 | 22.90 | 16.94 |
| 21 | ELEC A-S | 18.75 | 17.97 | 17.83 |
| 22 | ELEC SUN | 19.54 | 19.22 | 19.33 |
| 23 | CONNECTO | 26.96 | 27.55 | 27.69 |
| 24 | HARNESS | 19.23 | 21.09 | 21.44 |
| 25 | ELEC-VEL | 17.84 | 17.71 | 17.70 |
| 26 | ELPART 1 | 21.06 | 20.61 | 20.61 |
| 27 | ELPART 2 | 20.97 | 20.51 | 20.53 |
| 28 | ELPART 3 | 20.48 | 19.99 | 20.00 |
| 29 | NADIRRAD | 18.00 | 16.97 | 16.70 |
| 30 | P-AMP 4 | 27.10 | 25.76 | 25.01 |
| 31 | ESHIELDS | -77.88 | -75.96 | -81.33 |
| 32 | ESHIELDI | -33.79 | -31.50 | -39.52 |
| 33 | WING +V | -75.72 | -69.47 | -83.07 |
| 34 | WING -V | -83.97 | -74.83 | -89.83 |
| 35 | NOT USED | 18.01 | 16.98 | 16.71 |
| 36 | SCAN MOT | 20.79 | 15.20 | 15.89 |
| 37 | SCANMHSG | 20.26 | 14.76 | 16.28 |
| 38 | RAD ELEC | 18.15 | 17.89 | 17.66 |
| 39 | SCAN PS | 19.17 | 14.11 | 14.43 |
| 40 | SCAN M F | 26.68 | 15.60 | 27.34 |
| 41 | SCAN M B | 26.68 | 15.60 | 27.33 |
| 42 | CAVITY S | 18.33 | 14.08 | 14.73 |
| 43 | CAVITYAS | 17.58 | 13.25 | 14.14 |
| 44 | BASE CAV | 17.77 | 13.34 | 14.32 |
| 45 | CAL TGTL | 17.72 | 13.08 | 14.04 |
| 46 | CAL TGTS | 18.11 | 13.15 | 14.54 |
| 47 | BULK TEL | 16.34 | 14.28 | 14.42 |
| 48 | TELE | 32.02 | 22.06 | 7.50 |
| 49 | BULK CEN | 17.20 | 16.25 | 15.90 |
| 50 | BASE TEL | 16.36 | 15.17 | 15.07 |
| 51 | BASE OPT | 15.73 | 15.37 | 15.24 |
| 52 | COOL HSG | 17.33 | 15.99 | 15.24 |
| 53 | TEL OPTI | 25.70 | 20.90 | 14.57 |
| 54 | CH 1 REL | 25.91 | 21.17 | 15.12 |
| 55 | CH 2 REL | 26.02 | 21.30 | 15.09 |
| 56 | END -VEL | 17.75 | 16.93 | 16.54 |
| 57 | EL COVER | 3.91 | 9.23 | 10.11 |
| 58 | LW RELAY | 25.43 | 20.79 | 14.70 |
| 59 | INS +VEL | -25.16 | -9.70 | -67.68 |
| 60 | INS ASUN | -99.12 | -94.13 | -102.71 |
| 61 | INS -VEL | -44.32 | -43.81 | -56.01 |
| 62 | INS SUN | 41.21 | -8.78 | 44.47 |
| 63 | INS NAD | -10.89 | -11.85 | -26.44 |
| 64 | SPACE | -269.44 | -269.44 | -269.44 |

LOUVER EMISSIVITY = .4190 .2566 .2325

TABLE 8-1

## AVHRR/2 NODAL TEMPERATURES (°C)
## WORST CASE HOT

| NODE | DESCRIPTION | NODE | ORBIT 28° | ORBIT 68° | ORBIT 0° |
|---|---|---|---|---|---|
| 1 | PWR CONV | 1 | 34.14 | 34.05 | 33.97 |
| 2 | VOLT REG | 2 | 41.32 | 41.25 | 41.18 |
| 3 | RELAY123 | 3 | 28.38 | 28.26 | 28.18 |
| 4 | PATCH TM | 4 | 26.64 | 26.58 | 26.62 |
| 5 | TM # 2 | 5 | 28.00 | 28.03 | 28.09 |
| 6 | AUX SCAN | 6 | 30.31 | 30.38 | 30.44 |
| 7 | SCAN CTR | 7 | 29.21 | 29.29 | 29.36 |
| 8 | MTR LOGI | 8 | 30.48 | 30.55 | 30.62 |
| 9 | BLK BODY | 9 | 26.53 | 26.57 | 26.65 |
| 10 | AMPCH3&4 | 10 | 35.77 | 35.71 | 35.75 |
| 11 | POSTA1&2 | 11 | 37.61 | 37.63 | 37.69 |
| 12 | RAMP CAL | 12 | 34.10 | 34.16 | 34.22 |
| 13 | LOGIC #1 | 13 | 30.77 | 30.84 | 30.91 |
| 14 | LOGIC #2 | 14 | 31.18 | 31.24 | 31.32 |
| 15 | MULTPLX | 15 | 33.03 | 33.06 | 33.14 |
| 16 | POSTACH5 | 16 | 27.10 | 26.77 | 26.75 |
| 17 | P AMP3&5 | 17 | 28.21 | 27.67 | 27.60 |
| 18 | A/D CONV | 18 | 25.87 | 25.10 | 25.00 |
| 19 | CH 1 DET | 19 | 28.25 | 23.37 | 17.55 |
| 20 | CH 2 DET | 20 | 28.24 | 23.41 | 17.47 |
| 21 | ELEC A-S | 21 | 18.98 | 18.21 | 18.14 |
| 22 | ELEC SUN | 22 | 19.68 | 19.46 | 19.55 |
| 23 | CONNECTO | 23 | 26.91 | 27.60 | 27.74 |
| 24 | HARNESS | 24 | 18.92 | 20.92 | 21.25 |
| 25 | ELEC-VEL | 25 | 17.97 | 17.92 | 17.95 |
| 26 | ELPART 1 | 26 | 21.23 | 20.84 | 20.86 |
| 27 | ELPART 2 | 27 | 21.12 | 20.74 | 20.77 |
| 28 | ELPART 3 | 28 | 20.65 | 20.23 | 20.25 |
| 29 | NADIRRAD | 29 | 18.26 | 17.26 | 17.08 |
| 30 | P-AMP 4 | 30 | 27.37 | 26.00 | 25.34 |
| 31 | ESHIELDS | 31 | -71.07 | -68.59 | -76.00 |
| 32 | ESHIELDI | 32 | -29.98 | -27.19 | -37.77 |
| 33 | WING +V | 33 | -71.25 | -63.51 | -81.14 |
| 34 | WING -V | 34 | -80.06 | -68.60 | -87.97 |
| 35 | NOT USED | 35 | 18.27 | 17.27 | 17.09 |
| 36 | SCAN MOT | 36 | 22.00 | 15.91 | 18.15 |
| 37 | SCANMHSG | 37 | 21.42 | 15.46 | 17.50 |
| 38 | RAD ELEC | 38 | 18.49 | 18.24 | 17.95 |
| 39 | SCAN PS | 39 | 20.03 | 14.77 | 15.39 |
| 40 | SCAN M F | 40 | 29.30 | 16.70 | 30.46 |
| 41 | SCAN M B | 41 | 29.30 | 16.70 | 30.45 |
| 42 | CAVITY S | 42 | 19.09 | 14.63 | 15.54 |
| 43 | CAVITYAS | 43 | 18.40 | 13.82 | 14.99 |
| 44 | BASE CAV | 44 | 18.53 | 13.85 | 15.10 |
| 45 | CAL TGTL | 45 | 18.48 | 13.59 | 14.83 |
| 46 | CAL TGTS | 46 | 18.89 | 13.67 | 15.33 |
| 47 | BULK TEL | 47 | 17.33 | 14.66 | 14.96 |
| 48 | TELE | 48 | 33.65 | 22.94 | 8.21 |
| 49 | BULK CEN | 49 | 17.42 | 16.48 | 16.23 |
| 50 | BASE TEL | 50 | 16.60 | 15.40 | 15.42 |
| 51 | BASE OPT | 51 | 15.82 | 15.51 | 15.47 |
| 52 | COOL HSG | 52 | 17.60 | 16.23 | 15.57 |
| 53 | TEL OPTI | 53 | 26.55 | 21.43 | 15.11 |
| 54 | CH 1 REL | 54 | 26.76 | 21.71 | 15.68 |
| 55 | CH 2 REL | 55 | 26.86 | 21.83 | 15.63 |
| 56 | END -VEL | 56 | 18.00 | 17.22 | 16.93 |
| 57 | EL COVER | 57 | 2.86 | 8.44 | 9.26 |
| 58 | LW RELAY | 58 | 26.25 | 21.31 | 15.24 |
| 59 | INS +VEL | 59 | -9.07 | -6.11 | -70.46 |
| 60 | INS ASUN | 60 | -101.44 | -95.73 | -105.65 |
| 61 | INS -VEL | 61 | -51.38 | -43.55 | -57.26 |
| 62 | INS SUN | 62 | 46.92 | -5.30 | 50.54 |
| 63 | INS NAD | 63 | -14.88 | -9.09 | -24.58 |
| 64 | SPACE | 64 | -269.44 | -269.44 | -269.44 |
| | LOUVER EMISSIVITY = | | .4568 | .2839 | .2609 |

TABLE 8-2

## AVHRR/2 NODAL TEMPERATURES ($^{o}C$)
## WORST CASE COLD

| NODE | DESCRIPTION | | ORBIT 28° | 68° | 0° |
|---|---|---|---|---|---|
| 1 | PWR CONV | 1 | 33.69 | 33.87 | 33.85 |
| 2 | VOLT REG | 2 | 40.89 | 41.08 | 41.06 |
| 3 | RELAY123 | 3 | 27.89 | 28.05 | 28.04 |
| 4 | PATCH TM | 4 | 26.33 | 26.56 | 26.59 |
| 5 | TM # 2 | 5 | 27.73 | 28.05 | 28.10 |
| 6 | AUX SCAN | 6 | 30.06 | 30.42 | 30.48 |
| 7 | SCAN CTR | 7 | 28.96 | 29.33 | 29.40 |
| 8 | MTR LOGI | 8 | 30.23 | 30.59 | 30.66 |
| 9 | BLK BODY | 9 | [illegible].26 | 26.58 | 26.66 |
| 10 | AMPCH3&4 | 10 | 35.48 | 35.69 | 35.72 |
| 11 | POSTA1&2 | 11 | 37.36 | 37.65 | 37.70 |
| 12 | RAMP CAL | 12 | 33.85 | 34.19 | 34.25 |
| 13 | LOGIC #1 | 13 | 30.52 | 30.88 | 30.95 |
| 14 | LOGIC #2 | 14 | 30.93 | 31.28 | 31.35 |
| 15 | MULTPLX | 15 | 32.76 | 33.08 | 33.15 |
| 16 | POSTACH5 | 16 | 26.67 | 26.60 | 26.57 |
| 17 | P AMP3&5 | 17 | 27.75 | 27.47 | 27.32 |
| 18 | A/D CONV | 18 | 25.26 | 24.76 | 24.61 |
| 19 | CH 1 DET | 19 | 26.45 | 21.59 | 16.39 |
| 20 | CH 2 DET | 20 | 26.48 | 21.65 | 16.36 |
| 21 | ELEC A-S | 21 | 18.36 | 17.86 | 17.75 |
| 22 | ELEC SUN | 22 | 19.23 | 19.26 | 19.41 |
| 23 | CONNECTO | 23 | 26.97 | 28.00 | 28.12 |
| 24 | HARNESS | 24 | 19.66 | 22.11 | 22.39 |
| 25 | ELEC-VEL | 25 | 17.53 | 17.76 | 17.75 |
| 26 | ELPART 1 | 26 | 20.74 | 20.61 | 20.64 |
| 27 | ELPART 2 | 27 | 20.64 | 20.52 | 20.56 |
| 28 | ELPART 3 | 28 | 20.15 | 19.99 | 20.01 |
| 29 | NADIRRAD | 29 | 17.50 | 16.73 | 16.48 |
| 30 | P-AMP 4 | 30 | 26.66 | 25.54 | 24.89 |
| 31 | ESHIELDS | 31 | -82.34 | -81.31 | -84.87 |
| 32 | ESHIELDI | 32 | -41.71 | -40.65 | -45.79 |
| 33 | WING +V | 33 | -82.58 | -79.00 | -87.30 |
| 34 | WING -V | 34 | -90.20 | -84.61 | -94.34 |
| 35 | NOT USED | 35 | 17.51 | 16.74 | 16.49 |
| 36 | SCAN MOT | 36 | 19.00 | 13.65 | 15.06 |
| 37 | SCANMHSG | 37 | 18.52 | 13.25 | 14.54 |
| 38 | RAD ELEC | 38 | 17.69 | 17.75 | 17.62 |
| 39 | SCAN PS | 39 | 17.72 | 12.71 | 13.11 |
| 40 | SCAN M F | 40 | 22.59 | 12.52 | 22.38 |
| 41 | SCAN M B | 41 | 22.59 | 12.52 | 22.38 |
| 42 | CAVITY S | 42 | 17.13 | 12.99 | 13.68 |
| 43 | CAVITYAS | 43 | 16.31 | 12.17 | 13.03 |
| 44 | BASE CAV | 44 | 16.61 | 12.33 | 13.31 |
| 45 | CAL TGTL | 45 | 16.53 | 12.02 | 13.01 |
| 46 | CAL TGTS | 46 | 16.92 | 12.10 | 13.50 |
| 47 | BULK TEL | 47 | 16.07 | 13.72 | 13.89 |
| 48 | TELE | 48 | 30.35 | 19.31 | 6.40 |
| 49 | BULK CEN | 49 | 16.81 | 16.11 | 15.80 |
| 50 | BASE TEL | 50 | 15.94 | 15.01 | 14.93 |
| 51 | BASE OPT | 51 | 15.51 | 15.46 | 15.32 |
| 52 | COOL HSG | 52 | 16.89 | 15.77 | 15.12 |
| 53 | TEL OPTI | 53 | 24.70 | 19.58 | 13.95 |
| 54 | CH 1 REL | 54 | 24.91 | 19.88 | 14.49 |
| 55 | CH 2 REL | 55 | 25.04 | 20.01 | 14.48 |
| 56 | END -VEL | 56 | 17.25 | 16.69 | 16.33 |
| 57 | EL COVER | 57 | 5.49 | 11.81 | 12.45 |
| 58 | LW RELAY | 58 | 24.45 | 19.51 | 14.10 |
| 59 | INS +VEL | 59 | -27.65 | -17.87 | -64.89 |
| 60 | INS ASUN | 60 | -95.75 | -92.33 | -98.78 |
| 61 | INS -VEL | 61 | -45.75 | -45.46 | -56.10 |
| 62 | INS SUN | 62 | 34.56 | -17.74 | 37.70 |
| 63 | INS NAD | 63 | -16.69 | -19.83 | -31.84 |
| 64 | SPACE | 64 | -269.44 | -269.44 | -269.44 |

LOUVER EMISSIVITY = .3625 .1894 .1732

TABLE 8-3

# AVHRR/2 NODAL TEMPERATURES ($^{o}C$)
## WORST CASE COLD (Power Off)

ORBIT

| NODE | DESCRIPTION | $0^{o}$ | $68^{o}$ |
|---|---|---|---|
| 1 | PWR CONV | 7.54 | 10.95 |
| 2 | VOLT REG | 7.43 | 10.83 |
| 3 | RELAY123 | 7.41 | 10.81 |
| 4 | PATCH TM | 8.31 | 11.72 |
| 5 | TM # 2 | 8.13 | 11.52 |
| 6 | AUX SCAN | 8.06 | 11.44 |
| 7 | SCAN CTR | 8.03 | 11.41 |
| 8 | MTR LOGI | 8.02 | 11.39 |
| 9 | BLK BODY | 8.02 | 11.38 |
| 10 | AMPCH3&4 | 8.34 | 11.75 |
| 11 | POSTA1&2 | 8.16 | 11.55 |
| 12 | RAMP CAL | 8.09 | 11.47 |
| 13 | LOGIC #1 | 8.06 | 11.44 |
| 14 | LOGIC #2 | 8.05 | 11.42 |
| 15 | MULTPLX | 8.04 | 11.40 |
| 16 | POSTACH5 | 8.70 | 12.16 |
| 17 | P AMP3&5 | 11.04 | 14.62 |
| 18 | A/D CONV | 9.55 | 13.10 |
| 19 | CH 1 DET | 6.67 | 15.28 |
| 20 | CH 2 DET | 6.59 | 15.29 |
| 21 | ELEC A-S | 9.61 | 13.13 |
| 22 | ELEC SUN | 8.02 | 11.29 |
| 23 | CONNECTO | 7.29 | 10.64 |
| 24 | HARNESS | 5.86 | 9.14 |
| 25 | ELEC-VEL | 8.08 | 11.52 |
| 26 | ELPART 1 | 8.56 | 11.94 |
| 27 | ELPART 2 | 8.62 | 12.00 |
| 28 | ELPART 3 | 8.69 | 12.08 |
| 29 | NADIRRAD | 9.51 | 13.14 |
| 30 | P-AMP 4 | 10.34 | 14.38 |
| 31 | ESHIELDS | -84.94 | -81.33 |
| 32 | ESHIELDI | -45.83 | -40.65 |
| 33 | WING +V | -87.85 | -79.01 |
| 34 | WING -V | -94.40 | -84.61 |
| 35 | NOT USED | 9.51 | 13.14 |
| 36 | SCAN MOT | 13.06 | 14.90 |
| 37 | SCANMHSG | 12.28 | 14.22 |
| 38 | RAD ELEC | 6.40 | 9.84 |
| 39 | SCAN PS | 9.09 | 11.83 |
| 40 | SCAN M F | 19.32 | 13.52 |
| 41 | SCAN M B | 19.31 | 13.53 |
| 42 | CAVITY S | 9.40 | 11.97 |
| 43 | CAVITYAS | 9.06 | 11.44 |
| 44 | BASE CAV | 9.30 | 11.58 |
| 45 | CAL TGTL | 9.02 | 11.23 |
| 46 | CAL TGTS | 9.47 | 11.36 |
| 4 | BULK TEL | 8.86 | 11.99 |
| 48 | TELE | 1.55 | 17.56 |
| 49 | BULK CEN | 10.38 | 14.11 |
| 50 | BASE TEL | 10.06 | 13.54 |
| 51 | BASE OPT | 12.40 | 16.01 |
| 52 | COOL HSG | 10.34 | 14.38 |
| 53 | TEL OPTI | 6.37 | 15.37 |
| 54 | CH 1 REL | 6.55 | 15.32 |
| 55 | CH 2 REL | 6.44 | 15.34 |
| 56 | END -VEL | 9.92 | 13.68 |
| 57 | EL COVER | 2.32 | 5.47 |
| 58 | LW RELAY | 6.49 | 15.29 |
| 59 | INS +VEL | -65.62 | -17.34 |
| 60 | INS ASUN | -99.37 | -92.40 |
| 61 | INS -VEL | -57.56 | -47.10 |
| 62 | INS SUN | 30.67 | -19.10 |
| 63 | INS NAD | -33.10 | -19.94 |
| 64 | SPACE | -269.44 | -269.44 |

TABLE 8-4

LOUVER EMISSIVITY = .1500 .1500

Heater Pwr. (.94 of Nominal) = 23.5 watts

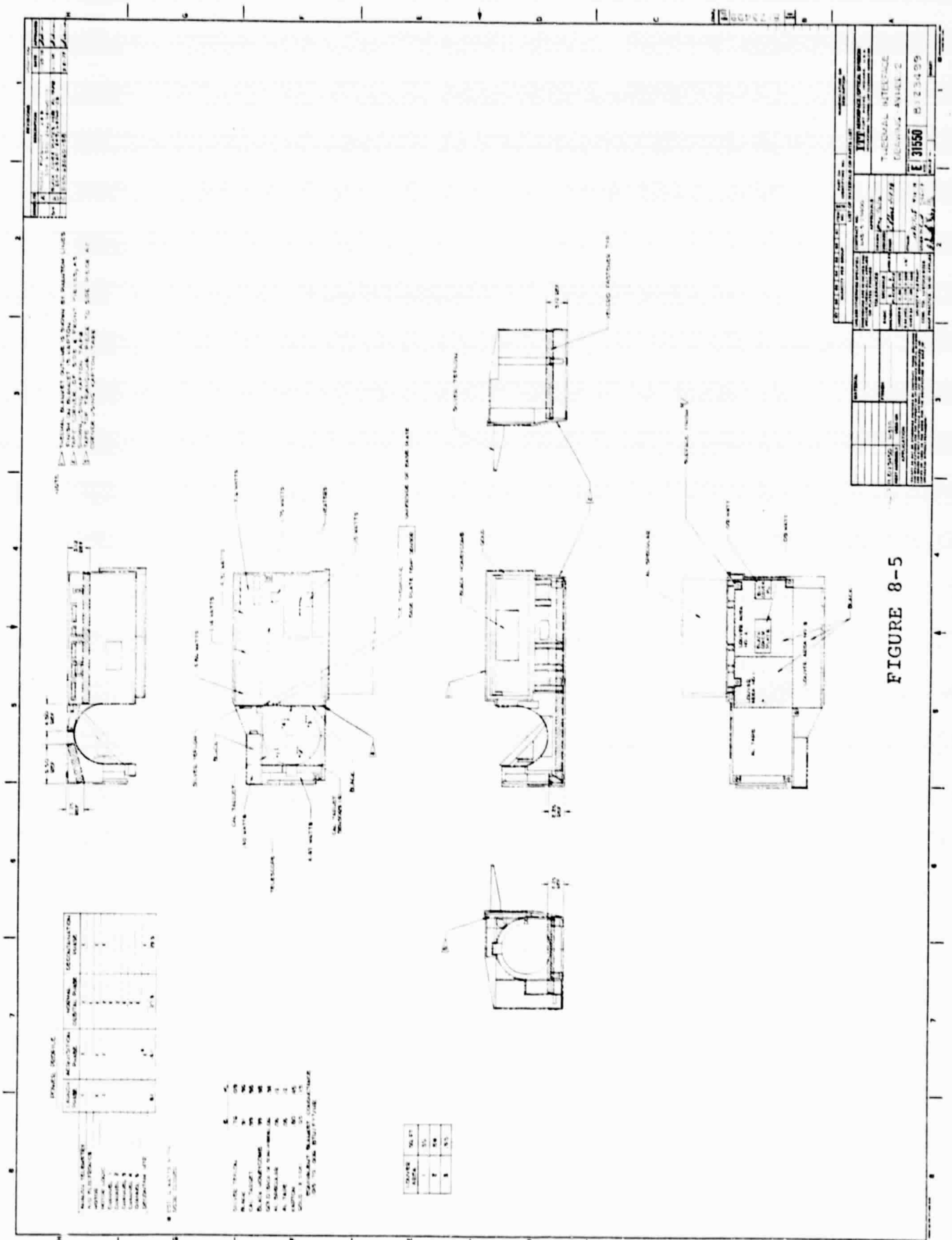


FIGURE 8-5

9.0 TEST AND CALIBRATION DATA

The test report for the Optical Test Model and a resume of the test results for the Protoflight Model are given on the following pages.

For detailed test results and calibration data, refer to

AVHRR/2 Test Report For Protoflight Model

Alignment and Calibration Data Book,
AVHRR/2 Protoflight Model

ADVANCED VERY HIGH RESOLUTION RADIOMETER

MOD 2

TEST REPORT

AVHRR/2

OPTICAL TEST MODEL

Prepared by

ITT AEROSPACE/OPTICAL DIVISION
FORT WAYNE, IN 46803

NATIONAL AEROANAUTICS AND SPACE ADMINISTRATION
GODDARD SPACE FLIGHT CENTER
GREENBELT, MARYLAND 20771

CONTRACT NAS5-23400

## 1.0 INTRODUCTION

The Optical Test Model (OTM) was constructed and tested to prove structural integrity and performance of the redesigned relay optics and the radiant cooler, these being modifications of the designs used on AVHRR/1.

The OTM consisted of elements of the AVHRR/1 Breadboard and Mechanical/Structural Models (BBM & MSM) in conjunction with the redesigned optics and cooler, the resulting assembly being nearly identical structurally to the design to be used on the Protoflight Model. Specifically the OTM consisted of

BBM telescope with new relay optics.
New cooler
MSM electronics module
MSM scanner
MSM baseplate (modified) with new brackets and covers.

## 2.0 OTM TEST PROGRAM

Figure 2-1 shows the tests which were performed on the OTM. Procedures followed were those utilized for AVHRR/1. Vibration levels were as specified for qualification by the AVHRR/2 instrument specification GSFC-S-726-5.

## 3.0 TEST RESULTS

The pages which follow give the results of the tests performed as presented at the AVHRR/2 MDR. It will be seen that the goals for the OTM have been achieved.

# OTM TEST PROGRAM

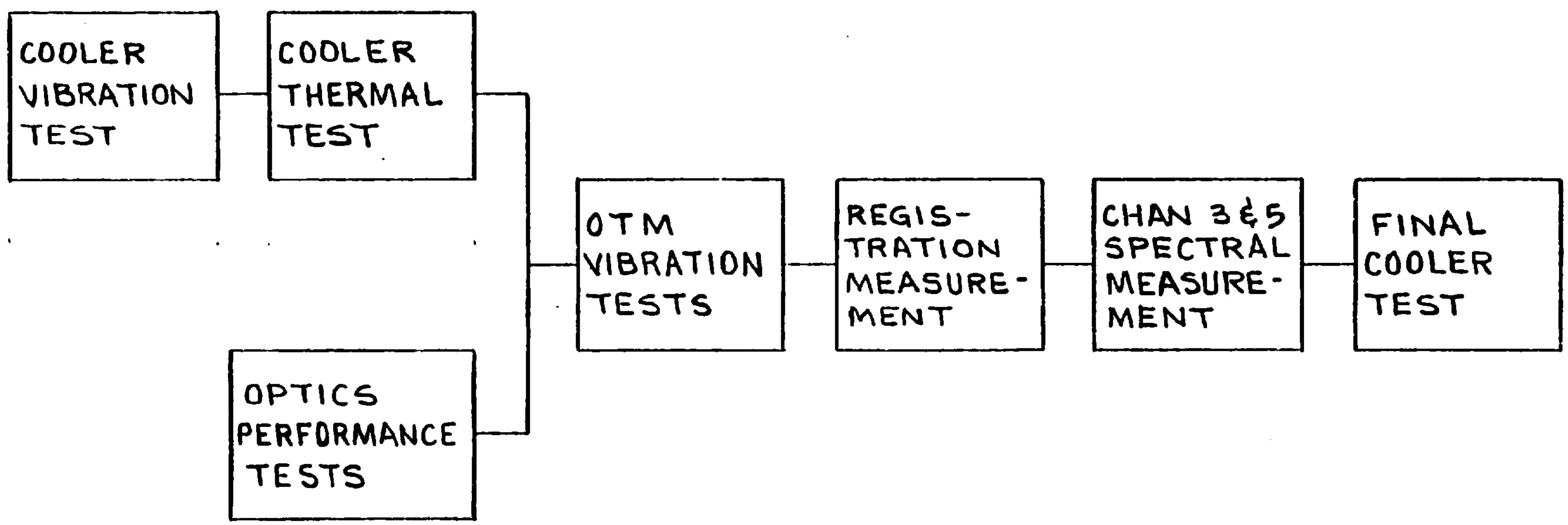


FIGURE 2-1

# OTM MECHANICAL TEST HISTORY

1. OTM Cooler - Qual level vibration

   No structural failures

2. OTM Qual Level #1

   Patch dichroic broke during first (Y) axis. (MR E03348)

   Registration of Ch 1, 2, and 4 in spec.

3. OTM Qual Level #2 and Sine Surveys

   Registration of Ch. 1, 2, and 4 in spec.

   Registration of Ch. 3 and 5 shifted 0.3 mrad. (MR E03349)

   Micro-crack in patch dichroic (MR E03350)

4. OTM Qual Level #3

   No dichroic damage.

   Registration of all channels maintained

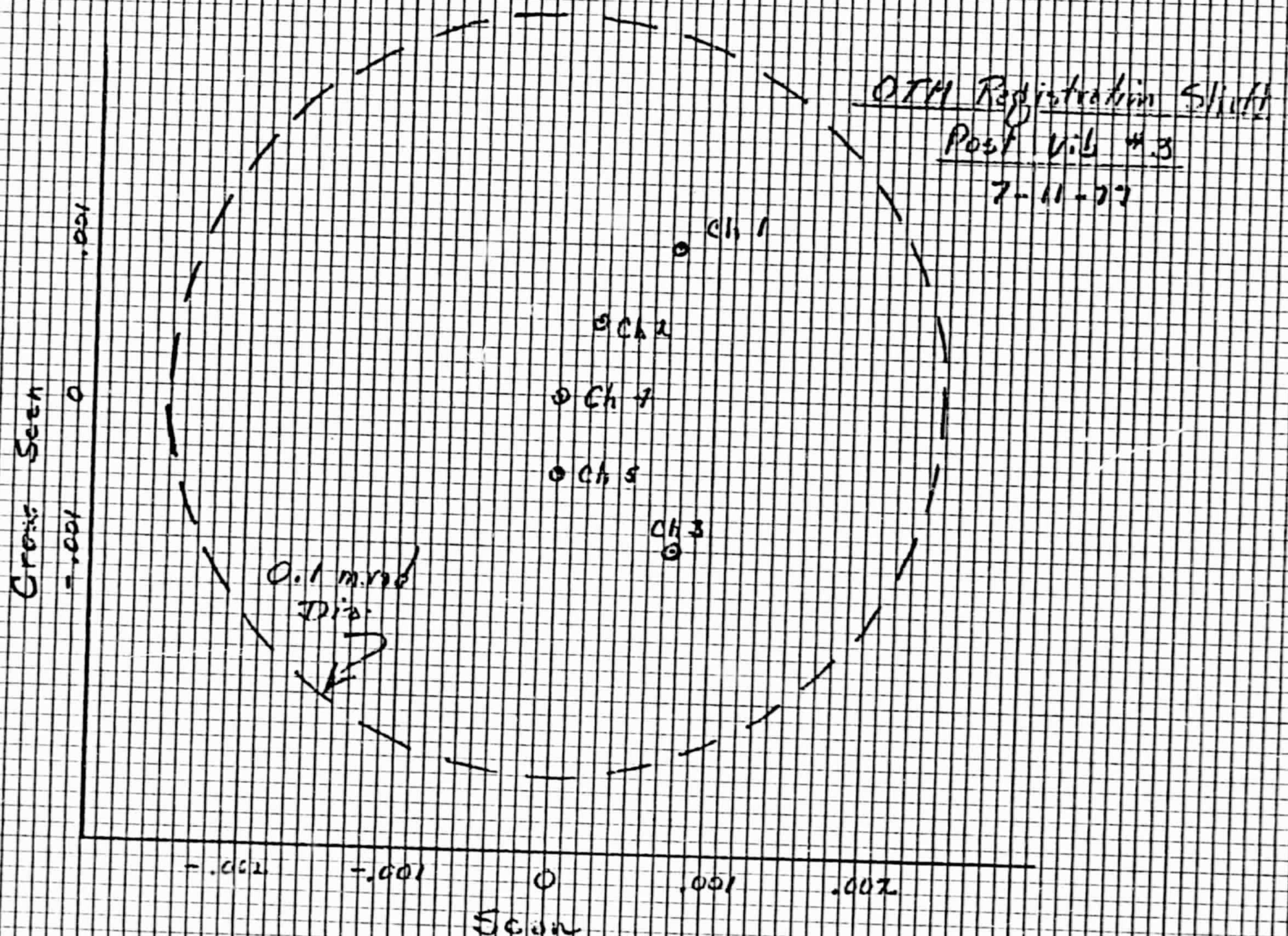
OTM Registration Shift
Post Vib #3
7-11-77
Ch 1
Ch 2
Ch 4
Ch 5
Ch 3
0.1 mrad
Dia.
.001
0
-.001
Cross Scan
-.002
-.001
0
.001
.002
Scan

## OPTICS SUBASSEMBLY MTF

| Spatial Freq. (cycles/radian) | ON AXIS SPEC. (MIN.) | ON AXIS MEASURED | EFOV EDGE SPEC. (MIN.) | EFOV EDGE MEASURED |
|---|---|---|---|---|
| | | **CHANNEL 3** | | |
| 96 | N.R. | 97.2 | N.R. | X |
| 192 | N.R. | 94.5 | N.R. | X |
| 257 | 90 | 92.7 | 90 | 92.4 |
| 385 | 86 | 89.0 | 86 | 88.0 |
| | | **CHANNEL 4** | | |
| 96 | N.R. | 96.8 | N.R. | X |
| 192 | N.R. | 93.7 | N.R. | X |
| 257 | 91 | 91.8 | 91 | 91.1 |
| 385 | 88 | 90.2 | 88 | 88.2 |
| | | **CHANNEL 5** | | |
| 96 | N.R. | 98.3 | N.R. | X |
| 192 | N.R. | 94.7 | N.R. | X |
| 257 | 90 | 92.6 | 90 | 93.5 |
| 385 | 86 | 88.9 | 86 | 89.2 |

## OPTICS SUBASSEMBLY FOV

| | On-Axis | Edge of EFOV |
|---|---|---|
| Ch. 3 | 1.36 m.r. | 1.34 |
| Ch. 4 | 1.35 | 1.37 |
| Ch. 5 | 1.26 | 1.24 |

## OTM - INSTRUMENT IFOV MEASUREMENTS

| | SCAN | CROSS SCAN |
|---|---|---|
| CH. 3 | 1.25 M.R. | 1.28 M.R. |
| CH. 4 | 1.22 M.R. | 1.22 M.R. |
| CH. 5 | 1.24 M.R. | 1.31 M.R. |

SPEC - 1.31 ± .2 M.R.

| PARAMETER | | SPECIFIED | MEASURED |
|---|---|---|---|
| **CHANNEL 3:** | | | |
| SHORT WVLN.* | 50% RESPONSE | 10.3±0.09µM | 10.28µM |
| LONG WVLN. | 50% RESPONSE | 11.3±0.09µM | 11.18µM* |
| CUTON SLOPE, | SHORT WVLN. | ≤4.0% | 2.3% |
| CUTOFF SLOPE, | LONG WVLN. | ≤4.0% | 3.7% |
| SHORT WVLN. | 1% RESPONSE | λ's≤9.8µM | 10.0 & BELOW |
| LONG WVLN | 1% RESPONSE | λ's≥ 11.8µM | 11.5 & ABOVE |
| **CHANNEL 4:** | | | |
| SHORT WVLN. | 50% RESPONSE | 3.55±0.06µM | 3.55µM |
| LONG WVLN. | 50% RESPONSE | 3.93±0.06µM | 3.95µM |
| CUTON SLOPE, | SHORT WVLN | ≤3.0% | 1.9% |
| CUTOFF SLOPE, | LONG WVLN | ≤3.0% | 1.8% |
| SHORT WVLN. | 1% RESPONSE | λ's≤3.40µM | 3.49µM & BELOW |
| LONG WVLN. | 1% RESPONSE | λ's≥4.12µM | 4.02µM & ABOVE |
| **CHANNEL 5:** | | | |
| SHORT WVLN. | 50% RESPONSE | 11.5±0.09µM | 11.43µM |
| LONG WVLN. | 50% RESPONSE | 12.5±0.09µM | 12.40µM** |
| CUTON SLOPE, | SHORT WVLN. | ≤4.0% | 1.8% |
| CUTOFF SLOPE, | LONG WVLN | ≤4.0% | 3.0% |
| SHORT WVLN. | 1% RESPONSE | λ's>10.9µM | 11.2µM & BELOW |
| LONG WVLN | 1% RESPONSE | λ's≥13.1µM | 12.6µM & ABOVE |

WVLN. = WAVELENGTH *OUT OF SPEC. BY 0.03µM
**OUT OF SPEC. BY 0.01µM

AVHRR/2, INFRARED SPECTRAL CHARACTERISTICS

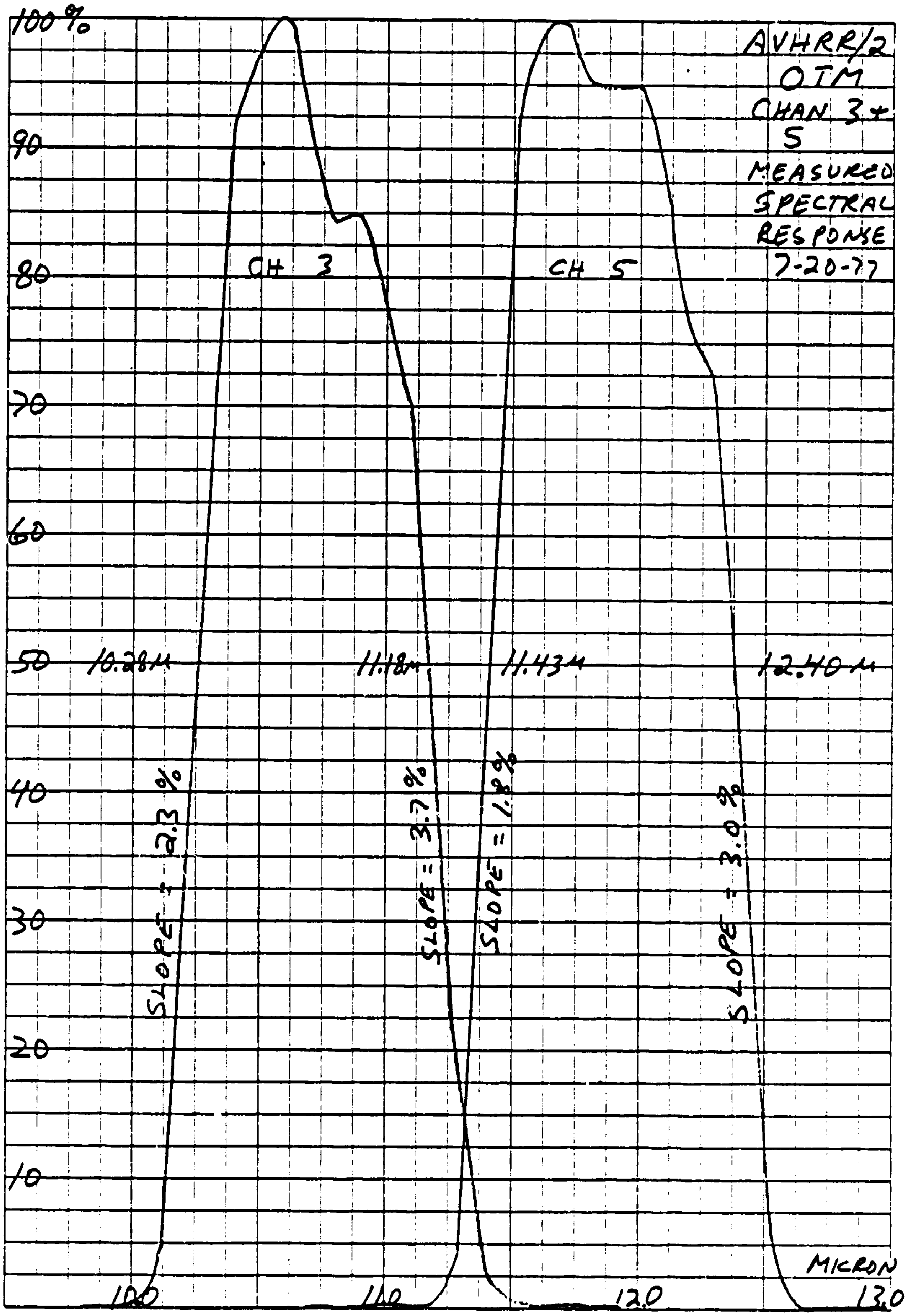
AVHRR/2
OTM
CHAN 3 + 5
MEASURED
SPECTRAL
RESPONSE
7-20-77
100%
90
80
70
60
50
40
30
20
10
CH 3
CH 5
10.28µ
11.18µ
11.43µ
12.40µ
SLOPE = 2.3%
SLOPE = 3.7%
SLOPE = 1.8%
SLOPE = 3.0%
10.0
11.0
12.0
13.0
MICRON

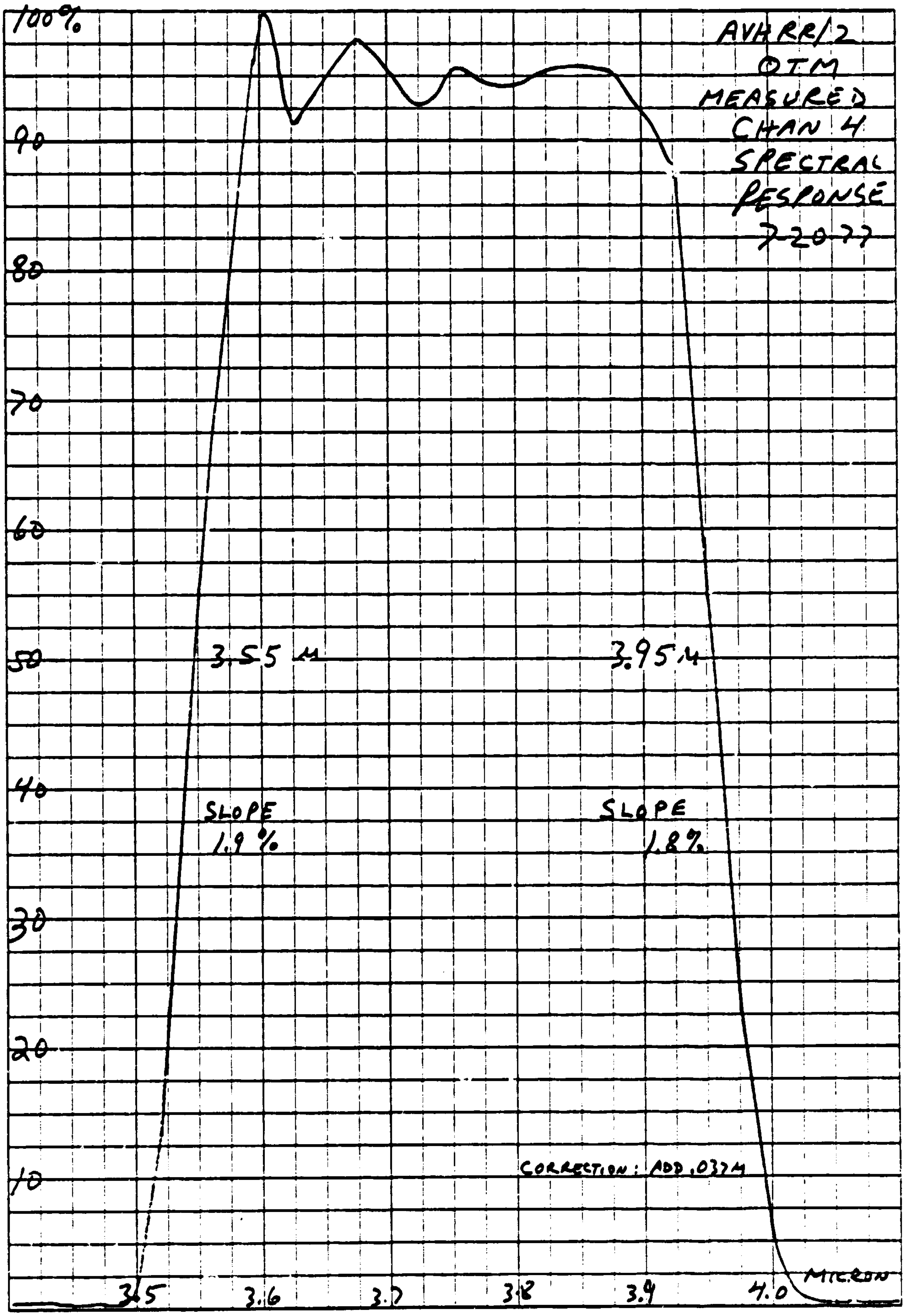


46 0253

K+E 4 X 4 TO THE INCH • 7 X 10 INCHES KEUFFEL & ESSER CO.

AVHRR/2 OTM RADIANT COOLER THERMAL PERFORMANCE

| | CHAMBER TESTS (A) | | ANALYTICAL MODEL |
|---|---|---|---|
| | MEASURED | CORRECTED (B) | PREDICTED |
| COOLER HOUSING | 3.3°C | 17.5°C | 17.5°C |
| OPTICS (C) | 13°C | 20°C | 20°C |
| RADIATOR | 167.7K, 167.4K | 171.0K, 170.7K | 168.8K - 171.2K (D) |
| UNCONTROLLED PATCH | - - | 96.9K, 97.1K | 95.4K - 96.3K |
| CONTROLLED PATCH | 103.4K, 108.3K | 105.0K | 105.0K |
| CONTROL POWER | 22.04mW, 41.04mW | 29.4mW, 28.7mW | 34.0mW - 31.3mW |
| JOULE HEAT | 1.46mW | 3.5mW | 3.5mW |

(A) FEB. 28 - MARCH 2, 1977

(B) TO NOMINAL ORBIT (833 KM ALTITUDE, 37.5° SUN ANGLE), INCL. ABSENCE OF SPACE TARGET INPUT.

(C) EXCEPT FOR CHANNEL 4 INPUT TO RADIATOR, WHICH IS AT HOUSING TEMPERATURE.

(D) FOR INSULATION FACTORS IN THE RANGE 65 TO 50.

## AVHRR/2 OTM RADIANT COOLER THERMAL PERFORMANCE - POST VIBRATION

| | CHAMBER TESTS (A) | | ANALYTICAL MODEL |
|---|---|---|---|
| | MEASURED | CORRECTED (B) | PREDICTED |
| Cooler Housing | 10.5C | 17 5°C | 17.5°C |
| Optics (C) | 14°C | 20°C | 20°C |
| Radiator | 169.4K | 171.4K | 168.8K - 171.2K (D) |
| Uncontrolled Patch | - - | 98.0K | 95.4K - 96.3K |
| Controlled Patch | 104.1K | 105.0K | 105.0K |
| Control Power | 18.8mW | 25.9mW | 34.0mW - 31.2mW |
| Joule Heat | 1.46mW | 3.5mW | 3.5mW |

(A) July 20-22, 1977

(B) To nominal orbit (833 Km altitude, 37.5° sun angle), incl. absence of space target input.

(C) Except for Channel 4 input to radiator, which is at housing temperature.

(D) For insulation factors in the range 65 to 50.

AVHRR/2

RESUME OF PFM TEST RESULTS

| ITEM | SPECIFICATION | MEASURED |
|---|---|---|
| SIZE | MAX. 30.75" x 11.5" x 14.5" | 30.25" x 11.19" x 14.31"<br>EXCLUDING THERMAL BLANKET |
| WEIGHT | 65 LB. | 63.31 LBS. WITH THERMAL BLANKET |
| POWER | 28.5 WATTS | 26.18 WATTS |
| CENTER OF GRAVITY | -- | DOOR OPEN / DOOR CLOSED<br>X 4.93" / 4.86"<br>Y 12.34" / 12.34"<br>Z 1.20" / 1.28" |
| VIBRATION | SEE SPEC. PARA. 4.4.4.3 | PASSED EXCEPT FOR<br>MR E03437 AND<br>MR E03438 |
| SCAN PLAN ALIGNMENT | MAX. CHANGE 0.5 MRAD AFTER VIBRATION | BEFORE / AFTER / CHANGE<br>NADIR +.04 / -.44 / .48<br>$90^{\circ}$ -.86 / -.76 / .10 |
| CHANNEL REGISTRATION | ALL IFOV CENTERS WITHIN 0.1 MRAD. | INITIALLY 0.08 MRAD.<br>AFTER VIB. 0.05 MRAD. |

| ITEM | SPECIFICATION | MEASURED |
| --- | --- | --- |
| SCAN JITTER | LINE-TO-LINE, 98% WITHIN ±17 μSEC | >98%, ±16 μSEC. |
| | SCENE, 98% WITHIN ± 27 μSEC | >98%, ±16 μSEC IN SCAN<br>100% ±16 μSEC IN X SCAN |
| | LONG TERM P-P, 34 μSEC MAX. | <34 μSEC. |
| IFOV SIZE AT 50% POINTS | 1.3 ± 0.2 MRAD. | CH 1: 1.44 X 1.43<br>CH 2: 1.43 X 1.42<br>CH 3: 1.28 X 1.46<br>CH 4: 1.42 X 1.42<br>CH 5: 1.32 X 1.31 |
| SYSTEM MTF | >30% AT IFOV FREQUENCY | CH 1: 44%<br>CH 2: 45%<br>CH 3: 42%<br>CH 4: 49%<br>CH 5: 37% |
| CH 1 & 2 SPECTRAL RESPONSE | SEE PARA. 3.4.2 OF SPEC | CH 1: IN SPEC.<br>CH 2: IN SPEC.<br>(SEE APPENDIX) |
| CH 1 & 2 SIGNAL STABILITY | CH 1 ± 100 MV, CH 2 ± 120 MV OVER $10^{0}$ TO $30^{0}$C RANGE | CH 1: 40 MV TOTAL<br>CH 2: 82 MV TOTAL |

| ITEM | SPECIFICATION | MEASURED |
|---|---|---|
| CH 1 & 2 S/N RATIO | 3/1 @ 0.5% ALBEDO (=10 MV NOISE) | CH 1: 2.96 MV.)<br>CH 2: 2.99 MV.) S/N = 10/1 @ 0.5% ALBEDO |
| CH 3, 4, & 5 SPECTRAL RESPONSE | SEE PARA. 3.4.2 OF SPEC | CH 3: LONG WAVE SLOPE OUT OF SPEC. (MR E03431)<br>CH 4 & CH 5: IN SPEC<br>(SEE APPENDIX) |
| CH 3, 4, & 5 SIGNAL STABILITY | CH 3 & 5 ± 100 MV, $10^{o}C$ TO $21^{o}C$<br>CH 4 ± 100 MV, $10^{o}C$ TO $30^{o}C$ | CH 3: 172 MV<br>CH 5: 49 MV<br>CH 4: 216 MV (MR F04271) |
| CH 3, 4, & 5 NE$\Delta$T (108K PATCH TEMP) | CH 3 & 4 0.12K<br>CH 5 0.13K | CH 3: .052K<br>CH 4: .056K<br>CH 5: .046K |
| SIGNAL AMPLITUDE CH 1 & 2 | 100% ALBEDO = 6.1 ± 0.1V | CH 1: 4.8416 @ 79.1% ALBEDO = 6.12 V @ 100%<br>CH 2: 5.658 @ 93.13% ALBEDO = 6.08 V @ 100% |
| | SPACE CLAMP = 0.25 ± .05 V | CH 1: 0.237 V<br>CH 2: 0.247 V |

| ITEM | SPECIFICATION | | MEASURED | | | |
|---|---|---|---|---|---|---|
| | | | | CH 3 | CH 4 | CH 5 |
| SIGNAL AMPLITUDE | 320K $\pm$1K = 0.3 $\pm$ 0.1 V | | @ 320K | 0.1377 | 0.1158 | 0.2137 |
| CH 3, 4, & 5 | ($15^{0}$ BASELINE) | | @ 319K | 0.2113 | 0.3239 | 0.2830 |
| | | | (CALCULATED) | | | |
| | SPACE CLAMP = 6.2 $\pm$ 0.05 V | | | 6.201 | 6.210 | 6.195 |
| COMMAND OPERATION | | | OPERATION AND DIGITAL TM LEVEL VERIFIED. | | | |
| ANALOG TM | | | INSTRUMENT STATUS MEASURED | | | |
| TURN ON TRANSIENT (28V) | | | | | | |
| ELECTRONICS | 1.4A MAX. @ 20 MA/$\mu$SEC | | 540 MA - 2.2 MA/$\mu$SEC. | | | |
| MOTOR | 1.4A MAX. @ 20 MA/$\mu$SEC | | 500 MA - 0.3 MA/$\mu$SEC. | | | |
| COOLER HEAT | 3.3A MAX. FOR 2 M.S. | | 2.3A FOR 500$\mu$SEC. | | | |
| EARTH SHIELD | 2.1A MAX. FOR 1 SEC | | 1.8A FOR .65 SEC | | | |
| CONDUCTED RIPPLE (28V) | $<$ 20 Hz | $>$20 Hz | $<$20 Hz | $>$20 Hz | | |
| MOTOR - LOW | 27 MA MAX. | 9 MA MAX | $<$5 MA | $<$5 MA | | |
| MOTOR - HIGH | | | $<$5 MA | $<$5 MA | | |
| ELECT. & ALL CH'S | | | 14 MA | $<$5 MA | | |
| FULL INST. | | | 8 MA | $<$5 MA | | |
| SUSCEPTIBILITY | .25V P-P TO 1.5 KHZ | | WORST CASE | | | |
| | .50V P-P TO 10 MHK | | 1.5 V @ 20 KHz. | | | |

| ITEM | SPECIFICATION | MEASURED | | | | |
|---|---|---|---|---|---|---|
| CONDUCTED RIPPLE (+10V) | 2 MA MAX. | 1 MA | | | | |
| CONDUCTED RIPPLE (+5V) | 1 MA MAX. | 1 MA | | | | |
| AMPLIFIER DROOP | .39% OF FULL SCALE (25 MV) | CH 1 | .1 MV | | | |
| | | CH 2 | 1.3 MV | | | |
| | .098% FULL SCALE | CH 3 | .08 MV | | | |
| | (6 MV) DESIGN GOAL | CH 4 | .15 MV | | | |
| | | CH 5 | .26 MV | | | |
| | | | TM | DATA | Δ | |
| VERIFICATION OF TM IN DATA STREAM | DIFFERENCE ± 12.5 M.V. MAX. | BB1 | 1.192 V | 1.185V | 7MV | |
| | | BB2 | 1.208 V | 1.2003V | 7.7MV | |
| | | BB3 | 1.207V | 1.2003V | 6.7MV | |
| | | BB4 | 1.267V | 1.2609V | 6.1MV | |
| | | PATCH TEMP | 2.911V | 2.906V | 5 MV | |
| | | | TM | DATA | Δ | |
| BB SAMPLE TM | DIFFERENCE ±12.5 MV. MAX. | CH 3 | 2483 | 2481 | 2 MV | |
| | | CH 4 | NO DATA | TEST EQUIP PROBLEM | | |
| | | CH 5 | 2373 | 2365 | 8 MV | |
| | | | 1 | 2 | 3 | 4 |
| VOLTAGE CAL VERIFICATION | 3 EARTH SCENE LEVELS | CH 1 | 1832 | 3468 | 5093 | 5900 MV |
| | 1 B.B. LEVEL | CH 2 | 1856 | 3481 | 5100 | 5908 MV |
| | | CH 3 | 1331 | 2950 | 4570 | 525 MV |
| | | CH 4 | 1337 | 2962 | 4594 | 525 MV |
| | | CH 5 | 1349 | 2968 | 4587 | 541 MV |
| | DETECTOR DISABLED | VERIFIED DET. DIS. | | | | |

| ITEM | SPECIFICATION | MEASURED |
|---|---|---|
| OVER-VOLTAGE | 28V TO 39V | ±15 V REGULATED VOLTAGES VARY 3 MV - +5 V SUPPLY VARIES 32 MV. |
| AMPLIFIER ZEROING | CH 1 .250 ± 0.050 V | 225 MV |
| | CH 2 .250 ± 0.050 V | 238 MV |
| | CH 3 6.2 ± 0.50 V | 6201 MV |
| | CH 4 6.2 ± 0.50 V | 6211 MV |
| | CH 5 6.2 ± 0.50 V | 6194 MV |
| AMPLIFIER LINEARITY | ± 12.5 MV MAX | CH 1 - 4 MV MEASURED WITH |
| | | CH 2 - 2 MV RAMP CAL AND |
| | | CH 3 - 6 MV DATA CONVERTER |
| | | CH 4 - 4.7 MV |
| | | CH 5 - 1.3 MV |
| RAMP CAL RANGE | 0.025 TO + 6.475 | CH 1 3247 |
| | | CH 2 3245 |
| | | CH 3 3238 |
| | | CH 4 3276 |
| | | CH 5 3242 |
| | | (HALF AMPLITUDE MEASUREMENTS. MULTIPLY BY 2 FOR FULL RANGE) |
| AUXILIARY SCAN | NONE | SYNC PULSE TO COLLIMATOR TARGET |
| | | VERIFIED OPERATION |

# AVHRR/2 PFM

## CALIBRATION EQUATIONS

| | | |
|---|---|---|
| RADIATOR TEMP | °K | $= 32.584\,V + 141.692 + .452V^2$ |
| PATCH POWER | MW | $= 2V^2$ |
| PATCH TEMP LOW RANGE | °K | $= 4.997\,V + 90.005 + .0297\,V^2$ |
| PATCH TEMP EX RANGE | °K | $= 34.826\,V + 90.769 + 2.074\,V^2$ |
| BB#1 TM | °C | $= .0349\,V^2 + 8.204\,V + 3.437$ |
| BB#2 TM | °C | $= .0349\,V^2 + 8.204\,V + 3.437$ |
| BB#3 TM | °C | $= .0349\,V^2 + 8.204\,V + 3.437$ |
| BB#4 TM | °C | $= .0349\,V^2 + 8.204\,V + 3.437$ |
| MOTOR CURRENT | MA | $= 60V$ |
| ELECTRONICS CURRENT | MA | $= 196.5\,V$ |
| EARTH SHIELD POSITION | | = <2V - CL  2-4 - MID  >4V - OPEN |
| ELECTRONICS TEMP | °C | $= -5.82V + 39.9$ |
| BASE PLATE TEMP | °C | $= -7.75V + 34.8$ |
| A TO D TEMP | °C | $= -8.33V + 86.16$ |
| MOTOR HOUSING TEMP | °C | $= -7.75V + 34.8$ |
| COOLER HOUSING TEMP | °C | $= -7.75V + 34.8$ |
| DETECTOR BIAS VOLTS | | $= 4.33V - 21.33$ |
| BB IR CH 3 | °C | $= 49.37 - 14.839\,V + .8329\,V^2 - .4582\,V^3 + .03498\,V^4$ |
| BB IR CH 4 | °C | $= 19.85 + 28.696\,V - 15.116\,V^2 + 2.939\,V^3 - .23074\,V^4$ |
| BB IR CH 5 | | $= 44.3544 - 2.397\,V - 9.581\,V^2 + 2.966\,V^3 - .37407\,V^4$ |
| OFFSET VOLTAGE | TM | $= 1.33\,V$ |

AVHRR/2

TEST DATA

APPENDEX

ITT AEROSPACE/OPTICAL DIVISION
FORT WAYNE, INDIANA, U.S.A.
INTERNATIONAL TELEPHONE AND TELEGRAPH CORPORATION



DRAWING NUMBER 8125979 REV

AVHRR S.N. 201 /PEM DATE 3/28/78 Q.C. ______

ENGINEER D. HARBER & L. OWENS

| | CHANNEL 1 | | CHANNEL 2 | |
|---|---|---|---|---|
| | SPEC. | MEASURED | SPEC. | MEASURED |
| SHORT WAVE 80% WV'LN. | WITHIN 0.04 µM OF 50% WV'LN. | .04 µm | WITHIN 0.02 µM OF 50% WV'LN. | .0093 µm |
| SHORT WAVE 50% WV'LN. | 0.58 ± 0.04 µM | .571 µm | 0.725 ± .025 µM | 712.7 µm |
| SHORT WAVE 5% WV'LN. | WITHIN 0.14 µM OF 50% WV'LN.*** | .016 µm | WITHIN 0.04 µM OF 50% WV'LN.* | .0137 µm |
| LONG WAVE 80% WV'LN. | WITHIN 0.02 µM OF 50% WV'LN. | .009 µm | WITHIN 0.2 µM OF 50% WV'LN. | .0599 µm |
| LONG WAVE 50% WV'LN. | 0.68 ± 0.04 µM | .6859 µm | 1.00 ± 0.05 µM | .9859 µm |
| LONG WAVE 5% WV'LN. | WITHIN 0.04 µM OF 50% WV'LN. | .031 µm | WITHIN 0.06 µM 50% WV'LN | .0921 µm |
| RESPONSE BETWEEN S.W. 80% WV'LN. AND L.W. 80% WV'LN. | 80% MIN. | >80% | 80% MIN. | >80% |

N.R. = NO REQUIREMENT

* S.W. 5% WV'LN. OF CHANNEL 2 MUST ALWAYS EXCEED 0.685 µM

** MINIMUM Δλ BETWEEN 50% POINTS SHALL BE 0.10 µM.

*** S.W. 5% WVLN. OF CH. 1 MUST BE GREATER THAN 0.46 µM

TABLE 5

CHANNEL 1 & 2 SPECTRAL CHARACTERISTICS

ORIGINAL PAGE IS OF POOR QUALITY

DWG SIZE A CODE IDENT NO. 31550 8125979

SCALE SHEET 10

FORM NO. FW ITTAOD D 105 LINCOLN-GRAPHIC CORP.

ITT AEROSPACE/OPTICAL DIVISION
FORT WAYNE, INDIANA, U.S.A.
INTERNATIONAL TELEPHONE AND TELEGRAPH CORPORATION



DRAWING NUMBER 8125979 REV A

AVHRR S.N. 201 /PFM DATE 3/28/78 Q.C.

ENGINEER D. HARBER L. OWENS

| | CHANNEL 3 | | CHANNEL 4 | |
|---|---|---|---|---|
| | SPEC. | MEASURED | SPEC. | MEASURED |
| SHORT WAVE 50% WV'LN. | 10.3 ± 0.09 μM | 10.362 μm | 3.55 ± 0.06 μM | 3.575 μm |
| S.W. 80% OF 1ST PEAK WV'LN. | SEE S.W. SLOPE | 10.410 μm | SEE S.W. SLOPE | 3.592 μm |
| S.W. 5% WV'LN. | SEE S.W. SLOPE | 10.230 μm | SEE. S.W. SLOPE | 3.528 μm |
| S.W. SLOPE* | <4.0% | 1.7% | <3.0% | 1.8% |
| LONG WAVE 50% WV'LN. | 11.3 ± 0.09 μM | 11.299 μm | 3.93 ± 0.06 μM | 3.983 μm |
| L.W. 80% OF 1ST PEAK WV'LN. | SEE L.W. SLOPE | 10.995 μm | SEE L.W. SLOPE | 3.961 μm |
| L.W. 5% WV'LN. | SEE L.W. SLOPE | 11.470 μm | SEE L.W. SLOPE | 4.032 μm |
| L.W. SLOPE* | <4.0% | 4.1% | <3.0% | 1.8% |
| RESPONSE BETWEEN S.W. 80% WV'LN. & L.W. 80% WV'LN. | 80% MIN. | 780% | 80% MIN. | 780% |
| RESPONSE AT WV'LN. <10.0 μM AND >12.0 μM | ≤1% | DID NOT MEAS. OUT OF BAND | N/A | N/A |
| RESPONSE AT WV'LN. <3.40 μM AND >4.12 μM | N/A | N/A | ≤1% | DID NOT MEAS. OUT OF BAND |

*SLOPE = [(80% OF FIRST PEAK WV'LN. - 5% WV'LN.) ÷ 50% WV'LN.] X 100%

TABLE 6
CHANNELS 3 AND 4 SPECTRAL CHARACTERISTICS

DWG SIZE A CODE IDENT NO. 31550 8125979

SCALE SHEET 11

DRAWING NUMBER 8125979 REV A

AVHRR S.M. 20: /PFM DATE 3/28/78 Q.C.

ENGINEER D. HARBER L OWENS

| | CHANNEL 5 | |
|---|---|---|
| | SPEC. | MEASURED |
| SHORT WAVE 50% WV'LN. | 11.5 ± 0.09 μM | 11.450 μm |
| S.W. 80% OF 1ST PEAK WV'LN. | SEE S.W. SLOPE | 11.500 μm |
| S.W. 5% WV'LN. | SEE S.W. SLOPE | 11.245 μm |
| S.W. SLOPE* | <4.0% | 2.3% |
| LONG WAVE 50% WV'LN. | 12.5 ± 0.09 μM | 12.424 μm |
| L.W. 80% OF 1ST PEAK WV'LN. | SEE L.W. SLOPE | 12.145 μm |
| L.W. 5% WV'LN. | SEE L.W. SLOPE | 12.545 μm |
| L.W. SLOPE* | <4.0% | 3.2% |
| RESPONSE BETWEEN S.W. 80% WV'LN. & L.W. 80% WV'LN. | 80% MIN. | >80% |
| RESPONSE AT WV'LN. <10.0 μM AND >12.0 μM | ≤1% | DID NOT MEAS OUT OF BAND |



*SLOPE = [(80% OF FIRST PEAK WV'LN. - 5% WV'LN.) ÷ 50% WV'LN.] X 100%

TABLE 7

CHANNEL 5 SPECTRAL CHARACTERISTICS

AVHRR/2 PFM SPECTRAL RESPONSE, CH. 1 3/28/78

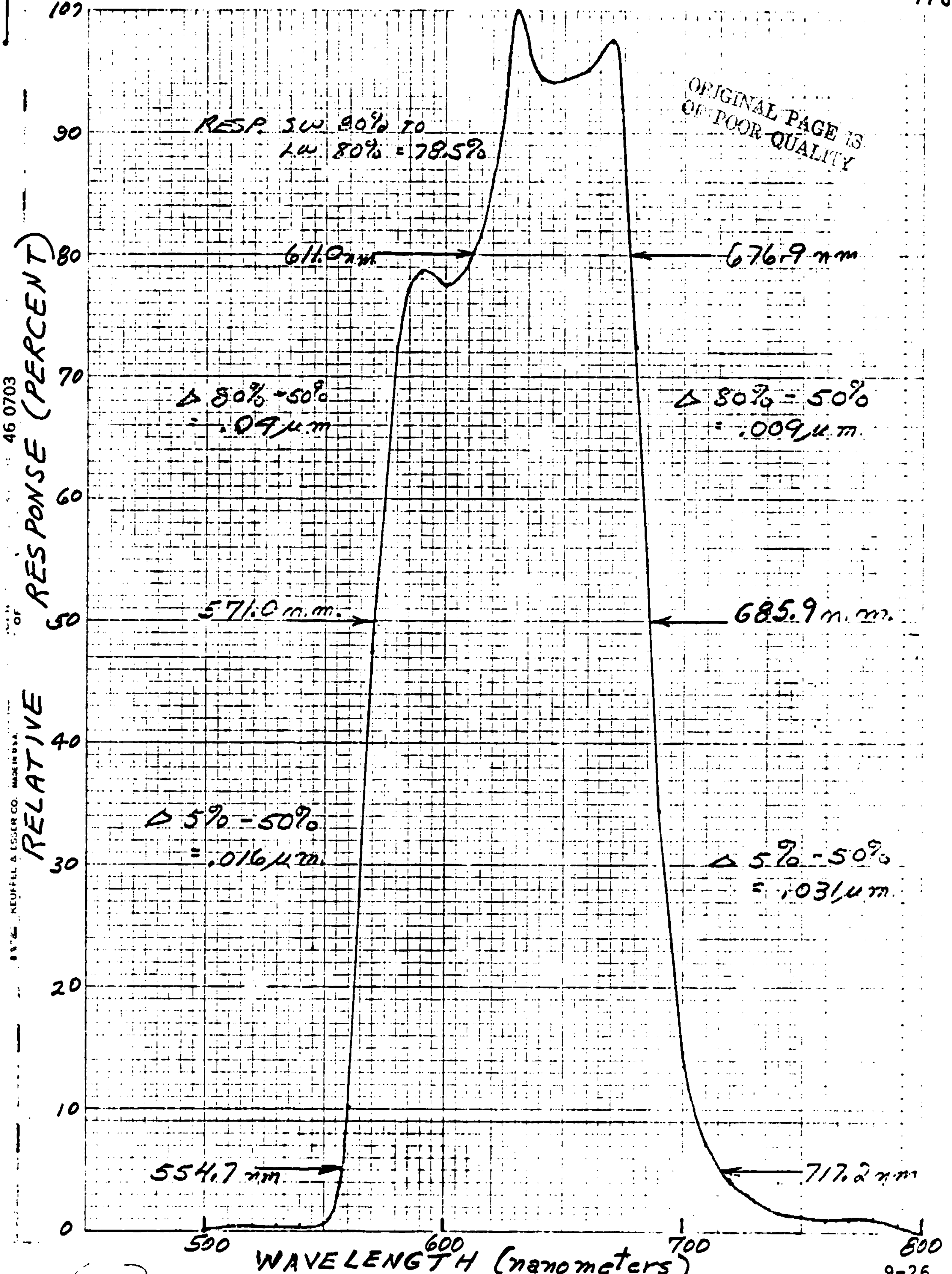

AVHRR/2 PFM SPECTRAL RESPONSE, CH. 2 3/28/78

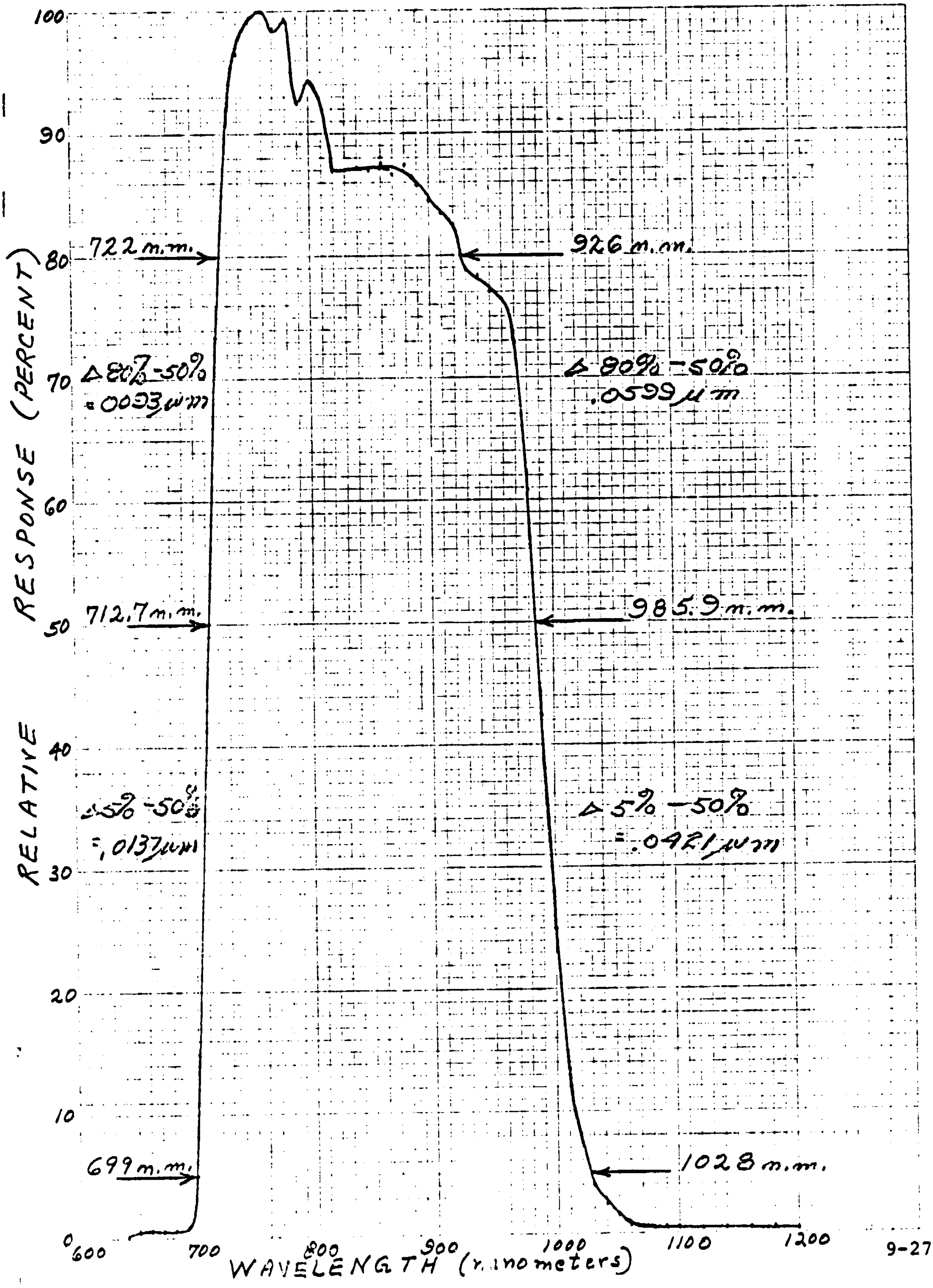

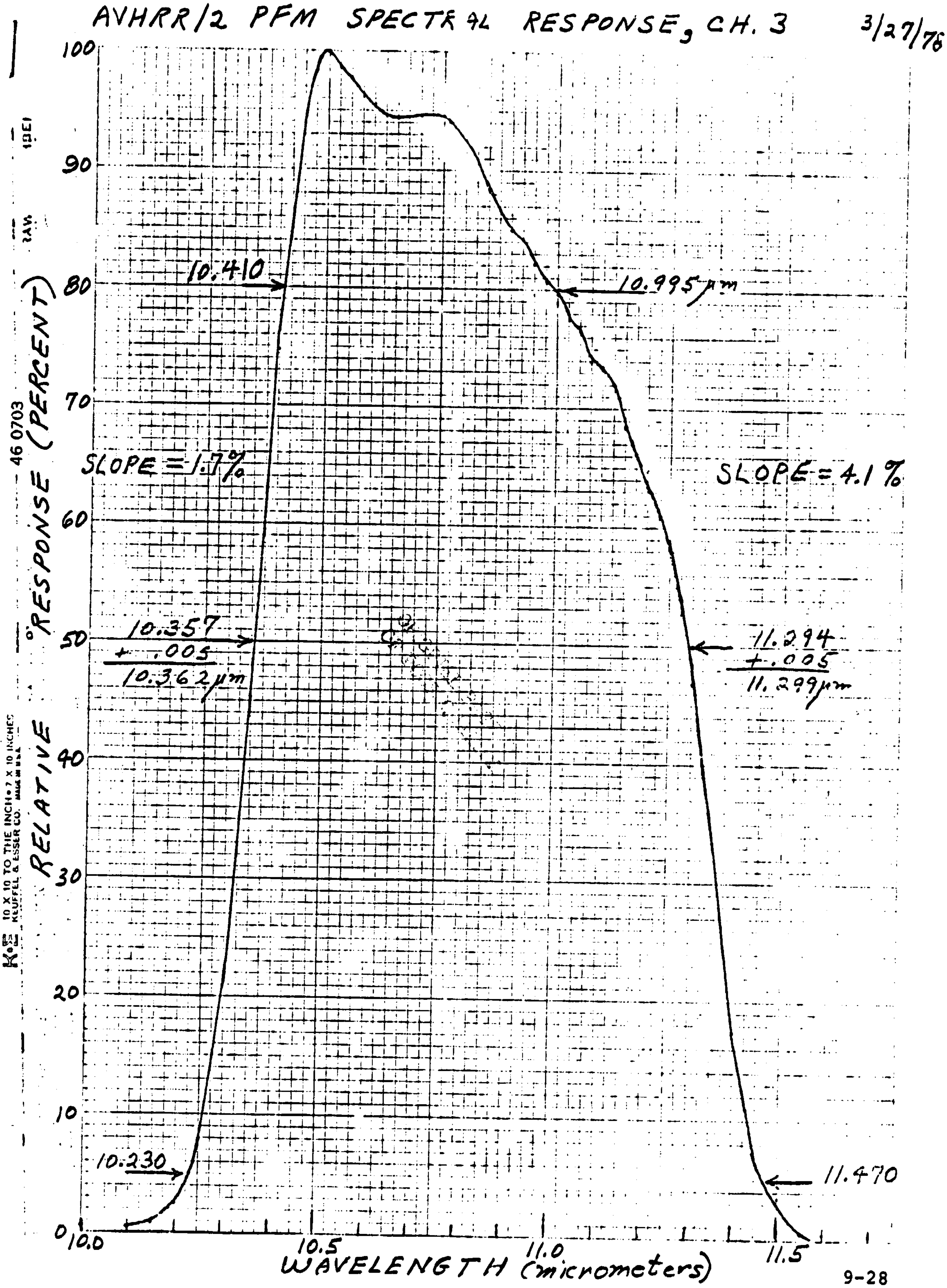

AVHRR/2 PFM SPECTRAL RESPONSE, CH. 3
3/27/78
RELATIVE RESPONSE (PERCENT)
WAVELENGTH (micrometers)
100
90
80
70
60
50
40
30
20
10
0
10.0
10.5
11.0
11.5
10.410
10.995 μm
SLOPE = 1.7%
SLOPE = 4.1%
10.357
+ .005
10.362 μm
11.294
+ .005
11.299 μm
10.230
11.470

AVHRR/2 P.F.M. SPECTRAL RESPONSE, CH. 4 3/27/78

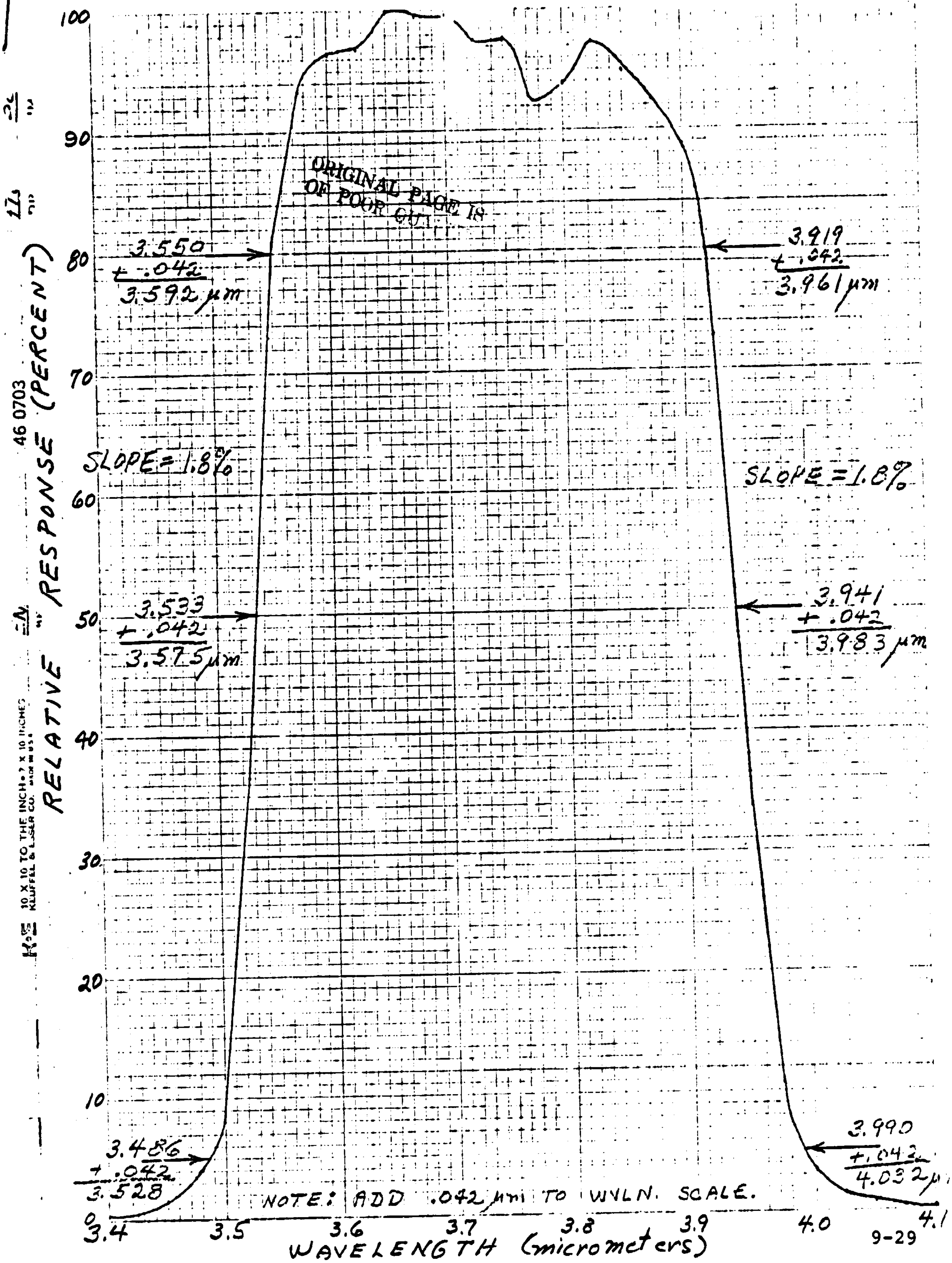

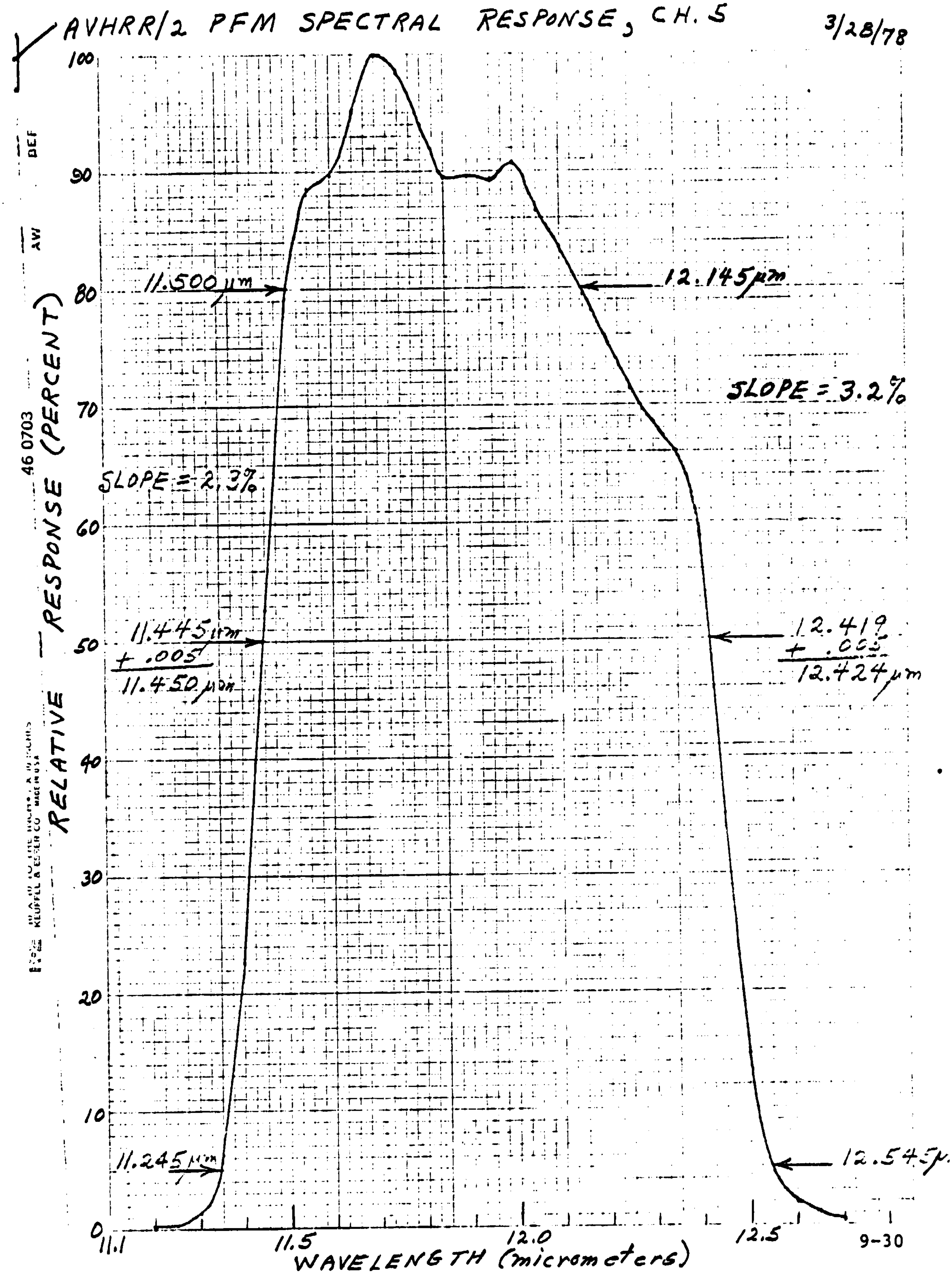
AVHRR/2 PFM SPECTRAL RESPONSE, CH. 5
3/28/78
RELATIVE RESPONSE (PERCENT)
WAVELENGTH (micrometers)
11.500 μm
12.145 μm
SLOPE = 3.2%
SLOPE = 2.3%
11.445 μm
+ .005
11.450 μm
12.419
+ .005
12.424 μm
11.245 μm
12.545 μ
0
10
20
30
40
50
60
70
80
90
100
11.1
11.5
12.0
12.5
9-30

## 10.0 LIST OF DESIGN INFORMATION REPORTS

Design Information Reports written on the AVHRR programs are listed below.

| DIR # | Subject |
|---|---|
| 1. | AVHRR Sensitivity - Harber/Koczor |
| 2. | AVHRR Collimator - Diffration Effects - R. Koczor |
| 3. | Effects of Optical Surface Errors on Diffraction Limited MTF - R. Annable |
| 4. | Approach to the Optical Alignment and Channel Registration of the AVHRR - R. Annable |
| 5. | The Effect of Detectors on the Instrument Spectral Response, Part 1, Channels 3 & 4 - R. Koczor |
| 6. | Theoretical Design to Meet the Polarization Requirements in Channels 1 and 2 - R. Annable |
| 7. | Polarization Design and Analysis Based on OCLI Measured Data - R. Annble |
| 8. | Using "Standard" Silicon Detectors for Channels 1 and 2 - R. Koczor |
| 9. | Effect of Scan Mirror Power on Diffraction Limited MTF - R. Annable |
| 10. | Visible In-Flight Calibration - R. Koczor |
| 11. | Orientation of the Visible Calibration D.R.T. - R. Koczor |
| 12. | Solar Channel Spectral Characteristics, Part 1 - R. Koczor |
| 13. | Solar Channel Sensitivity - R. Koczor |
| 14. | The Absence of Coma in an Afocal Pair of Confocal, Coaxial Parabolic Mirrors - R. Annable |
| 15. | Heating of the Radiator Window for Contamination Protection - R. Annable |
| 16. | AVHRR Test Collimator Design - R. Koczor |
| 17. | The Effect of Collimator Aberrations on the Diffraction Limited MTF - R. Annable |
| 18. | Worst Case Honeycomb Temperature Gradient in the In-Flight Thermal Calibration Target - R. Annable |
| 19. | Cool Down and Decontamination Times for the Radiant Cooler - R. Annable |
| 20. | Scanner Jitter, Linearity, and Alignment Tests - R. Koczor |
| 21. | Optimization of IFOV Size and Shape, Pre-Sampling Filter, and Sample Rate - R. Foote |
| 22. | Thermal Math Model Analysis - Crawford/Wright |
| 23. | Thermal Math Model Analysis, OFF Instrument - Crawford/Wright |
| 24. | Measurement of Low Emissivity - R. Koczor |

| DIR # | Subject |
|---|---|
| 25. | AVHRR Scan Motor Lubricant Evaluation and Selection - J. Stark |
| 26. | AVHRR TM Calibration - N. Franklin |
| 27. | MSM Vibration Test - J. Stark |
| 28. | BBM Acceptance Test Results - Owens/Koczor |
| 29. | Completion of Thermal Math Model - J. Crawford |
| 30. | MSM Vibration #2 - J. Stark |
| 31. | Effect of Loss of Radiant Cooler Temperature Regulation - R. Harber |
| 32. | Worst Case Analysis - L. Roffelsen |
| 33. | AVHRR MSM Vibration #3 - J. Stark |
| 34. | Spectral Response Measurements on AVHRR ETM - R. Harber |
| 35. | Pinning of Critical Parts - C. Soest |
| 36. | Cooler Door Momentum - C. Soest |
| 37. | Scattered Light Test Results of AVHRR BBM - R. Koczor |
| 38. | Final Thermal Model Analysis - J. Crawford |
| 40. | LTM Final Report - C. Soest |
| 42. | AVHRR Data Amplifier Signal Droop - H. Kalina |
| 43. | Channel 4 Coherent Noise in AVHRR PFM - R. Foote |
| 44. | AVHRR Scanner Long Term Drift Measurement-Larry Howell |